INVESTIGATION INTO SUITABILITY OF GEOPOLYMERS (ILLITE & METAKAOLIN) FOR THE SPACE ENVIRONMENT

DISSERTATION

Brandon T. Cesul

AFIT/DS/ENY/12-14

DEPARTMENT OF THE AIR FORCE
AIR UNIVERSITY

AIR FORCE INSTITUTE OF TECHNOLOGY

Wright-Patterson Air Force Base, Ohio

AFIT/DS/ENY/12-14

INVESTIGATION INTO SUITABILITY OF GEOPOLYMERS (ILLITE & METAKAOLIN) FOR THE SPACE ENVIRONMENT

DISSERTATION

Presented to the Faculty

Department of Aeronautics & Astronautics

Graduate School of Engineering and Management

Air Force Institute of Technology

Air University

Air Education and Training Command

In Partial Fulfillment of the Requirements for the

Degree of Doctor of Philosophy in Astronautical Engineering

Brandon T. Cesul, B.S.E, M.Eng.

September 2012

AFIT/DS/ENY/12-14

INVESTIGATION INTO SUITABILITY OF GEOPOLYMERS (ILLITE & METAKAOLIN) FOR THE SPACE ENVIRONMENT

Brandon T. Cesul, B.S.E, M.Eng.

Approved:

15 June 12

Dr. Shankar Mall, Professor of Aerospace Engineering (Chairman) Date

15 JUN 12

Dr. Richard Cobb, Associate Professor of Aerospace Engineering (Member) Date

Paul T. Murray

15 JUN 12

Dr. P. Terrence Murray, Professor, University of Dayton, Materials Engineering (Member) Date

Dr. Lawrence Matson

15 June 12

Dr. Lawrence Matson, Senior Researcher, Air Force Research Laboratory (Member) Date

Accepted:

MU Thomas

24 Jul 2012

M.U. THOMAS Date

Dean, Graduate School of Engineering and Management

Acknowledgments

I would like to express my sincere appreciation to my faculty advisor, Dr Shankar Mall, for his guidance and support throughout the course of this thesis effort. I would also like to thank Dr Lawrence Matson from Air Force Research Laboratory for his support and guidance of the experimental work performed as part of this thesis effort. I would also like to thank my committee for their patience and assistance. Finally, I would like to thank my wife for all her support, emotionally and physically, during this long adventure.

Brandon T. Cesul

Table of Contents

List of Figures

Page

List of Tables

List of Acronyms

AFM	Atomic force microscopy
AFIT	Air Force Institute of Technology
AFRL/RX	Air Force Research Laboratory Materials & Manufacturing Directorate
Al	Aluminum
AMSD	Advanced Mirror System Demonstrator
AO	Atomic oxygen
ASTM	American Society for Testing and Materials
Be	Beryllium
C	Carbon
Ca	Calcium
Cs	Cesium
CSM	Continuous scan method
CTE	coefficient of thermal expansion
CVCM	Collected Volatile Condensable Materials
ESA	European Space Agency
ESH	Equivalent solar hours
EUVS	Equivalent ultraviolet suns
eV	Electron-volt
Fe	Iron
GSFC	Goddard Space Flight Center
H	Hydrogen
IIT	Instrumented indentation testing
IR	Infrared
ISS	International Space Station
JAXA	Japan Aerospace Exploration Agency
K	Potassium
KOH	Potassium hydroxide
LDEF	Long Duration Exposure Facility
LEO	Low earth orbit
MISSE	Materials International Space Station Experiment
MWIR	Mid-wave infrared
Na	Sodium
NaOH	Sodium hydroxide
NASA	National Aeronautics and Space Administration
NIST	National Institute of Standards and Technology
NML	Net mass loss
NRO	National Reconnaissance Office
O	Oxygen
OH	Hydroxide group
RMS	Root mean square
SCEPTRE	Space Combined Effects Primary Test & Research
Si	Silicon

SiC	Silicon carbide
SLV	Space launch vehicle
STS	Space Transportation System (NASA's "Space Shuttle")
TML	Total mass loss
ULE	Ultra low expansion (glass)
UV	Ultraviolet
VOC	Volatile organic compound
VUV	Vacuum ultraviolet
XPS	X-ray photoelectron spectroscopy

AFIT/DS/ENY/12-14

Abstract

The United States has utilized high resolution imaging platforms for national defense since the beginning of the space age. In order to improve the resolution and swath width of imaging satellites, the primary restriction in optical hardware is the mirror size, specifically mirror diameter and mirror mass. This research addresses one of these concerns, reducing the mass of a spacecraft mirror by the use of innovative materials.

In contemporary imagery satellites, monolithic glass is the material of choice to produce large aperture mirrors that can survive the space environment. However, material performance requirements for future imaging mission mirrors necessitate a lower areal density than glass with similar if not superior mechanical strength. Additionally, any material chosen must also be able to deal with the unique environment of low earth orbit, namely the near-vacuum conditions, radiation environment and interaction with atomic oxygen.

This research focuses on investigation of a class of inorganic polymers known as geopolymers for use in the space environment. Geopolymers are based on aluminosilicate chemistry and have advantages of high specific strength combined with low densities, tailorable coefficients of thermal expansion, and easier curing processes than traditional space qualified epoxies. Geopolymers have a long history for use in terrestrial

applications, but empirical data is not available addressing their suitability for the space environment.

This research focused on determining whether the geopolymer as a bulk material will respond favorably to environmental conditions as experienced during typical spaceflight operations. Two different formulations of geopolymer were investigated, one based on metakaolin chemistry, and the other based on illite chemistry. Three primary objectives were identified for assessing whether geopolymers could survive the space environment: could the materials be processed to minimize curing shrinkage, characterizing the outgassing performance, and analyzing the materials for damage following exposure to typical radiation and atomic oxygen levels seen in a short duration LEO mission.

The results of the test campaign showed promising results. Curing shrinkage was controlled using pressure as a primary variable, but a cracking failure mode was present due to thermal shock effects. Neither geopolymer emitted significant organic volatiles during outgassing, but water emission and re-absorption during test, qualification, and pre-launch storage associated with launch cycles may be an issue. Finally, space environmental exposure of ultraviolet radiation, high energy particles, and atomic oxygen bombardment resulted in only minor surface changes to the bulk material with structural performance maintained throughout the rest of the material. Overall, geopolymers show great promise as a spacecraft material due to their resistance to space environment effects, but specific caveats need to be considered for application development.

AFIT/DS/ENY/12-14

INVESTIGATION INTO SUITABILITY OF GEOPOLYMERS (ILLITE & METAKAOLIN) FOR THE SPACE ENVIRONMENT

I. Introduction

Chapter Overview

This chapter will introduce the general motivation of the research, present the research problem statement, define the objectives of the research, establish a generic methodology within to conduct the research, state assumptions associated with the research campaign, delineate expected outcomes, and outline the dissertation document.

General

A spacecraft designer's primary concern in the design phase most times is the conservation of mass margins. Spacecraft mass can affect the choice of space launch vehicle, which then affects the cost of a space mission. (Mosher 1999) Anytime that mass savings can be gained on a spacecraft project due to a change in material without affecting the structural strength or mission performance, the designers will be able to realize those savings and then book those savings to other subsystems such as batteries or propellant that can directly improve the spacecraft duty cycle or mission lifetime.

In modern imaging spacecraft, a major mass component in the design is the optics. Imaging spacecraft optics are typically comprised of a large primary mirror and smaller mirrors and lenses in the optical train. In terms of mass and system performance, the most important optic is the primary mirror which controls the diffraction limited resolution of the imaging system, as defined by the equation:

Ideal Theoretical Angular Resolution = 1.22 λ/D (Hecht 2002)

Where:

λ = wavelength
D = diameter of primary mirror

By this, a larger mirror generally gives better resolution performance. The choice of mirror material since the beginning of the space age has been monolithic glass. Monolithic glass mirrors have enabled spacecraft designers to achieve mirror diameters of over 1 m, and they are well understood in terms of mechanical and thermal performance as monolithic glass variants have been one of the first man-made construction materials. (Carlin 2000) The optical and design properties of a standard monolithic glass mirror and other traditional optical materials used in imaging spacecraft optics are listed in Table 1.

Table 1. Traditional optical material properties (Stahl 2009)

Material	ULE	ULE & Be	Beryllium	Various Glass	SiC
Use	Hubble Space Telescope	AFRL AMSD Program	James Webb Space Telescope	Terrestrial Observatory	Herschel
Optic Size (diameter)	2.8 m monolithic	< 1 m	6.5 m segmented	3.67 m (AEOS)	3.5 m fused
Areal Density (kg/m^2)	180	18	26	300-500	33
Areal Cost ($\$M/m^2$)	10 ($0.05M/kg)	4 ($0.22M/kg)	6 ($0.23M/kg)	0.5 ($0.0017M/kg)	< 24.6 (<$0.67M/kg)
Year Built	1984	2005	2008	Continuous	2003

[NOTE: money is not time indexed]

However, imaging spacecraft designers, in a never ending quest to achieve either larger mirrors or maintain current mirror diameters while reducing mass of the optic, have run into a barrier. (Coulter 1998) Monolithic glass mirrors cannot be made larger on spacecraft without encountering substantially increased mass (thereby reducing mass available to other subsystems) or endangering the mission by introducing unstable structural designs in the hopes of “hollowing out” the mirror backing. The trend is for spacecraft to become smaller and lighter in hopes of saving costs by reducing launch mass, which is accommodated by a smaller space launch vehicle.

The Materials and Manufacturing Directorate, Air Force Research Laboratory (AFRL/RX) has attempted to tackle this issue on behalf of the United States Air Force (USAF) and other US national customers. Instead of glass, composite materials (metals, ceramics, polymers, or combinations), foams, and hybrid engineered materials would form the basis of the structural substrate. Reflecting surfaces can be attached to these substrates in a number of ways which include direct thick film deposition techniques (cladding) followed by grinding, polishing, and reflective coating application, or by adhesion of a replicated reflecting foil or nano-laminate. Recent work at AFRL/RX using this replication approach has made possible small flat mirrors with areal densities less than 7 kg/m^2, a 50% reduction over the currently best available lightweight glass substrate. (Matson 2008) Composite materials being developed for this purpose also allow for a tailorable coefficient of thermal expansion (CTE) and high structural modulus.

Problem Statement

A key in developing these hybrid lightweight composite mirrors is to control the CTE of the substrate, adhesive, and reflecting material so as not to induce strains on the optical surface which would then cause distortions. These distortions end up resulting in non-focusing mirrors or optics with severe aberrations. Government laboratories have pioneered replicated nano-laminate foil technology to use as a reflecting surface as seen in Figure 1 and have produced half-meter diameter foils of visible optics quality. (Sandia

2000 & Wang 2007) Currently, the CTE of substrate and reflecting materials are close to being matched to a near zero level (~ 3 ppm/deg C). (Matson 2003) However, development of an adhesive to match these CTE values has been a challenge. Current space qualified adhesives (see Table 2) have CTE's on the order of 40 ~ 50 ppm/deg C. (Licari 2005) Furthermore, the high cure temperature (> 300 deg C) necessary for many of these space qualified adhesives results in dimensional expansion beyond acceptable limits for optical applications. (Monib 2003)

One path toward new space optic development, that has attracted attention, has been in the field of non-organic polymers. Organic polymers would seem to be a good solution for reducing the mass and cost of space optics without sacrificing mechanical performance as has been done with terrestrial optics since the mid 20th century, like polycarbonate lenses. However, organic polymers do not react well to the space environment since they frequently have issues with effluent release in the vacuum of space, significant degradation of their mechanical strength due to UV radiation exposure, and have thermal expansion rates high enough to cause destructive stresses on the optics.

Table 2. CTE values of common high temperature and space qualified adhesives ("Ablebond 84-1" 2006)

Material	***CTE Value (ppm/deg C)***
Amicon D125 F3 low T curing epoxy	70-80
Silica filled amine-cured epoxy	55
Loctite 3610	45
Uralane 7760	29
Cyanate Ester	21
Silver glass paste	16
Ablebond 84-1 space adhesive	55
AFRL/RX geopolymer (as tested)	8-15

As shown in the last row of Table 2, the inorganic polymers (commonly called geopolymers), start with a CTE of approximately 8 - 15 ppm/deg C. The addition of negative CTE dispersions such as zirconium tungstate, glass microballoons or carbon fiber strands has been successful in tailoring their CTE from 10 to -5 ppm/deg C. (Mah 2003) Geopolymers are made using an aluminosilicate sol-gel chemistry which cures at low temperatures, this being 100 deg C or less. (Davidovits 1991) This combination of low curing temperature and relatively low CTE values results in a potential small curing shrinkage.

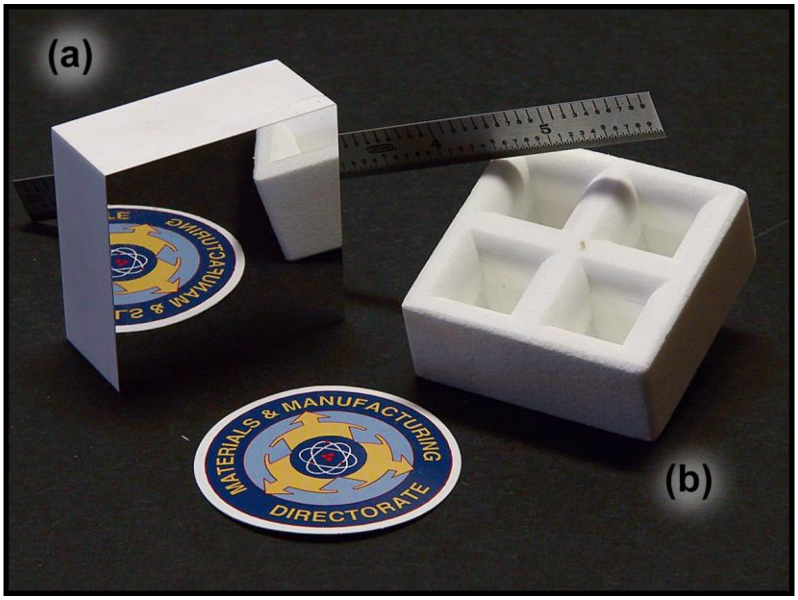

Figure 1. Sample AFRL/RX mirrors made of cast organic adhesives and reflective thin films

Inorganic polymers, or "geopolymers" (the word being formed from "geologic polymers") as they are commonly known, are generally based on aluminosilicate powders. They have been studied for literally thousands of years as replacements for traditional cements because of lower densities and easier curing conditions. Generally, geopolymers have fewer effluents than their organic counterparts (due to the lack of organic volatiles used in making organic polymers). They cure at lower temperatures than epoxies, reducing the production costs and increasing the categories of materials they can be bonded with (since the other materials don't have to survive extreme temperature environments). Finally, geopolymers have another property advantageous to space optics over organic polymers: they have a low baseline CTE. AFRL/RX began a geopolymer research program in the mid-2000's. For space optics, geopolymers have promise in two ways- as an adhesive, or as a structural material.

There have been preliminary efforts by AFRL/RX to reduce the curing shrinkage of geopolymers. However, the mechanisms involved in this process were not completely understood. The understandings about the role of polymerization, optimal water content in both free and hydrate forms, and mass loss during the curing process in the geopolymers are needed for additional improvements. Further, preliminary results show that there is a large dependence of the curing shrinkage on the environment.

Since no polymer is ever "fully" cured and the space environment is essentially a vacuum, the suitability of these geopolymers in the space environment must be addressed before their use. In other words, it would be most disastrous if a spacecraft telescope made of a hybrid composite mirror with a geopolymer adhesive became distorted or damaged on orbit due to the liberation of outgassing species (like water).

Importantly, geopolymers have never been rigorously evaluated in regards to their response to space environmental effects at a bulk material level. The space environment poses unique hazards for materials. In addition to atomic oxygen attack, electrical charge buildup, and micrometeoroid impact, there is a specific concern with any material, including geopolymers, and it is about the behavior under the radiation environment encountered in orbit. Historical experimentations both on the ground and in-flight experiments have shown that significant degradation of the organic polymer strength occurs due to increased cross linking of polymer networks after absorbing the radiation emitted from the sun or deep space. The typical radiation environment includes exposure to ultraviolet and gamma radiation, in addition to high energy charged particles like electrons and protons. (Dressler 2001)

Geopolymers have great potential to become structural materials and / or adhesives acceptable and qualified for composite mirror applications. However, important questions remain unanswered regarding the use of the material in a general sense for the space environment before evaluation of specific applications can be performed. During the production process, there is uncertainty about the primary factors which control curing shrinkage of the material. In the post-production stage, questions remain about whether the evolution of water species as a result of the polymerization reactions will impact the spacecraft mission as a result of the outgassing mechanism. A significant question also remains in terms of whether the geopolymer will be subject to similar problems as its organic polymer brethren encounter in the space environment. This is, namely, material degradation resulting from ultraviolet radiation exposure or reactions with atomic oxygen present in the low earth orbit (LEO) environment. All these questions need to be answered to a sufficient depth to ensure the baseline physics, chemistry, and material science processes are understood enough to proceed with application development and testing.

Research Objectives

The work presented in this dissertation answer three essential questions toward the use of geopolymers for spacecraft applications. Two different geopolymer formulations will be used in the course of the experimental series: an illite based geopolymer and a metakaolin based geopolymer. Two different formulations are selected in order to not be biased by a single geopolymer chemistry performance. Both materials are relatively inexpensive as well as being readily available, and both materials have been evaluated for some terrestrial applications. (Kumar 2008)

In Objective 1, the question of curing shrinkage during the polymer curing process needs to be addressed. Is there a curing variable (pressure and temperature) that impacts curing shrinkage greater than others, or is curing shrinkage a result of coupled curing variables? In addition, how do simply optimized geopolymers compare to other space qualified polymers quantitatively in terms of curing shrinkage?

In Objective 2, the geopolymers will be evaluated to control the phenomenon of outgassing, the evolution of volatile materials following exposure to the near vacuum conditions of space. Following the subjection of the geopolymer samples standard outgassing tests as defined by NASA, can we quantify their outgassing performance in comparison to accepted metrics?

Finally in Objective 3, the geopolymers needs to be evaluated against typical space radiation and reactive species exposure levels seen during a typical low earth orbit (LEO) mission. Samples will be tested against ultraviolet radiation and atomic oxygen exposure, the two primary material degradation drivers for organic polymers. After the exposure periods have been completed, are there significant deviations in performance with respect to standard mechanical performance values between exposed and non-exposed samples? Are there additional signs of failure mechanisms visible through other inspection methodologies?

Methodology

Experiments were performed according to ASTM standards when applicable. Geopolymer formulations were kept constant within a set specification to ensure consistency of results. The experiments involved three major tasks with several sub-tasks in support of each objective.

Objective 1 - Curing shrinkage

This task involved the investigation of the mechanisms associated with the curing shrinkage of geopolymers with a goal to control it. This research effort attempted to optimize the primary variables (temperature and pressure) in the curing process in order to reduce curing shrinkage to a level at least below organic polymers qualified for space utilization. Temperature and pressure were varied to investigate the coupling of these variables in curing shrinkage performance. Following a defined cure time, the samples were removed from the molds and measured in length, width and height. These measurements were then used to provide both linear dimension change and volumetric change.

Objective 2- Outgassing

This task involved investigation of the mechanisms resulting in the geopolymer outgassing volatile species. A volatile species in this context is a constituent that readily evaporates, due to pressure or temperature. In terms of the geopolymer, the only expected volatile was water vapor generated and captured in the geopolymer matrix during the formulation reaction. Outgassing water vapor in significant levels can invalidate the material for use in spacecraft applications as deposition of water vapor on an optical surface can disrupt the focusing of the optical train. Additionally, there is a concern that if water vapor is liberated from the internal polymer matrix and driven to the surface due to diffusion mechanisms, it might cause "bubbling" of the optical reflecting surface if the geopolymer is used in an adhesive application. The milestone for this task is to determine the performance of the bulk materials with respect to outgassing and optimize either the chemistry or production process to reduce outgassing to a level consistent with ASTM E-595, the NASA accepted standard for space qualified material outgassing performance.

This test series used the officially designated NASA outgassing chamber at NASA Goddard Space Flight Center in Greenbelt, MD. Samples were prepared at AFRL/RX and then shipped in protective containers to NASA Goddard where the testing was performed and results reported back to AFRL/RX. At that point, analysis was performed on the results to determine performance and key variables associated with outgassing qualification.

Objective 3 - Space radiation and LEO environment exposure testing

This objective investigated the effects from radiation and environmental exposure as seen in a typical LEO mission profile. While many, if not most, space missions in LEO have spacecraft on-orbit for years, due to budgetary concerns with this research project, exposures were only performed for an equivalent 6-month on orbit timeframe. This does not invalidate the research however. During the space system design process, it is necessary to simulate long mission times in reasonable ground times.

Because of this reason, it is necessary to perform accelerated testing. Previous work has shown that for some inorganic siloxane polymers, UV exposure effects were seen as early as 20 hours exposure. (Haffke 2002) On the mission planning side, militarily useful missions that would benefit from the lightweight structures enabled by this research, such as the NRO Colony program small satellites and Operationally Responsive Space (ORS) satellites, have planned lifetimes of 1 month to 1 year, so a 6-month test exposure is reasonable. This test sequence investigated both bulk material property changes and microstructure alterations occurring due to exposure regimes. Evaluation of the material will be made looking for changes in chemistry, surface structure, and mechanical performance.

Control samples in addition to chamber exposure samples were prepared for both geopolymer formulations. The AFRL/RX SCEPTRE space environment simulator facility was used for the UV and high energy particle exposure tests. The geopolymer was also exposed to atomic oxygen (AO) in a separate chamber than the UV and high energy particle exposure tests. Atomic Force Microscopy (AFM) was used to look at surface structures of the exposed and non-exposed samples. A nanoindenter at AFIT was used to document the changes in hardness and modulus as a function of surface depth to determine the extent of chemical reaction changes due to exposure. As part of the standard test series at AFRL/RX for UV exposure testing, spectrographs from the ultraviolet through infrared wavelengths were also recorded. Finally, x-ray photoelectron spectroscopy (XPS) was performed to determine chemical composition changes in the materials, pre- and post-exposure, for the AO specimens.

Assumptions

Materials used were consistent in reactant composition and purity. The commercial chemicals used were not significantly different among batches. Equipment used in the process of the research work was calibrated and precision maintained to applicable significant figures or statements of precision.

Expected Outcomes

In the three primary test series that have been identified as the basis of the doctoral work, the following results are expected:

- For the curing shrinkage objective, it is expected both temperature and pressure to have an effect on reducing the curing shrinkage. Curing shrinkage in cements and concretes have been identified as being caused by excessively rapid evaporation of water from the surface, and in fact many cement manufacturers have identified atmospheric conditions as major controlling agents when cracking from curing shrinkage occurs. (Graniterock 2009) Geopolymers are more similar to concretes and cements than organic polymer based plastics. It is postulated that by increasing pressure or temperature in this gas-evolving, exothermic reaction, the reaction rate will be slowing down consistent with elementary chemical reaction engineering and not allowing water to exit the material. This causes the polymer network to form around the water particles and physically resist the collapsing of the polymer network to minimize the voids in the polymer matrix. Since the primary control mechanism in this theory is to control the water release and subsequent diffusion out of the polymer matrix to equalize humidity levels, applying pressure to the surface will likely be more effective than temperature increase alone.

- Regarding the concerns about outgassing, the chemistry of the geopolymer reaction should exclude all evaporating species except for water, unless volatile organic components (VOC) are present due to contamination or lack or purity of the reactive species. Water outgassing might be a problem if enough water particles are trapped in the polymer matrix during curing. Surface water absorption will likely be the most significant outgassing source concern, although there is an additional worry that water re-absorption following a period of storage may result in undesirable mass gains.

- With respect to the question about space environment exposure, the intermolecular bond energies of the geopolymer constituents should be high enough to resist cleaving by all ultraviolet frequencies except for the highest energy UV photons. When these higher energy photons impact the geopolymer, they should be at fluence levels small enough to not cause massive changes. Chemical reactions as a result of high energy UV photon exposure should only be present at minimal surface depth penetrations. Atomic oxygen also should not be a concern since the Al-O-Si bonding provides theoretical protection against further oxidation of the Al or Si species. High energy charged particles impacting the surface may cause pitting of the surface that may sever polymer bonds and reduce the bulk material properties. It is expected that none of the space environmental effects will significantly negatively impact the bulk material performance, and any effects will be limited to superficial surface effects.

The experiment campaign as described was performed in fulfillment of the requirements to complete this research. The remainder of this document will capture the different aspects of the work. Chapter 2 is a literature review presenting the motivations for this work, and providing an extensive history of the past work on space qualification testing, geopolymers, and previous space missions dedicated to evaluating material performance in the space environment. Chapter 3 provides an in-depth explanation of the methodology behind the work accomplished for each of the three primary objectives comprising this research. Chapter 4 presents the results and analysis of the data collected during the experimental campaign. Chapter 5 summarizes the conclusions of the campaign and lays out the unique contributions to the scientific community as well as potential benefits resulting from this campaign.

II. Literature Review

Chapter Overview

The purpose of this chapter is to provide an overview of space optics, define the space environment as it applies to the work and describe the current state of geopolymer research in space and non-space applications.

Overview

Use of optics in space

Since space became "the ultimate high ground" in the 1960's with nations realizing the importance of placing optical systems on-orbit, telescope and optical design has undergone quantum leaps in improvements. Consequently, the terrestrial and aerial optical industries have benefited from these improvements once they hit the "civilian" world. Starting with switching from film to electro-optical systems, introduction of lens coatings to isolate specific wavelengths or bandwidths of light, computer aided optical design software, the use of lightweight materials in mirror building, and the employment innovative mechanical designs to lighten the loads on the mirrors themselves, the race has always been to try and improve one of three key metrics in satellite imaging design: spatial resolution, imaging area (specifically swath width & length), and spectral resolution. (Kishner 2006)

In order to improve the spatial resolution and swath width of imaging satellites operations, the primary restriction in optical hardware is the mirror size, specifically mirror diameter, and subsequently mirror mass. While simply building bigger mirrors may have been sufficient in the past, we are now approaching a point where additional mass on the mirror structure due to increases in mirror diameter is harming the overall design of the optical system by increasing dynamic loads during the launch stage and thermal stresses during heating/cooling cycles on orbit, not to mention increasing cost and complexity.

Issues with space optics

Mirror diameters are essentially limited by the size of the launch vehicle fairing. In order to get larger mirrors on-orbit than a launch vehicle fairing diameter will allow, the designer of the optical system must consider ways to fold a mirror or to segment a mirror that can then be unfurled or deployed on orbit. NASA's James Webb Space Telescope will employ a foldable mirror system on orbit to observe IR and X-ray wavelengths in deep space. (Stockman 2006) For low earth orbit (LEO), high-resolution, visible wavelength imaging satellites, thin film foldable mirrors have been proposed for this purpose; however, difficulties in maintaining the optical grade flatness on the mirror surface without a solid backing structure have been persistent.

A mirror's mass is limited by the ability to survive the tremendous forces placed upon the mirror structure by the rocket launch event. In both declassified national programs and current commercial high resolution imagery satellites, monolithic glass is the material of choice to produce large aperture mirrors that can survive the space environment. Glass is used because it can be easily formed into complex curvatures in order to accommodate different telescope designs, soft enough to be polished to a high finish rapidly and is relatively stable thermally due to chemical tailoring. Past research programs, like the Advanced Mirror System Demonstrator (AMSD), have incorporated new processing techniques to drive the mass of the ever increasing diameter mirrors to an areal density of around 15 kg/m^2. However, requirements for future imaging missions necessitate an even lower areal density with similar if not superior mechanical strength.

Materials chosen for imaging satellite applications must also be able to deal with the unique environment of low earth orbit. Solar emissions in the form of UV, X-ray, and gamma radiation and high energy particle streams, significant atomic oxygen concentration, a local environment that promotes the build-up of electrical charge, near vacuum pressures, and extreme temperature gradients are the most serious of the difficulties that spacecraft materials encounter. (Tribble 2003)

Spacecraft optical materials

In creating a hybrid composite mirror, the payload designer typically has to consider the compatibilities of the mirror substrate (backing structure), the reflecting surface, and the bonding agent (or adhesive) used to mate the substrate to reflecting surface. In this research campaign, we are concerned primarily with how the bulk material acts, not necessarily how the material affects a particular application. So for this purpose, differences in the qualification process between a structural component and an adhesive component are minimal when obtaining bulk material performance. The geopolymers proposed for use in this research can be used in either application, bonding a reflective surface to a mirror substrate while maintaining thermal expansion stability, or as the mirror substrate itself. Looking at space qualified adhesives used in contemporary imaging missions for a point of comparison, the current practice is to use organic based polymers, such as two part epoxies, or inorganic silicone based chemistries.

A comparison case: Silicone based adhesives

Some space qualified adhesives used in optical systems include some resin systems like polyimides, cyanate esters, silicone, epoxy, polyurethane and acrylic resins. Silicone based adhesives have some properties that make them more desirable to the aerospace engineer. Phenyl-based silicones can withstand the temperature extremes that are experienced in orbit and are able to maintain a good degree of flexibility at very low temperatures where other materials would stiffen and crack, as seen in Figure 2. (Monib 2003) The silicone shown in Figure 2 demonstrates that even at extreme temperatures of as low as -100 deg C, the material still has some displacement flexibility on the order of multiple microns. While this is not much, it does allow for some ability to withstand stress introduced by mismatched CTE materials when bonded to them.

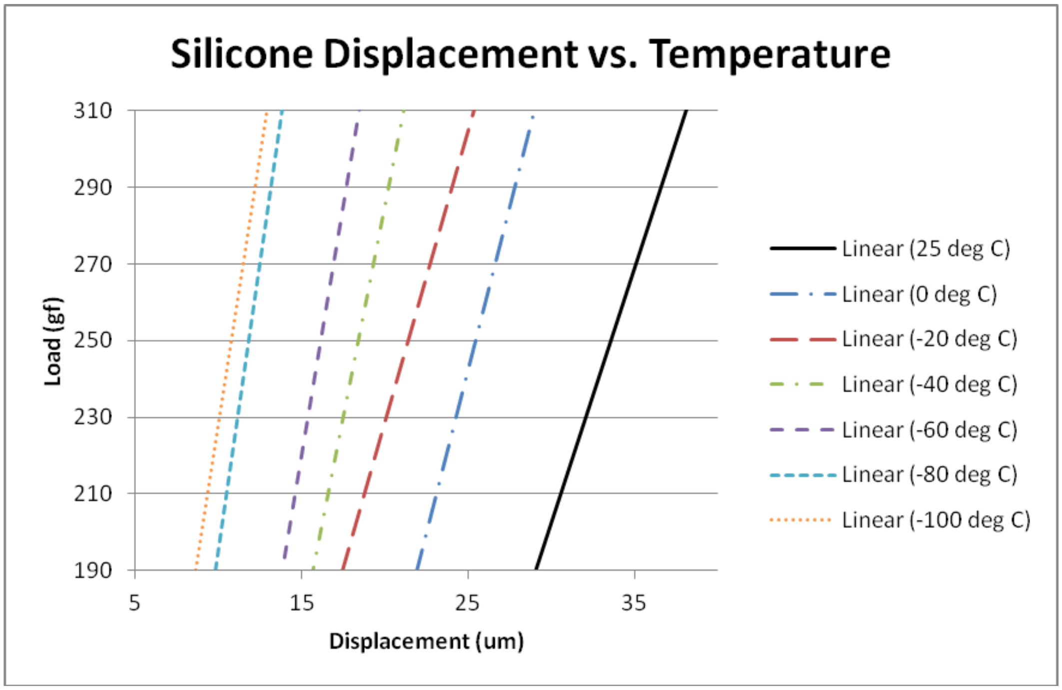

Figure 2. Silicone displacement at different temperatures (recreated from Monib 2003). The x-axis is displacement of the silicone after being subjected to gram-force loads (y-axis) in terrestrial surface gravity conditions.

The most significant drawback to silicone use in space applications has been outgassing. Untreated silicones generally contain volatile species that outgas and contaminate sensitive surfaces, such as optics. The already referenced test method ASTM E595 gives the maximum allowable amounts for a material to be considered as low outgassing. There are two components to this specification, the total mass loss (TML) and the Collected Volatile Condensable Materials (CVCM). TML is simply the amount of material given off during a 24 hour time period at 125 deg C and less than 5 x 10^{-5} torr. CVCM is the amount of volatiles that will condense on a collector plate controlled to 25 deg C. For aerospace applications, TML must be less than 1%, while CVCM must be less than 0.1%. Standard silicones can yield more than 5% TML and 1% CVCM. Specialty silicones employing optimized cure cycles have been able to achieve as low as 0.06% TML and 0.02% CVCM. (Gross 2002)

A typical silicone formulation for space applications is the Dow Corning 93-500 (DC 93-500) silicone based encapsulant. It is a proprietary 100% silicone resin content material used as an adhesive in spacecraft electronics bonding applications. It has TML of 0.25% and a CVCM of 0.05% after ASTM E-595 outgassing testing, both values within accepted NASA limits. It cures at room temperature after about 24 hours, but does have issues with UV exposure like most silicones. While utility after exposure to high energy radiation is relatively high—the material is usable in a bonding application after exposure to 200 megarads-- testing has shown that DC 93-500 degrades with respect to mechanical properties such as a reduction in Young's modulus. (Dever 2006)

Commercial literature abounds with examples of different silicone chemistries available for spacecraft usage. Silicones are popular due to the wide varieties of processing techniques that can a range of performance characteristics. Commercial manufacturers are able to produce special grades of silicones having brittle points below –101 deg C. (O'Neill 2002) With regard to assisting the mitigation of the launch environment, elastomeric properties of silicones dampen primary launch vibration modes. Silicone is also used as an adhesive to bond materials that have different CTE values, since when two bonded surfaces experience the dramatic temperature changes encountered during spaceflight one surface will contract or expand. In the case of electronic circuit boards that are bonded to metal heat sinks, stresses on the circuit board solder joints could cause failure in the joint and irreparably damage the electrical connection vital to that electronic components' function. Silicones can absorb that expansion or contraction without losing mechanical function.

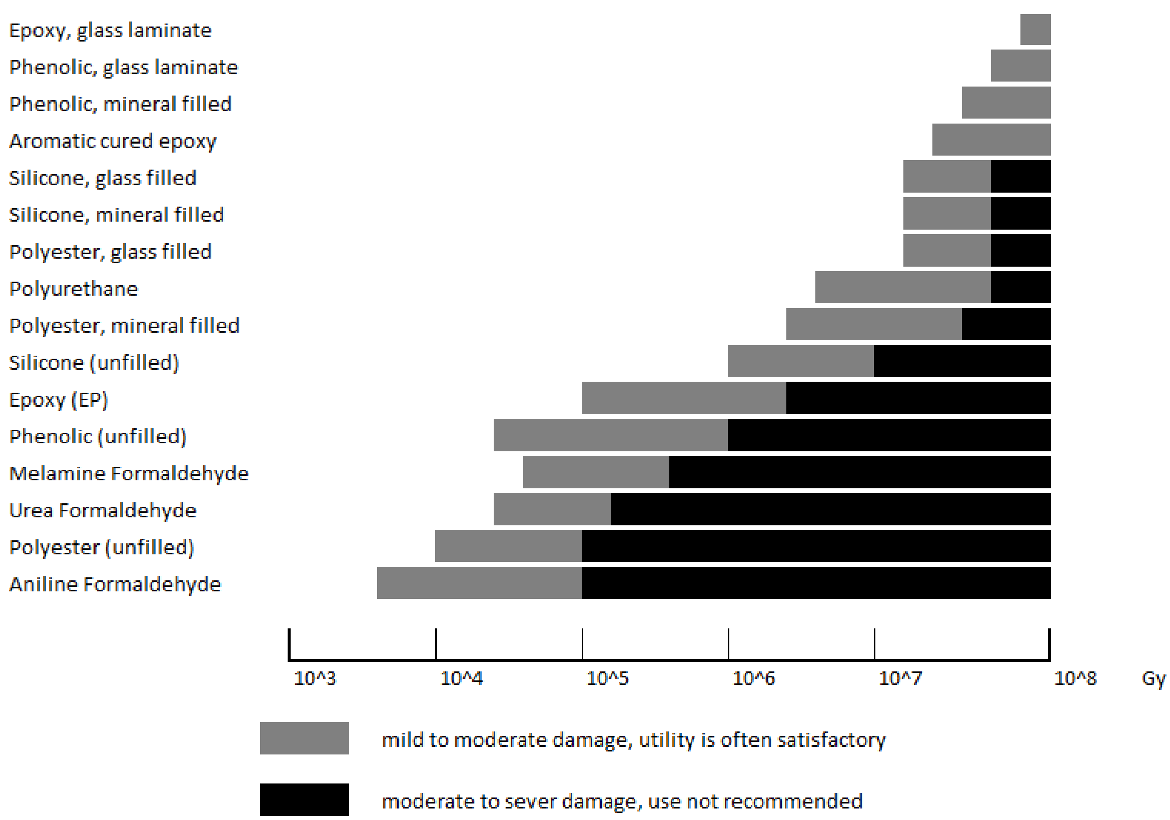

Figure 3. Radiation exposure limits of common polymers (recreated from Monib 2003). Radiation units on the x-axis are in Grays (Gy)

However, silicones do have significant problems with the space environment as a whole. Similar to organic polymers, silicone is susceptible to radiation exposure by UV photons and some high energy particles, breaking down the polymer bond chains, and causing changes in the properties of silicone rubber similar to those caused by heat aging in terrestrial applications. Some commercial specialty silicones are available that possess excellent resistance against radiation (see Figure 3) but are expensive. (Monib 2003)

In addition to photonic and particle radiation, atomic oxygen (AO) reacts with organic polymers causing erosion, which is a threat to material, and hence spacecraft durability. Nearly 90% of the atmosphere from 100 to 350 miles from the Earth's surface is comprised of AO. (Haener 2003) Silicone adhesives used on spacecraft would generally not be exposed to AO, as they would be sandwiched between two surfaces; however, if silicone was used as a structural material, this exposure issue would come to the forefront.

AFRL AMSD program

The Materials and Manufacturing Directorate, Air Force Research Laboratory at Wright-Patterson Air Force Base (AFRL/RX) is focusing on developing mirrors with reduced areal densities. In a spacecraft trade study, the mass savings from a lighter weight mirror can be used to either increase the mass available to other subsystems (like propulsion fuel carried) or reduce the total spacecraft mass (thereby reducing launch costs, requirements on attitude control actuators, etc). Instead of glass, composite materials (metals, ceramics, polymers, or combinations), foams, and hybrid / composite materials would form the basis of the structural substrate. Reflecting surfaces can be attached to these substrates in a number of ways to include direct thick film deposition techniques (cladding) followed by grinding, polishing, and reflective coating application, or by adhesion of a replicated reflecting foil or nano-laminate. Recent work at AFRL/RX using this replication approach has made possible small flat mirrors with areal densities less than 7 kg/m^2, a 50% reduction over the currently best available lightweight glass substrates. (Matson 2008) The composite materials being developed allow for a tailorable CTE and modulus, have low densities, and show high specific strength, stiffness and toughness.

Geopolymer background

According to the Dictionary of Composite Materials Technology, (Lee 1989) a geopolymer is defined as:

"A family of refractory ceramics used for composite matrices that can be fabricated at low temperature that are prepared from an aluminosilicate oxide precursor (Si2O5·Al2O2)n…. In an exothermic poly-condensation reaction below 100°C a three-dimensional macromolecular structure is formed from the above precursor and alkali polysilicates to form polymeric Si-O-Al bonds".

Geopolymers and geopolymer composites are a relatively newly defined class of ceramic materials whose intrinsic properties and potential applications are still relatively under-explored, although evidence of the human knowledge of geopolymers can be traced to

Ancient Egypt. Pure geopolymers are rigid, inorganic, aluminosilicate, hydrated gels, charge balanced by the presence of Group I cations such as Na^{+1}, K^{+1}, or Cs^{+1}. They have a range of compositions but are totally inorganic. Geopolymers are acid resistant, thermal shock resistant and are refractory adhesives. Upon heating, these refractory adhesives become even stronger as the gel converts to a ceramic of corresponding starting composition. The intrinsic microstructure is nano-porous (~3.4 nm radius) and nano-particulate (= 5 nm in size), and the porosity constitutes ~40 % by volume of the material. The porosity can be modified and enhanced by choice of Na^+ or K^+ charge balancing cations, addition of aluminum (Al) nano-particles, curing with hydrogen peroxide (H_2O_2), addition of micron sized hollow spheres of graphite or glass, alumina (Al_2O_3), silica (SiO_2), or organics (e.g. polyethylene). (Mah 2005)

Basic Chemistry of Geopolymer Reaction

In a basic sense, the geopolymer reaction is a typical polymeric reaction instead substituting mineral functional groups for carbon based functional groups. Davidovits in his fundamental work on the topic has identified the primary mers in the geopolymer reactions.

–Si–O–Si–O– siloxo, poly(siloxo)
–Si–O–Al–O– sialate, poly(sialate)
–Si–O–Al–O–Si–O– sialate–siloxo, poly(sialate–siloxo)
–Si–O–Al–O–Si–O–Si–O– sialate–disiloxo, poly(sialate–disiloxo)
–P–O–P–O– phosphate, poly(phosphate)
–P–O–Si–O–P–O– phospho–siloxo, poly(phospho–siloxo)
–P–O–Si–O–Al–O–P–O– phospho–sialate, poly(phospho–sialate)
–(R)–Si–O–Si–O–(R) organo–siloxo, poly–silicone

Figure 4. Common geopolymer oligomers (Davidovits 2008)

In the geopolymer reactions, the mineral base (Al, Si, or Al & Si) which forms the primary constituent of the oligomer is combined with an aqueous hydroxide solution, typically potassium hydroxide (KOH) or sodium hydroxide (NaOH). Silicate solution (SiO2) can be added to the solution to provide additional Si-O groupings to improve cross linking in the final polymer matrix. (Xu 2000)

Using Davidovits' text book as a reference for the drawings below, the chemical mechanisms for a generic geopolymer can be shown. In this example, NaOH is used as the polymerization triggering agent.

Step 1: The Al double bonded to the oxygen has the double bond broken by the OH anion. The open oxygen then strips off a hydrogen atom from the water molecule to form a

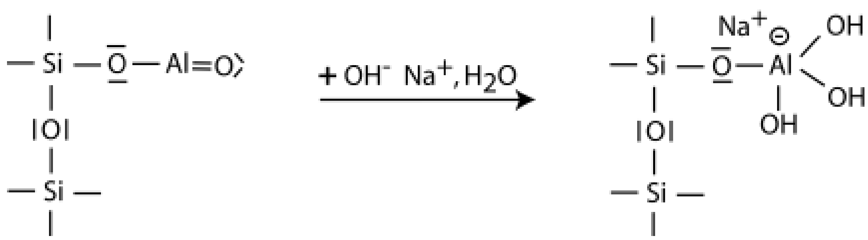

(1)

second OH, and the resulting third OH group then bonds covalently to the Al atom causing the Al atom to concentrate the negative charge. The Na cation in solution then stays in ionic proximity to the Al negative grouping for charge balance.

Step 2: More OH anions in solution proceed to bond to the Si forming a pentahedron with a net negative charge,

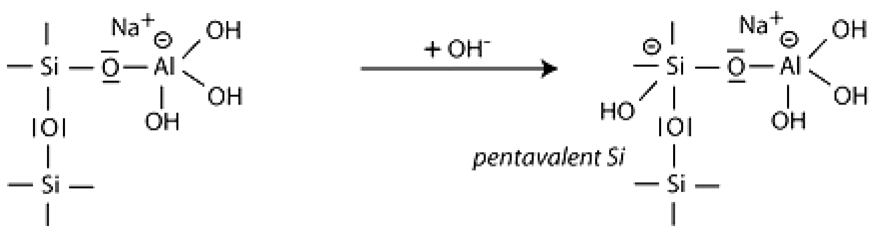

(2)

Step 3: A hydroxide shift occurs cleaving the secondary Si group of from the main chain.

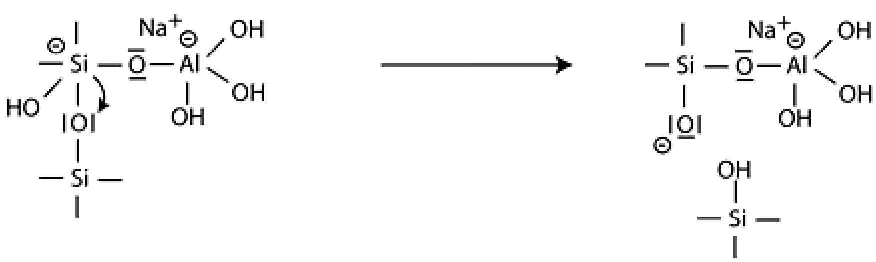

(3)

Step 4: More OH anions in solution continue to replace the bonds from Si to other constituents leaving a negatively charged oligomer, the base unit of polymerization for the geopolymer reaction. The base unit is called the ortho-siolate oligomer.

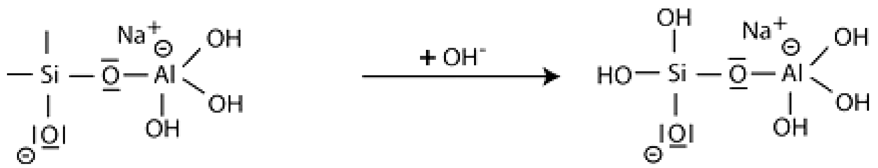

(4)

Step 5: The negatively charged siloxo grouping gains a Na cation in ionic bonding to balance charge and create the terminal bond for the polymerization.

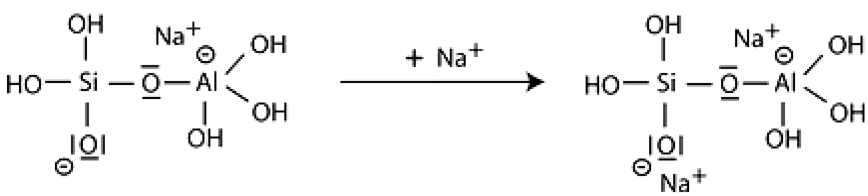

(5)

Step 6: Now the polymerization chain reactions occur as condensation reactions between the single oxygen bonded to the Si molecule reacts with OH groups attached to the Al in the oligomer. This now forms the fundamental Al-O-Si bond prevalent in geopolymers. Water molecules are liberated as a result of the polymerization reaction. In the graphic below, a cyclic polymer is formed, but chains can be formed as well. As the polymerization continues, NaOH in solution is regenerated until all the OH groups are used up in the polymerization reactions.

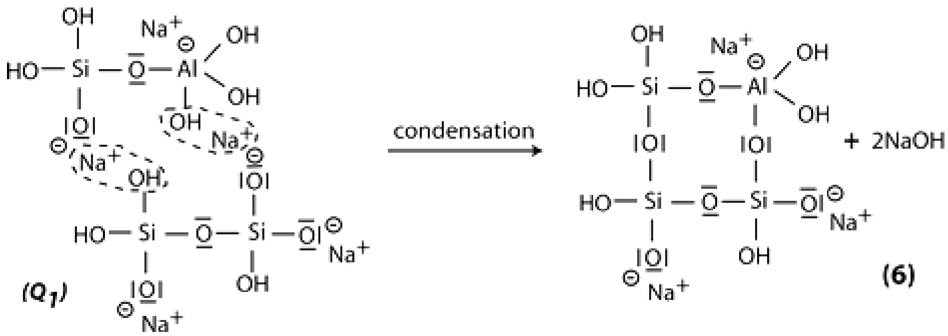

Step 7: The polymerization chain reactions continue until all the OH anions are used up. The Na cations form ionic bonds with the negatively charged Al atoms in the polymer matrix. As you can see by the diagram below, the geopolymers can grow in both linear and 3-D fashion. It is the 3-D growth in which the liberated water molecules from condensation reactions get “trapped” in the polymer matrix.

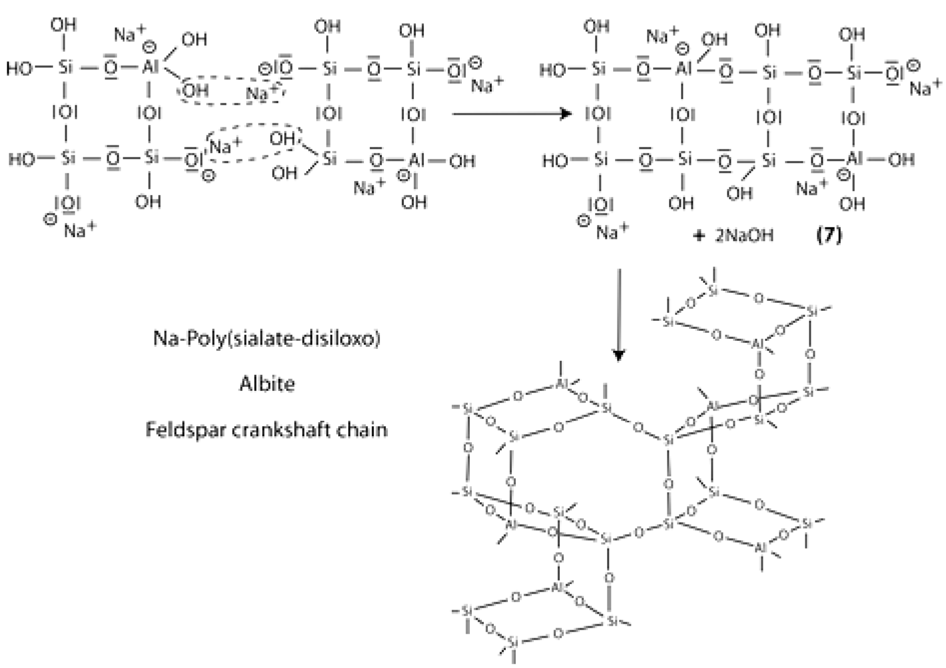

Since the Si and Al atoms form covalent bonds with the oxygen atoms and not ionic bonds in a crystal structure, the bond strength of the molecule is much stronger than what would be expected utilizing crystalline structure of solids theory. The only ionic bond in the material is with the Na cations which are highly attracted to the siolate anion at the Al atom negative charge locale. This covalent model is the explanation for the geopolymer exceptional bulk material strength.

The chemical kinetics of geopolymerization can be characterized by anionic polymerization rate equations. Specifics of the rate law will require the individual reaction to be defined in terms of the stoichiometry of the anion initiated activation reaction to determine the reaction order. Alternatively, geopolymerization reactions can be modeled as condensation reactions since that is the primary chemistry mechanism occurring in the individual polymerization reactions. Specific geopolymer formulation kinetics work has been performed by De Silva (2007) and Provis (2005) and would direct the reader there for an in-depth discussion of the issue.

Geopolymer characteristics

Davidovits performed much of the initial characterization of modern geopolymers. The great potential in developing these materials has been the ability to synthesize the geopolymer at low temperatures. As such, the cost has been reduced and the flexibility in application has been increased. The ability to cast and cure a ceramic system near room temperature could result in great advantages in fabrication structures.

The two geopolymers being investigated in this study are an illite based geopolymer and a metakaolin based geopolymer. Both are made from commercially available base materials. Illite is a potassium alumino-silicate. The commercial form used in this study does have trace amounts of Ca as well due to the mineral source used by the manufacturer. Classically, illite's chemical formula is given as

$$(K,H_3O)(Al,Mg,Fe)_2(Si,Al)_4O_{10}[(OH)_2,(H_2O)]$$

but most references identify that illite has considerable cation substitution. (Gualtieri 2000) The illite geopolymer trigger solution for this study is a sodium silicate solution with some cation substitution. Metakaolin is a processed form of the kaolinite mineral. The classical chemical formula for kaolinite is

$$Al_2Si_2O_5(OH)_4$$

To process kaolinite to metakaolin, endothermic dehydroxylation (i.e., dehydration) is performed by raising the temperature of the kaolinite to as high as 550-600 deg C to produce disordered metakaolin, $Al_2Si_2O_7$. (Bellotto 2005) The trigger solution for metakaolin geopolymers is a sodium silicate solution with some cation substitution.

Current Geopolymer Uses

According to a paper presented by Davidovits in 2002, geopolymers have been utilized in a number of fields and can be separated by their polymeric character, meaning the 3-dimensional polymer network. There are two ends of the spectrum for geopolymer character: 2-D crosslink geopolymers which have a similar structure to graphite where the polymer forms in "sheets" with minimal cross linking between layers; and 3-D network geopolymers which form more like glass with complex interlocking 3-dimensional matrices. This can also be sorted by their Si:Al ratio in the core mer of the geopolymer—high Si:Al ratios are more 2-D in structure while low Si:Al ratios are more 3-D in structure. Both illite and metakaolin used in this work, based on their chemical formulas, are at lower Si:Al ratios suggesting they are more 3-D in structure.

The primary commercial applications for geopolymers up to this point are in the production of so-called "green cements" which are environmentally friendlier to produce than the traditional Portland cement, and as coatings for fire resistant materials. Since geopolymers have an easy application process and a low toxicity, as well as the fire retardant properties of base ceramics, this is projected to be an application with healthy growth in the next decade. (Davidovits 2002) Geopolymers are also being investigated as a casing material for radioactive materials, being proven to have excellent resistance to nuclear waste radiation effects. (van Jaarsveld 1997)

Geopolymer processing

Geopolymers are usually made by mixing a powder with a basic solution (although water can be used in some cases), forming a paste which is poured into a mold or applied on to a metal, glass or ceramic surface. Typically, geopolymers are cured at room temperature and pressure although it is suspected that the mechanical properties are influenced by water content in the geopolymer matrix and as such, different curing processes have been investigated. (Duxson 2005)

Because of the simple preparation of geopolymer material, complex shapes (such as parabolic solids) can be made by pouring the uncured material over a mold. Additionally, geopolymers have an adhesive quality, shown to be able to bond to a wide variety of materials including 1018 steel, 6061 aluminum, alumina, and borosilicate glass. (Bell 2005) However, at times significant bonding enhancement agents are needed to improve the tackiness and overall adhesion strength of geopolymer based adhesives.

When curing, geopolymers exhibit a color change associated with the creation of water particles and hydrate formation. Researchers at Rutgers University funded by the New Jersey Department of Transportation had previously characterized the curing color changes of geopolymers. (Balaguru 2008)

Geopolymer Optics: Advantages

Geopolymers have intrinsic properties that make them interesting as a possible solution to the space optics problem as described above. Since they can be cast into almost any shape in the uncured state, mirror designs of essentially any curvature or shape can be made without expensive grinding or polishing techniques, in almost any quantity. Since geopolymers can also be made into an adhesive, ultra-lightweight materials (like foams) could be used as the optic structure with geopolymer acting as the bonding agent between structure and reflecting surface without the high temperature cure processes used in many space qualified adhesive epoxies. Work by Papakonstantinou, et al has shown that geopolymers have significant strength retention at high temperatures, even though they are cured at such a low temperature compared to other materials with similar retention. (Papakonstantinou 2001)

Geopolymers are also advantageous from a densities point of view. As shown in Table 3, while geopolymers are approximately as dense as polycarbonate, they have similar specific strength performance properties to currently used materials, making them ideal for optical applications. This high specific strength, low density property is suitable for spacecraft applications as well where mass is at a premium to the designer.

Table 3. Densities of optical materials (Matweb 2012)

Material	Density (kg/m^3)
Cured geopolymer	~ 1500
Borosilicate glass	2440
Silicon carbide	3217
Polycarbonate	1300

Geopolymer CTE tailorability is a huge potential benefit as discussed previously. AFRL/RX has done initial investigations into tailoring CTE of organic polymers with the addition of zero or negative CTE valued nanostructured materials such as carbon nanotube fibers and nano-sized zirconium tungstate with great results. (Matson 2003) The concept of this is shown in Figure 5. The red arrows are the thermal expansion of the polymer while the yellow arrows indicate thermal shrinkage from negative CTE additive materials.

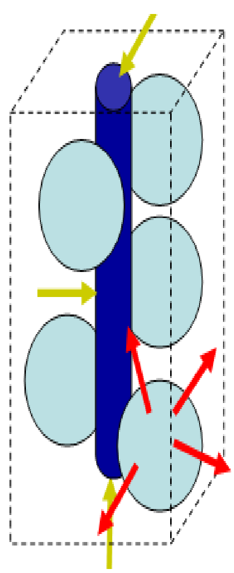

Figure 5. Graphic showing concept of CTE tailoring

The theory is that the producer does not try to radically change the CTE of the expanding material, but to affect the bulk properties of the materials by offsetting the expansion of the higher CTE material with the contraction of the negative CTE material. The positive CTE material, represented by the light blue spheres, is expanding when exposed to heat. The negative CTE material represented by the dark blue rod is contracting. The overall "unit cell" either stays the same or decreases depending on the ratio of the two materials and their relative CTE values.

There is a limit to the benefit of this approach however in that as you add more negative CTE material you begin to alter other bulk properties of the mixture farther away from the baseline material you desired. This is where the geopolymer is an excellent fit since it already has a low CTE value and would not require addition of negative CTE materials in quantities enough to significantly change other bulk geopolymer properties.

A second approach to tailoring CTE and shrinkage of a bulk material tried by AFRL/RX is to introduce glass microballoons with near zero CTE. The theory is that the glass microballoons will form the majority of the volumetric structure with the geopolymer acting as an adhesive between the balloons. When the geopolymer is cured, it can only shrink until the glass microballoons touch. At this point, if the geopolymer needs to shrink more it can only do it in the void space between the balloons, while the bulk material stays volumetrically stable. The shrinkage and CTE are then controlled by the amount of microballoons that form the syntactic foam. This has the advantage of not affecting the chemistry of the geopolymer, but you also lose some of the rheological advantages of the pure geopolymer. (Matson & Mollenhauer 2003)

Geopolymer Uncertainties

Geopolymers have been subjected to a number of characterization tests for terrestrial applications, most notably Kriven, et al. at the University of Illinois. (Kriven 2009) However up to this point, the question of using geopolymers in space applications have focused on if they can be *built* into applications needed in the spacecraft, not if the bulk material *would perform* in the space environment. Inorganic polymers such as geopolymers have, as one of the products of the polymerization reaction, free water molecules that are typically trapped in the voids of the polymer matrix. Since geopolymers also tend to have large molecular surface areas with available Van der Waals bonding sites, they tend to be hydrogopic as well. As will be seen in Chapter III, qualifying hydrogopic materials for the space environment presents unique challenges.

Space Environment

It is important to define what the general characteristics of the "space environment" are. The "space environment" can be considered unique due to the presence of three characteristics: vacuum, large thermal variations and a specific radiation exposure regime different from the surface of the Earth. There are other conditions which also contribute to the uniqueness of the space environment and these will also be discussed. While there is some debate as to where "space" begins, the commonly understood "Karman line" at 100 km altitude, named after Theodore von Karman, is a good reference and as such will be used a reference point for delineating between "space" and "terrestrial atmosphere". (Cordoba 2004)

Vacuum

One of defining and best understood characteristics of the space environment is that "outer" space is a near vacuum. Space is, on average, a vacuum because there is so much nearly empty void between galaxies, stars, and planets. All of the mass of the universe is

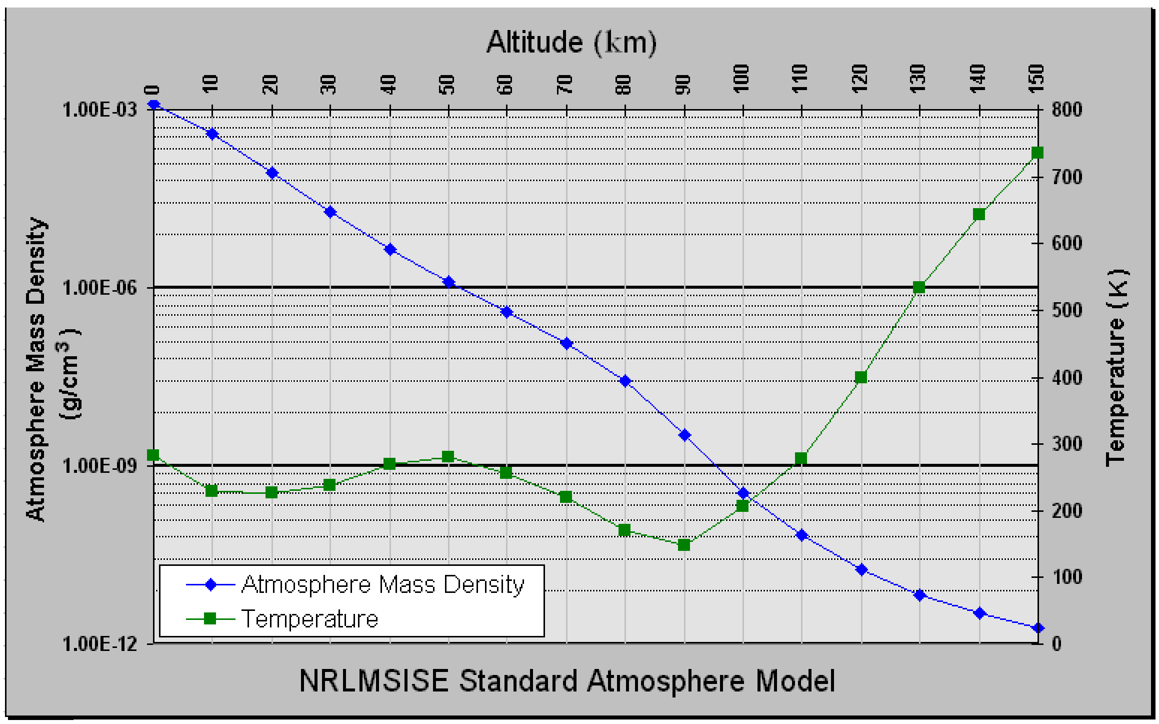

Figure 6. Atmospheric properties as a function of altitude, Naval Research Laboratory Standard Atmosphere Model (Picone 2003)

caught up in stars (which make up galaxies) and planets. In between are vast, almost unimaginable distances, where there is nothing but a few hydrogen atoms (thus virtually a vacuum) every cubic meter. As can be seen by this graph (see Figure 6) from the Naval Research Laboratory standard atmospheric model, at the transitional altitude of 100 km, the atmospheric mass density of the local environment is less than $1x10^{-9}$ g/cm^3 and begins to flatten out. (Picone 2003)

In pressure terms, 100 km altitude corresponds to an average pressure of less than 0.03 Pa. (US Standard Atmosphere 1976) Ultimately, geostationary orbit altitude (~36000 km) space settles at an estimated pressure of 3.0E-9 Pa.

This environment is a danger on materials as sublimation is a common vapor release mechanism. These vapor species can either re-attach to other spacecraft surfaces creating a coating (possibly disastrous in the case of optical surfaces or electrically conductive materials), or simply releasing to the general local environment causing structural defects in the original material that ages or weakens the original material’s strength. If the vaporization is massive and directional, a thrust force can be imparted on the spacecraft. Additionally, if the total mass loss is great enough, the center of mass of the spacecraft can drift to a significantly different location, causing complications in attitude control of the spacecraft.

The outgassing problem

All spacecraft launched from Earth will outgas a little due to atmospheric water vapor that has attached to the spacecraft exterior during shipping and the launch preparation cycle. Most launch locations in the US and worldwide are located in coastal climates with high humidity and a spacecraft will wait typically months at a launch location in preparation for launch operations. Organic polymers are particularly susceptible to bulk outgassing as the volatile chemicals used in the formulation and present during and after the curing process typically are easy to evaporate or sublimate in a vacuum, not to mention upon application of heating due to exposure to the sun while in orbit.

Thermal

The thermal environment is dramatically different than terrestrial environs, because of the near vacuum nature of space as described above. In the relatively molecularly dense regions of Earth's near surface atmosphere, the air particles and natural wind movements provide an effective heating / cooling mechanism in the form of convective heat transfer in addition to the conductive and radiative heat transfer mechanisms. This allows material used in terrestrial applications to normally not exceed a 10 deg C difference in a 24 hour period unless the application drives a large exothermic or endothermic action. Even over the course of a year in the upper latitudinal regions with significant human populations, the temperature extremes of application materials may range from near 0 deg C in dead of winter to 20-30 deg C in the heat of summer buffered by the layers of thick atmospheric air.

However in space, the local gas environment is not dense enough to sustain meaningful convective heat transfer, and as such, the only heat transfer mechanisms available to a spacecraft component are conduction and radiation. As deep space is a near absolute zero background, radiative transfer is very effective at sinking heat off a spacecraft provided the tremendous heating source of the sun is not present (i.e. eclipse conditions). So, as the spacecraft goes from a near absolute zero heat sink background to a high power heating source such as the sun, in a span as short as 90 minutes for a LEO mission, a spacecraft typically has to account for a significant change in heat loading.

Empirical evidence has determined that a good temperature regime to test against while designing and integrating a spacecraft is dependent on whether it is an external or internal component. For external components, such as solar arrays and antennas, operational temperatures can range from -150 to 110 deg C. For internal components, the ranges are much smaller and can vary wildly depending on if it is a component that has a large heat load (like transmitters or batteries) or low heat load (like internal base plates or passive sensors). For large heat load components, typical operational temperatures are tight, such as 0 to 15 deg from some battery boxes. For low heat load components, an expanded operational temperature profile is seen, with -10 to 40 deg C being not out of the ordinary. (Gilmore 2004) The spacecraft designer has to take this all into consideration when designing the thermal design requirements and test regime.

Atomic oxygen

Another unique aspect of the space environment is the presence of chemical constituents not found in normal terrestrial environments. One component of particular danger to the spacecraft that has to be accounted for in material selection choice is that of atomic oxygen (AO). Created by the fissure of O_2 molecules by solar radiation and sustained in the bulk charge neutral ionosphere region, AO is the predominant atmospheric species from 200 to 600 km. (Hedin 1986)

AO is highly reactive, and LEO AO can not only erode the external surfaces of polymers on spacecraft, but can cause degradation to internal spacecraft surfaces where openings to the local environment exist. The large flux of AO can produce serious erosion of surfaces through oxidation. Thermal cycling of surfaces, which go in and out of the earth's shadow frequently in this orbit, can remove the oxidized layer from the surface. Some surfaces respond differently by having their surface structure dramatically altered and hence the heat transfer properties, which are important for spacecraft thermal control, are changed. Experiments by NASA have identified that materials on the ram direction of the spacecraft (forward velocity vector) are those predominantly affected. (Banks 2003)

AO has a number density and ram impact energy between the altitudes of 180 km and 650 km that is sufficient to pose a threat to the long term durability of solar arrays and other material surfaces being considered for use on the Space Station. (Banks and Rutledge 1988) Typical AO number densities in LEO (~250 km) are about 109 atoms/cm^3. This is approximately equal to the density of residual gas in a vacuum of 10^{-7} torr. However, due to the high orbital velocity (approximately 8 km/s), the flux is high, being of the order of 1015 atoms/cm^2*sec. The effect of this exposure is seen when examining the surface erosion and mass loss. In addition, AO exposed materials exhibit a significantly altered surface morphology with needle-like peaks having vertical walls. (Visentine 1988)

Radiation

The near vacuum environment in space also allows another unique characteristic of the space environment to threaten spacecraft materials-- radiation exposure. Materials in terrestrial environments are buffeted from significant levels of UV and high energy particle (proton and electron) bombardment through absorption of these radiation forms by atmospheric constituents. Unprotected from layers of thick gas, spacecraft materials are attacked by these radiation components that cause molecular bond breakdowns and in some cases atomic dissociation. Research as early as the 1970's identified six primary sources of external radiation to spacecraft: geomagnetically trapped radiation belts (like the van Allen belts), solar flares, solar wind, solar electromagnetic radiation (typical of an emitting blackbody), galactic cosmic rays, and auroral radiation released from the interaction of charged particles re-entering the Earth's atmosphere through the magnetic poles. (Tribble 2004) The three predominant radiation concerns in LEO from a material degradation perspective are almost all solar originating: UV, high energy proton and high energy electron.

The sun produces a wide spectrum of photons, nearly in accordance with a blackbody emanation. UV radiation from about 250-400 nm wavelengths can cause photo-dissociation and photo-transformation of molecular bonds below that energy threshold. A typical broadband source of UV radiation for ground testing purposes is considered to be 185-400 nm. Research has shown that UV radiation in the 185-200 nm bands is more effective in causing spacecraft material degradation than the 140-185 nm bands. (Dever 2006)

The effect of UV irradiation on organic polymers is well studied. (Decker 1984) Typical reactions that occur with organic polymers exposed to UV radiation are cross linking and chain scission. Cross linking increases Young's Modulus, impedes viscous flow when in a liquid phase, decreases elongation of the solid, increases hardness of the bulk material, and leads to embrittlement of the bulk material over time. Chain scission results in a decrease in Young's Modulus, reduced yield stress for plastic flow, increased elongation, decreased hardness, and decreased elasticity. The reactions are keyed by the presence of oxygen bonds that are severed by the irradiation and this leads to the formation of free radical oxygen at the end of a polymer chain that is available for further reactions. (“Nuclear & Space” 1970) The main visible sign of UV irradiation effects on organic polymers is a chalky appearance, and a color shift of the surface. There is also typically a noticeable increase in brittleness of the surface, but examination of some commercial thermoplastics showed that under conditions similar to long term LEO exposure, the degradation effects didn't penetrate deeper than 0.5 mm in depth of the sample disk. (Zeus 2006)

Exposure levels for UV differ according to altitude, orbit inclination, and orbit phasing. One JAXA study estimated that the International Space Station received about 3.5×10^4 J/cm^2 in a 6-month period of UV radiation in the 250-400 nm bands. (Nakamura 2006) For a test sequence, previous work has varied in exposure simulation time (equivalent solar hours, ESH) from 1000 ESH at NASA Glenn to 3200 ESH by Aerospace Corporation simulating a 5-yr LEO mission. The Aerospace Corporation research group identified that UV degradation effects stabilize after about 5000 ESH, but measurable effects are seen much earlier, around 3000 ESH. (Meshishnek 2001)

The Apollo 11 mission's Lunar Surface Experiments Packages determined that more than 95% of the particles in the solar wind are electrons and protons, in approximately equal numbers. (Lunar 2009) While most of the interest in proton and electron bombardment in space focuses on biological system effects, there is a concern with polymer damage because of the intricate molecular linking structure similar to many biological compounds. When a high energy-proton or electron collides with an atom, it causes the ejection of an electron from the outer layer of the atom in the case of the proton collision, or the negative ionization of the atom in the case of the electron collision. These now ionized species can react quickly with other nearby species and liberate from their bulk material. High energy particle exposure levels have been documented well over time.

NASA has published general exposure levels for a multitude of radiation sources at different altitudes. For LEO altitudes, one can expect electrons at an energy level of < 0.5 MeV to have a flux of 2×10^7 particles/cm^2sec and protons at an energy level of < 1 MeV to have a flux of 5×10^5.

Space environment effects on materials

There has been an extensive effort by NASA, ESA, JAXA, and both Soviet and Russian space agencies to study the effects of the space environment on materials. Multiple dedicated missions and experiment packages have been flown on unmanned as well as manned spacecraft. The Russians in particular were probably the first space agency to dedicate long term orbital research facilities to studying space environment effects on materials during the Mir space station lifetime. Two notable contemporary missions dedicated to materials science and spacecraft engineering are the NASA Long Duration Exposure Facility (LDEF) and the NASA Materials International Space Station Experiment (MISSE).

The LDEF was an unmanned spacecraft launched in 1984 off of the Space Shuttle Challenger and had a nearly 6 year lifetime in orbit before retrieval by Space Shuttle Columbia in 1990. The entire satellite was returned to Earth for analysis. Flying an approximately 480 km circular orbit at 28 deg inclination, LDEF was NASA's first attempt at doing dedicated long term spacecraft component testing in orbit. Fifty-seven science and technology experiments from nine different nations flew on the LDEF mission testing a variety of spacecraft technologies. Notably for this study, LDEF carried about 10,000 individual material samples for space environment suitability testing. Some specimens were exposed to the space environment on the outer surface of LDEF, while others were positioned internally, shielded, or had time-controlled exposure doors. (NASA Langley 2009) A 9700-kg, school bus sized satellite, LDEF was a tremendous achievement in material science & satellite engineering.

Due to the extremely long duration of the experiment some thin organic polymer films and thermal blanket materials were essentially destroyed and disintegrated into small debris pieces which collected on adjacent spacecraft surfaces. A low-density debris cloud from these particles was created in LDEF's wake. Of particular note was that severe darkening of interior vent paths was noticed and attributed to UV exposure of polymer linings used. (Pippin 1995) Even that notwithstanding, the LDEF is remarkable in that the LDEF data depository is the best single database for understanding space environmental effects and has resulted in several volumes of published data. (Dooling 1999)

The MISSE set of experiments are a direct descendent of the LDEF heritage and the Mir Environmental Effects Payloads (MEEP) that were attached for over a year to the Mir Docking Module of the space station Mir between shuttle flights STS-76 and STS-86 (1996-1997). Utilizing the long term nature of the ISS, the MISSE units (see Figure 7) are approximately 1 square meter trays that are mounted to the exterior of the ISS for between 0.5 – 2 years and contain at least 400 sample containers of material coupons or small components that are exposed to all the major factors of the LEO space environment. (NASA MISSE 2009)

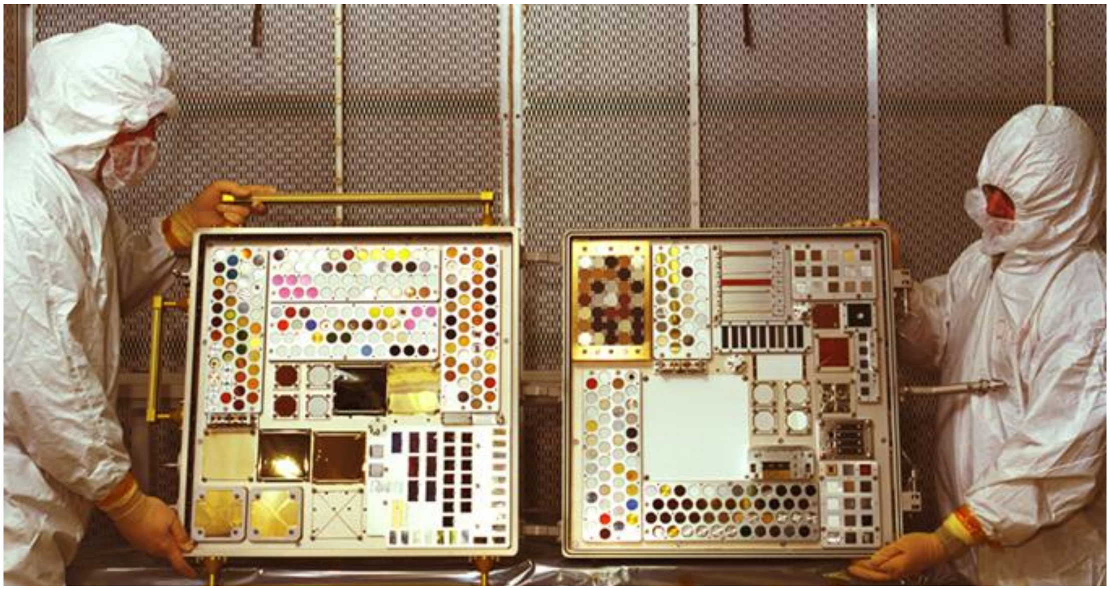

Figure 7. Photo of MISSE-1 pre-flight

There have been seven MISSE missions up to this point, with MISSE-8 on orbit from 2011-2013. Once the MISSE equipment is installed on the ISS exterior, the trays are photographed whenever the astronauts are near it on a spacewalk. At mission completion, the astronauts collect the experiment trays for packaging in the Space Shuttle or Soyuz capsule, the trays are returned to NASA Langley Research Center, and the samples returned to the preparer. Of note, MISSE-7 (2009-2011) carried samples of the geopolymers being investigated in this study, but have not been released for analysis in time for comparison as part of this research project.

A common failure mechanism for organic polymers in orbit is the breakdown of the polymer matrix caused by exposure to UV radiation on orbit. While this phenomenon is also experienced on the surface of the Earth, it is especially troublesome in orbit where the protective UV absorption of the terrestrial atmosphere is not present. As UV rays tend to increase cross linking in these types of polymers, their bombardment of spacecraft adhesives based on organic polymer chemistry can become “over cross-linked” and brittle. (Boboev 1969) The increasing brittleness of the polymer adhesive then becomes a danger if thermal expansion/contraction effects are increased due to a loss of flexibility as a result of increasing brittleness. The polymer can fracture or lose structural integrity causing a spacecraft failure. (Grossman 2003) The effect of ultraviolet radiation on spacecraft materials in orbit has been likened to heat aging in terrestrial applications.

The mechanism of UV absorption by the polymer molecule and subsequent breakdown is due to the fact that with organic polymers, the primary bond energies between the common carbon – carbon (C-C), carbon-oxygen (C-O), and carbon-nitrogen (C-N) bonds is below the energy threshold of typical ultraviolet-A (UVA), -B (UVB), and -C (UVC) photon, instigating a reaction where the photon disassociates the polymer bond, typically at the cross links.

Radiation in operational space orbits affects standard organic polymers in two ways: at lower energies (e.g. UV), cross linking increases. At higher energies, the organic polymers react by cleaving some of these C-C bonds and affecting the overall strength of the polymer. Si-O-Al bonds in inorganic polymers have higher bond energies than C-C bond (511 kJ/mole and 460 kJ/mole for Al-O and Si-O, compared to 347 kJ/mole for C-C) and should be less susceptible to the cleaving of organic polymer chains seen in some spaceflight experiments. Table 4 below shows the bond energies for typical organic and non-organic bond components. (Sanderson 1976)

Table 4. Intermolecular bond energies for common polymer bonds with UV photon energies (Sanderson 1976)

Polymer bond	Bond Energy (kJ/mole)	Photon Wavelength	Photon energy (kJ/ mole photons)
C-C	347	400 nm (UV-A)	298
C-O	357	314 nm (UV-B)	381
C-N	305	280 nm (UV-C)	434
Al-O	511		
Si-O	460		

UV resistance of geopolymers has not been adequately studied under space-like conditions. The most significant research on UV exposure of geopolymers has been a State of New Jersey Department of Transportation study on the UV resilience of a geopolymer coating on a test strip of highway retainer wall. (Balaguru 2006) The results from this indicate that UV was not a factor in geopolymer degradation under ambient atmospheric conditions, but begs answers for other environmental conditions. Terrestrial UV exposure levels are radically lower than orbital exposure profiles due to absorption by the Earth’s atmosphere.

Geopolymers form their polymer matrices on the basis of higher energy bonds than organic polymer bonds, like aluminum-oxygen (Al-O) and silicon – oxygen (Si-O). Because of these higher bond energies, they should be able to resist the typical cleaving effect that UV radiation has on organic polymer bonds. In order to validate this assumption, a series of UV exposure tests for the geopolymer materials could be conducted. A common methodology to test the effect of UV exposure for organic polymers is to perform a hardness test, since the exposed surface of the polymer will be the area of greatest change. The breakdown of organic bonds in the polymer matrix causes the polymer to become brittle, and prematurely age. This changes the hardness of the surface and depending on the extent of UV photon penetration, the bulk material itself.

Research by the nuclear industry has shown geopolymers to be quite absorptive to radiation in the form of neutrons and gamma rays, but no characterization has been made yet specifically to levels and types of radiation seen in the space environment, such as high energy protons and electrons. (Snead 2005) Both species can cause erosion of an exposed material due to ionization of surfaces and then increased reactivity with ionospheric components.

AO has the possibility of inducing reactions at matrix bond locations and initiating chemical reactions to allow for the sublimination and erosion of the bulk material. The LDEF and MISSE experiments answered some questions on general material and polymer / AO interaction effects; most of the established literature knowledge of the actual space environment performance of organic polymers and other space qualified materials was established as a result of these two flight experiments. Since geopolymers are a relatively new class of materials with respect to being considered for spacecraft applications, the question of geopolymer with AO effects has not been dealt with empirically.

Summary of Background

This chapter presented background information on geopolymers and the space environment. Geopolymers were defined according to the base chemistry involved. Geopolymers are a promising material for space applications due to their high strength & low density, their low initial CTE, and the theoretical resistance to radiation environments. However, investigation is needed into the materials in their bulk state to assess their applicability in space optical systems due to potential interactions with harmful parts of the space environment. The components of the space environment that are likely the most troubling to geopolymers include the vacuum nature of outer space, the thermal environment, the radiation environment, and the atomic oxygen environment. All of these space environment components were defined and given context with regards to this research campaign. The existing literature on geopolymer applicability in a space environment shows that the studies on this topic are limited even though a number of terrestrial based studies have some applicability.

III. Methodology

Chapter Overview

The purpose of this chapter is to describe the experimental methodology used in this work.

The objective of the research performed here is a step forward in the direction toward making geopolymers space qualified. As defined in Chapter I, there are three objectives that need to be accomplished to determine whether geopolymers are suitable for space applications. In order to properly characterize geopolymers for use in the space environment, problems have to be overcome in the processing of the materials themselves, determining the response of these materials to basic space environment concerns such as outgassing, and more extreme space environmental concerns such as radiation and AO exposure.

Following the radiation and AO exposure testing, evaluation of the materials by comparing their behavior before and after exposure was completed. Referenced to a set of control samples, the illite and metakaolin samples exposed to UV, high energy particle, and AO sources were evaluated for surface feature changes (including differences in average surface roughness) and changes in structural properties (hardness, modulus) as a function of bulk material depth. Finally, the pre- and post-exposure samples were examined with XPS, a technique used to determine chemical composition of materials to see if significant alterations in bulk material chemistry had occurred as a result of the space environmental exposure.

Experimental Work

Formulation procedure

For the curing shrinkage tests, there were two formulations. The illite formulation was prepared in a 5:3 ratio of commercial powder to sodium silicate solution. The data sheet for the commercial illite material is listed in Appendix C. The metakaolin formulation was prepared in a 1:2 ratio of metakaolin powder to sodium silicate solution. The trigger solution was a mixture of 26.1% SiO_2, 23.9% NaOH, and 49.9% H_2O (percentages by weight). After each formulation, the materials were mixed together in a Thinky ARE-250 centrifugal mixer (see Figure 8) for 2 minutes at 2000 rpm. After that, the materials were transferred in their slurry form to a mold to cure. The illite mixture solidified beyond slurry manipulation after approximately 20 minutes. The metakaolin mixture initially solidified typically after 40-60 minutes. The curing conditions were specific to each objective—multiple curing conditions were used during the curing shrinkage testing in order find an optimal condition. After the optimal condition was determined, the rest of the test series specimens were cured in the same manner (for the outgassing and radiation / atomic oxygen exposure tests, this was with vacuum sealed bags providing pressure on the slurry in mold with an elevated local temperature of 60 deg C).

Figure 8. Thinky ARE-250 centrifugal mixer

Objective 1- Curing shrinkage testing

The purpose of Objective 1 is to identify and determine the key variable associated with minimizing curing shrinkage, quantify the amount of shrinkage, and then compare to other similar space qualified materials. All flowable materials either contract or expand when forming a network of bonds during the transition to a solid state. For polymers that require time and the right environmental conditions, this is typically a contraction and the term "curing shrinkage" is used to describe the phenomenon. (Pocius 2002) Geopolymers are no different than other flowable pre-cured polymers in that when the 3-D network of bonds begins to form, the structure of the geopolymer matrix begins to take shape and the volume of the bulk material reduces.

Initial estimates by AFRL/RX showed that geopolymer curing shrinkage for two selected geopolymers (illite and metakaolin) was a significant concern. The need to quantify the amount of curing shrinkage in a controlled manner and determine the key environmental variables that would control the shrinkage is a key problem in future geopolymer applications. This work was to perform a series of experiments where for each geopolymer, the temperature or pressure would be varied during the curing process and measurements would be taken before and after the curing process to quantify the shrinkage.

Description of experimental plan & test setup

The general approach was to prepare the geopolymers by mixing the solid powder and liquid reaction initiator chemicals to form the geopolymer paste, pour these samples into molds which had been dimensionally characterized before the testing began, allow the geopolymer to cure and then extract the solid samples for dimensional measurements. By using a linear dimension metric of height + length + width (mold shrinkage), this would allow us to take into account curing across all three dimensions, instead of just trying to monitor the reduction in cross sectional area.

Change in variable

Curing shrinkage is dependent on the two principally controllable environmental variables, temperature and pressure. Previous work suggested that adding compression force would be effective in controlling curing shrinkage. For this experiment, compression was introduced by using vacuum bagging of the samples after initial solidification was completed. The samples were prepared according to the procedure outlined above and each geopolymer formulation was subjected to one of the following test curing conditions:

- room temperature and ambient atmosphere
- vacuum bagged and left at room temperature (approx 23 deg C)
- vacuum bagged and placed in a 60 deg C oven
- vacuum bagged and placed in a -17 deg C freezer

Measurements taken before / after test

For each formulation, the mass of the material in the mold was recorded along with the ambient temperature of the curing chamber and the ambient pressure. Additionally, the dimensions of the internal mold cavity were recorded to the nearest 0.1 mm by hand dialed calipers. Following the cure cycle, the molds were re-weighed and the samples extracted and measured.

Objective 2- Outgassing testing

The purpose of Objective 2 is to characterize the performance of the geopolymers with respect to outgassing using a standard NASA accepted test procedure. If the materials do not pass the standards, then work needs to be performed to determine if there are alternative preparation procedures that can be utilized to qualify the materials under the NASA standard. If not, then the results need to be quantified and failure modes identified.

<u>Test requirements</u>

National space agencies around the world including NASA, the European Space Agency (ESA), Japan Aerospace Exploration Agency (JAXA), and Russian Federal Space Agency (Roscosmos) have realized the danger of high outgassing materials to spacecraft mission success and have established standards to test materials against levels of outgassing. NASA uses ASTM Standard E-595-07 for testing, and in general (but not all cases) uses a metric of < 1% Total Mass Loss (TML) to qualify a new material as being acceptable for the space environment from an outgassing point of view. TML is calculated by looking at the mass difference before the 125 deg C vacuum oven exposure and immediately after. Water Vapor Regained (WVR) is a measure of how much water vapor is reabsorbed by the material and compares the mass following the two humidity chamber treatments. Taking TML and subtracting WVR gives you a "Net Mass Loss" (NML) that tells you essentially how much mass of your tested material was lot during the vacuum exposure, excluding the water that was absorbed during the first humidity soak and then released during the outgassing.

Understanding the differences in TML, WVR, and NML is particularly important for hydrogopic materials, the class of materials that readily absorb atmospheric water. For hydrogopic materials, the classic TML standard indicates a huge mass loss and likely a failure in qualification, but in reality the majority of that mass loss during the vacuum exposure was the water absorbed before the vacuum exposure either in storage, or in the high humidity soak chamber used in ASTM E-595-07 before vacuum exposure. A NML of < 1% for hydrogopic materials can be acceptable for applications where the evolution of water vapor immediately upon entry to orbital atmosphere is not a large concern. Since geopolymers are hydrogopic materials, the TML, WVR, and NML issue becomes a concern that needs to be addressed.

Because of the hydrogopic nature, geopolymer qualification with regards to outgassing necessitated the use of NML versus TML for consideration of the materials worthiness. Essentially if the geopolymer polymer constituents outside of water vapor do not outgas and if the water loss is manageable (especially if surface water is the only water source pre-launch operations), then the geopolymer can qualify as a space qualified material even thought the < 1% TML standard would be violated. If the application of geopolymer in the spacecraft can reduce the susceptibility to water vapor absorption and short duration exposure (such as use as an adhesive bonding between two tightly fitting surfaces), then geopolymers should be an outgassing friendly material with none of the Collected Volatile Condensable Materials (CVCM) problems that are common with organic polymers.

Description of test setup & procedure

ASTM outgassing standard

The standard for outgassing tests is ASTM Standard E-595. This ASTM test involves taking a small sample of material, subjecting to a "soak" condition in a high humidity (50% relative humidity) and elevated temperature environment for 24 hours to simulate storage conditions at the two main space launch sites in the United States, Cape Canaveral in Florida and Vandenberg Air Force Base in California. Then the mass is taken, and the sample is placed in a vacuum oven for 24 hours at 125 deg C and 1.5 x 10^{-5} torr. The specimens are monitored for release of CVCM, considered potentially hazardous to manned spaceflight missions. The CVCM value cannot be higher than 0.10%. Following the vacuum exposure, the samples are taken out of the oven, measured for mass, returned to the high humidity chamber for a "re-soak" of 24 hours and then masses are measured again. (Campbell 1993) A detailed description of the outgassing apparatus and the test procedure is in the following subsection.

NASA GSFC test setup

The preparation of the samples was performed at AFRL/RX at Wright-Patterson AFB. The curing process is described along with the results in Chapter IV. The actual outgassing tests were performed at NASA Goddard Space Flight Center Materials

Figure 9. Photo of NASA GSFC outgassing test laboratory

Engineering Branch laboratory. The equipment there is based on the Stanford Research Institute developed micro-CVCM apparatus (see Figure 9), first built in the 1960's for NASA.

The micro-CVCM chamber consists of multiple parts and is run at a high vacuum condition (see Figure 10). A number of samples can be tested at one time in the micro-CVCM vacuum chamber. Each sample- typically 250 milligrams - is placed into a pre-weighed aluminum foil boat, which has been thoroughly cleaned and dried. Following a 24-hour pre-conditioning at 25deg C, 50% relative humidity and standard atmospheric

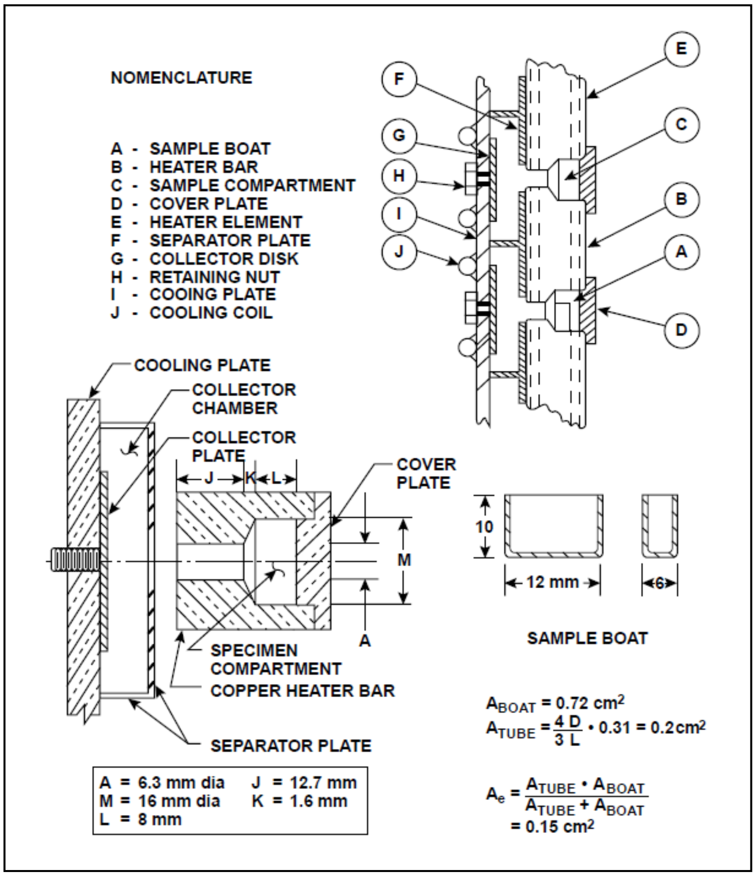

Figure 10. Diagram of Micro-CVCM apparatus (Scialdone 2000)

pressure to ensure that the samples receive a common preliminary treatment, the individual samples are weighed. The samples are then loaded into individual compartments in a solid copper bar that can be heated. Each compartment is closed by a solid copper cover, requiring that all gaseous materials escape only through the 6.3-mm (0.25-in.) diameter exit port.

The copper heater bar, having 12 sample compartments, is heated to 125 deg C for 24 hours. The sample is also heated to approximately 125 deg C by conduction with the copper bar and radiative heating. This causes the volatile materials to be driven off, with their only escape being through the exit port. At a distance of 12.7 mm (0.5 in.), a chromium-plated collector is in direct line of sight of the exit port and is maintained at 25 deg C. A significant portion of the escaping volatiles collects on the chromium-plated disk if the condensation temperature is 25 deg C or above. Barriers are near the collector plate to prevent cross-contamination between adjacent samples.

The mass loss of the sample is determined from the weights before and after the heated vacuum exposure, and the percentage loss is calculated to provide the TML. In a similar manner, the difference between the weight of a clean collector and of the collector having condensed materials will provide the mass of condensed materials. This mass of condensed materials is calculated as a percentage of the starting mass of the sample, and stated as CVCM. (Fisher 1971)

The first set of outgassing samples was a second set of specimens from the last batch of curing shrinkage tests. The illite samples were made on 4 Jan 2008 from a mixture of illite powder and trigger agent in a 5:3 ratio (powder:liquid). Cure was at room temperature in a sealed vacuum bag following initial setting time of 45 minutes in a nitrile rubber mold. The sample was kept in a vacuum bag for 5 days. The sample was then exposed to ambient atmosphere in AFRL/RX laboratory facilities prior to shipping. The metakaolin sample was made from a mixture of metakaolin powder and trigger solution in 1:2 ratio (powder:liquid). The metakaolin cure was at room temperature in a sealed vacuum bag following initial setting time of 60 minutes in a nitrile rubber mold. The sample was kept in vacuum bag for 6 days. The sample was then exposed to ambient atmosphere in AFRL/RX laboratory facilities prior to shipping.

A second set of samples was prepared again at AFRL in April 2008 and sent off to NASA GSFC as well for testing. The illite sample was made from a mixture of commercial illite powder and curing agent in a 5:3 ratio (powder:liquid). Cure was at room temperature in a sealed vacuum bag following initial setting time of 45 minutes in a nitrile rubber mold. The sample was kept in vacuum bag for 1 day. The sample was then baked at 60 deg C overnight and subjected to 24 hour vacuum bake at 0.7 $x10^{-4}$ torr, 140 deg C for 24 hours. A final room temperature vacuum exposure at 10^{-6} torr was performed for 24 hours prior to shipping.

The metakaolin sample cure was at room temperature in a sealed vacuum bag following initial setting time of 90 minutes in a nylon mold. Sample was then placed in high pressure autoclave for 1 hour. Sample was then baked at 60 deg C overnight and then a

24 hour vacuum bake-out at 140 deg C. A final room temperature vacuum exposure was performed for 24 hours prior to shipping.

All samples were tested at NASA GSFC according to ASTM E-595 standards. Test reports were received following completion of the testing and are included in Appendix B. The results of that testing is discussed in Chapter IV.

Objective 3- Space environment testing

The purpose of Objective 3 is to evaluate geopolymer performance following the exposure of the geopolymer to a representative space environment of radiation and atomic oxygen bombardment. Stated another way, Objective 3 is to answer the essential question of whether the materials lose any appreciable performance after exposure to an inclusive space environment for a relevant period of time. Objective 3 included two separate exposure tests, a combined UV & high energy particle exposure, and an atomic oxygen exposure. The space environment as noted earlier is a harsh operating condition and especially so for compounds that are chemically reactive with one or more of its constituents. Since an actual flight opportunity is expensive and fraught with potential of delays and single point failures, the choice was made to simulate an orbital exposure by using the AFRL/RX Space Combined Effects Primary Test and Research (SCEPTRE) chamber. For UV and high energy particle testing, the standard exposure duration for the SCEPTRE chamber is a 3000 ESH campaign. For AO exposure, no standard test campaign duration is currently defined. Ground-based AO exposure campaigns at NASA

Glenn used 18-40 hour continuous exposure times at 2-3 times the fluence of LEO levels seen on-orbit. LDEF results have shown that for missions of 5-6 years in duration, only 0.0127cm (127 micrometers) erosion was noted for Mylar and Kapton materials.

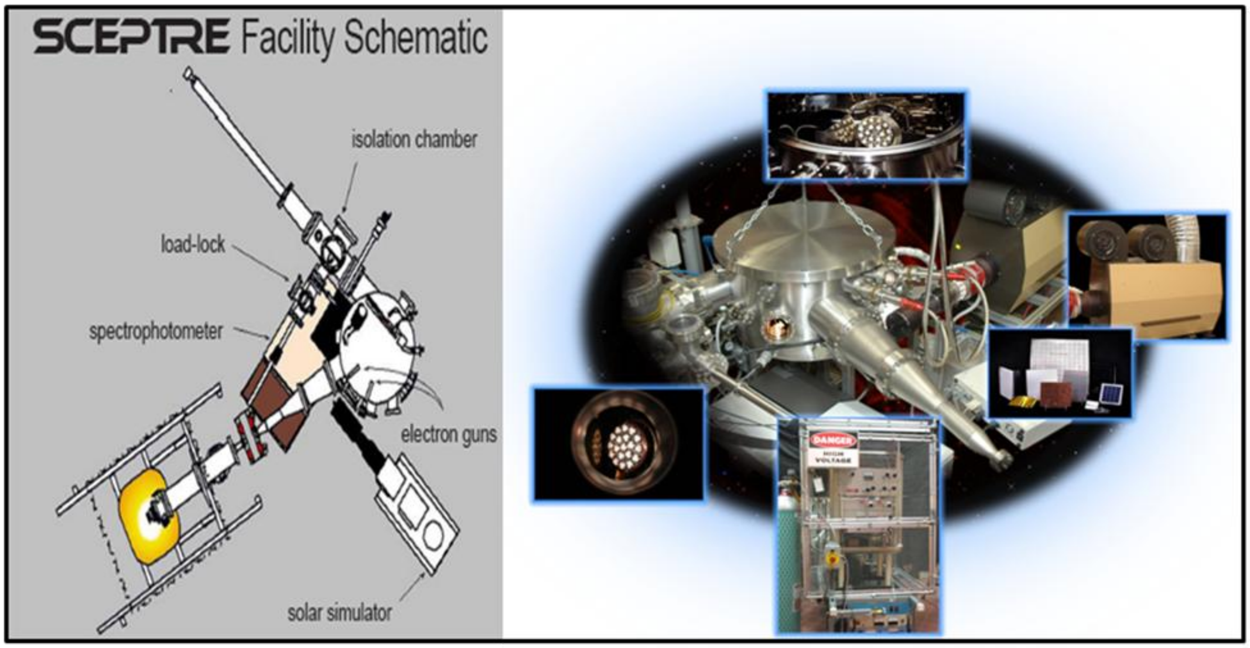

Figure 11. SCEPTRE facility schematic & photo (courtesy AFRL/RX)

<u>Simulating the space environment- the SCEPTRE chamber</u>

Although other government owned facilities exist, SCEPTRE is the AFRL/RX owned facility designed specifically for testing and qualification of spacecraft thermal control coating materials. (Cerbus 1994) SCEPTRE (see Figure 11) is a chamber capable of researching spacecraft material charging and space environment exposure effects all at the same time. (AFRL 2007)

Testing at the facility is performed in accordance with the guidelines established by the American Society for Testing and Materials ASTM E 512-94, Standard Practice for Combined, Simulated Space Environment Testing of Thermal Control Materials with Electromagnetic and Particulate Radiation. (ASTM 2008) The system has the capability of providing synergistic UV, vacuum ultraviolet (VUV), proton, and electron radiation environments similar to those experienced by satellites orbiting in mid-to-high earth orbits. In addition, the system has the ability to perform in situ measurements of sample temperature and in-vacuo reflectance as a function of wavelength. The vacuum level is maintainable from approximately 5 x 10^{-8} to 5 x 10^{-7} torr, the sample temperatures have achieved extremes ranging from 200 deg C down to 0 deg C depending on their thermo-optical properties, and the UV intensity averages around three equivalent ultraviolet suns (EUVS) in the 200 – 400-nm wavelength range. The VUV radiation is provided by a Hamamatsu 150-W deuterium lamp, and it provides approximately 17-EUVS (120 – 200-nm wavelength range). This combination provides an accelerated testing environment with synergistic effects of vacuum, accelerated UV and electron radiation, and limited thermal cycling.

Vacuum System

The vacuum system is composed of a 76.22-cm (30-in.) diameter chamber pumped by a Shimadzu TMP-1003LM hybrid turbomolecular pump (backed by a BOC Edwards XDS35i dry scroll vacuum pump) and a Helix Technologies, Inc., CTI-Cryogenics® Products ON-BOARD® 8 cryo-pump. The chamber is monitored via two Helix

Technologies, Inc., Granville-Phillips® Products ion gages, both of which are Series 360 STABIL-ION®. The chamber has the capability of exposing a maximum of nineteen 2.38 - 2.54-cm (15/16 - 1-in.) diameter, specimens to the synergistic VUV and UV radiation. This provides area for eighteen test samples with a single calibration sample mounted in the middle.

Solar Simulator

The solar simulator consists of a moderately filtered 2500-Watt Xenon arc lamp mounted in a modified Spectral Energy Corporation solar simulator. The Xenon arc lamp is water filtered and is capable of generating 4 EUVS at the target area in the vacuum chamber and has a fairly uniform intensity distribution (varying less than 30%) across the profile of the beam. The output of the solar simulator is measured with an Optronic Laboratories, Inc. model OL 754 spectroradiometer that is calibrated using an Optronic Laboratories, Inc. model OL 752-12 40-Watt deuterium lamp (200 – 400-nm) traceable to the National Institute of Standards and Technology (NIST) data. The deuterium lamp spectra are shown in Figure 12.

The vacuum ultraviolet (VUV) source is a water-cooled 150-W deuterium lamp with a magnesium fluoride (MgF_2) window. It is mounted in a vacuum flange that mounts directly on the SCEPTRE facility's vacuum chamber. The output of this model of

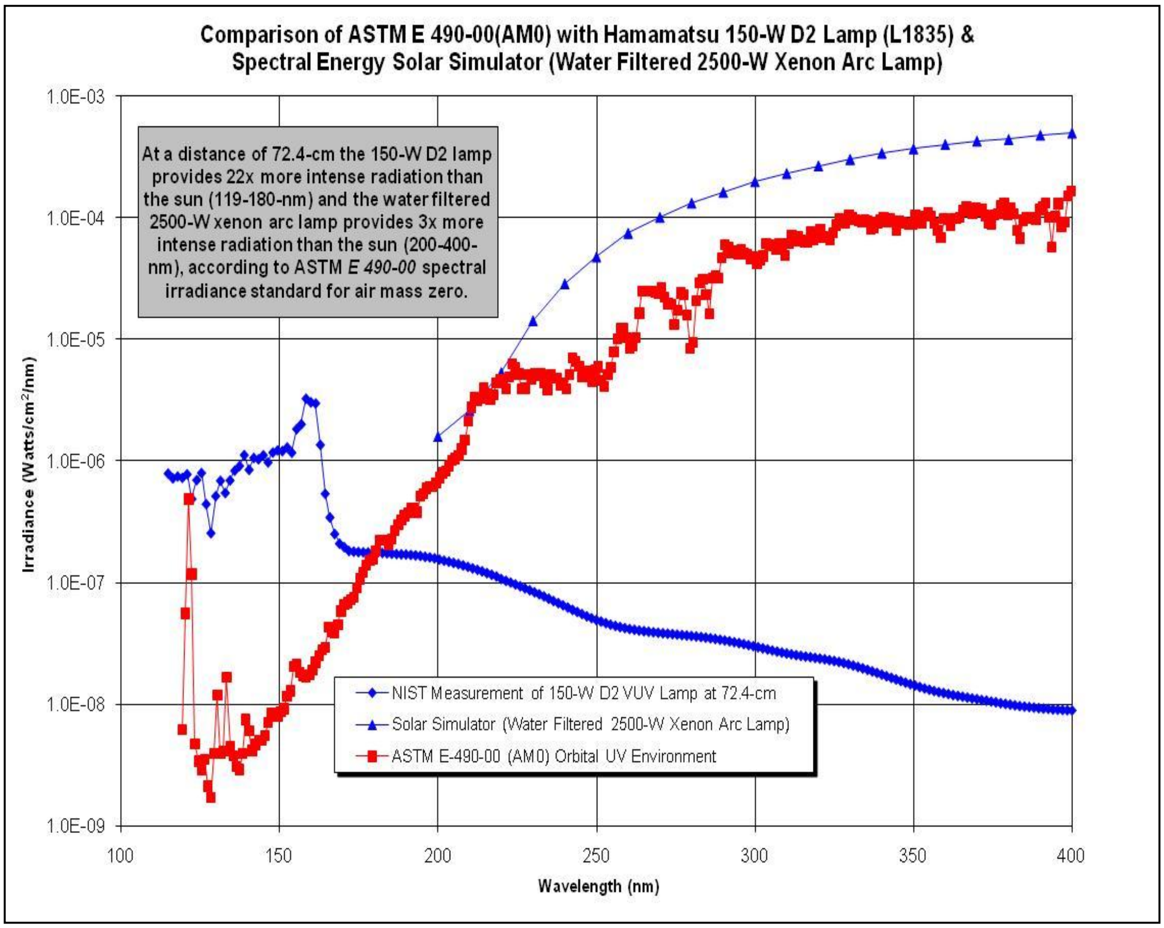

Figure 12. SCEPTRE deuterium lamp spectra (AFRL 2007)

deuterium lamp has been measured by NIST between the wavelengths of 115 – 400-nm and shown to be essentially a line source of radiation with a peak irradiance at 158.5-nm. At a distance of 81.3-cm (32-inches), the NIST measurement shows that the L1835 lamp is approximately 150-times more intense than the sun as compared to the ASTM E 490-

00 Standard Solar Constant and Air Mass Zero Solar Spectral Irradiance Tables. (ASTM 2004) The output of the VUV is not measured nor monitored directly at the SCEPTRE facility. It is no trivial matter to measure radiation in the extreme UV region of the spectrum. VUV measurements obviously require measurements in a vacuum environment and special detectors that are sensitive to radiation at this wavelength. Additionally, it is known that the output of deuterium lamps decrease with time, due to both the degradation of the lamp and the propensity for the VUV radiation to fix contamination to its window.

The SCEPTRE facility utilizes two Kimball Physics Inc. EFG-11 electron flood guns. These guns are designed to provide a flood of electrons with energies ranging up to 20-keV. Their output are monitored by a Faraday cup situated about 10.16-cm (4.0-in.) below and to the left of the center most sample position. A Keithley 617 programmable electrometer is used to measure the electron current generated by the Faraday cup. The electron beam is adjusted using a phosphor screen and determined to be relatively uniform across the specimens.

Spectrophotometers

The spectrophotometer used to monitor the specimens' solar absorptance *in vacuo* is a Perkin-Elmer *Lambda 19* UV-Vis-NIR double beam spectrophotometer and is fiber-optically coupled to a Labsphere Inc. integrating sphere located inside the vacuum chamber. The spectrophotometer is designed to provide *in situ* NIST traceable reflectance measurements and is utilized periodically throughout the duration of a test. However, because the materials being evaluated in this test were not thermal control materials and there was no other reason for monitoring their optical performance, the spectrophotometric setup was not utilized. The facility also has a second spectrophotometer which is used to measure spectral reflectance and transmittance *ex vacuo*. It is a Perkin-Elmer *Lambda 950* UV-Vis-NIR double beam spectrophotometer and it utilizes a Perkin-Elmer 60-mm reflectance sphere attachment.

Emissometer

The emissometer used to monitor the specimens' thermal emittance is an AZ Technology, Inc.'s *TEMP-2000A*. This emissometer is designed to be a portable instrument that performs total hemispherical reflectance measurements over a wavelength range from less than 3 to greater than 35 micrometers and is not limited by filters, windows, or coatings placed in the optical path. The *TEMP-2000A* provides both normal and hemispherical room temperature reflectance measurements and for opaque specimens, whatever radiation is not reflected is absorbed. Due to the physical behavior of materials, the radiation that is absorbed will also be emitted. Thus, the emittance of a material is equated to its absorptance within the spectral region of interest.

Temperature

The SCEPTRE facility indirectly cools the specimens via a chilled (-35 deg C) ethyl alcohol coolant filled line. The temperature control system reduces the exposed specimens' temperatures by on the order of 50 deg C. This cooling set-up relies heavily on the thermal conductivity of the mounting and construction materials and is dependent on limited physical contact between the cooling plate and the specimen platen for heat transfer. There are two different methods of monitoring the specimens' temperature. One is with a thermocouple on the backside of one of the outer specimens and the other is with a non-contact IR thermometer through a zinc-selenide viewport. The non-contact IR thermometer is manufactured by Raytek GmbH (model no. *DC3TXSLTCF3L2*) and is in their *Thermalert*® *TX* series of instruments.

Data Acquisition

The data acquisition is performed by a personal computer, in conjunction with hardware from a variety of vendors, and utilizes IEEE-488, RS-232, and analog-to-digital interfaces. The system monitors the electron flux, vacuum level, specimen backside temperature, the temperature of the center position specimen, and residual gases present in the vacuum chamber. Data is sampled periodically, usually at 15-min intervals, throughout the duration of a test.

<u>Ultraviolet radiation exposure testing</u>

For the UV exposure test, the SCEPTRE facility was configured to hold up to eighteen 2.5-cm diameter disks identical to MISSE disk sample size (2.5 cm D x 0.3 cm H). UV beam size is approximately 35-cm diameter conic at the test surface. The samples were loaded into the chamber using pressure clips to hold the samples in place. The sample surface was rotated to ensure equal exposure to the source over the test period. Each disk was weighed and photographed before and after exposure. There were also control samples kept outside of the chamber and used to compare with the exposed samples.

The SCEPTRE test chamber conditions are listed in Table 5. As seen, the test went for ~ 3000 ESH in the primary UV exposure wavelengths (200-400 nm). This translates to approximately 4 equivalent solar months of UV exposure. In LEO since spacecraft typically spend half their time in eclipse and half in sunlight, this exposure period actually equates to an approximately 8 month LEO mission lifetime, surpassing the 6 month mission lifetime minimum required for the test series.

Table 5. SCEPTRE test conditions for geopolymer exposure

Exposure time (real)	1096 hrs
Equivalent Solar Hours (ESH)	3014 for 200-400 nm wavelengths 2800 for 115-200 nm wavelengths
Solar environment	
UV	2500 W Xe arc lamp 2.75 EUVS @ 200-400 nm
VUV	150-W deuterium lamp 20 EUVS @ 115-400 nm
High energy particle	
Electron flux (1 keV e-)	3 E 9 e-/cm^2/s
Electron flux (10 keV e-)	6 E 9 e-/cm^2/s
Electron fluence	3.2 E 16 e-/cm^2 @ 1096 hrs
Vacuum level	2.3 E -7 torr

Evaluation of UV exposure effects

Since one of Objective 3's purposes is to determine if the geopolymers can survive the UV radiation environment of space, the primary investigation in this exposure test series is to identify whether chemical reactions are occurring due to exposure to UV radiation. For the case of polymers, while the polymer itself may stay intact, the significant shortening, elongation, or cross linking of polymer chains are individual chemical reactions. One can identify a chemical reaction that has occurred through many means, but a simple observation of a few key properties can identify if a reaction has occurred. These are:

- color change signifying a new chemical compound present
- mass change signifying the release of reaction products
- significant change in temperature (raised if exothermic, lowered if endothermic)
- change in physical properties associated with polymer performance such as hardness, strength (in the form of Young's modulus signifying that the polymer chains have been severed or additionally cross linked due to a chemical reaction affecting the polymer bonds), and emissivity

Chemical evidence of exposure effects

XPS was used to establish chemical profiles of the surface of both pre- and post-exposure samples. XPS is a quantitative spectroscopic technique that measures the chemical composition and state of the elements that exist within a sampled material. XPS spectra are collected by irradiating a material with X-ray beams while at the same time measuring the kinetic energy and number of electrons that escape from the top 1 - 10 nm of the material being analyzed. XPS requires ultra high vacuum conditions.

XPS is a surface chemical analysis technique that can be used to analyze surfaces of a material in an “as-is” state, such as after exposure testing. It is important to note that XPS detects only those electrons that have actually emitted as a result of X-ray excitation--since deeper photo-emitted electrons at the micron scale are recaptured or trapped in excited states closer to the surface, degradation of the material does not occur unless that material is susceptible to x-ray irradiation breakdown, such as most biological materials. In this non-organic application, XPS is essentially a non-destructive test means that still provides chemical composition of surfaces. (Moulder 1992) In this experiment series, XPS resources were limited and prioritization of which geopolymer specimens were tested occurred. Due to factors which will be discussed later, only the atomic oxygen exposed samples of geopolymers had XPS testing conducted with it, both a control and the AO exposed samples.

Visual evidence of exposure effects

Each sample pre- and post-exposure was photographed using a commercial digital camera, and each sample had a spectrograph of reflectivity from UV through midwave infrared (MWIR), 200-2500 nm wavelength, collected. The spectrographs were collected using the Perkin Elmer spectrophotometer mentioned previously.

Atomic force microscopy (AFM) was also performed on representative samples to check for changes in average surface roughness and inspect for evidence of surface pitting. AFM is a very high-resolution type of scanning probe microscopy, with demonstrated resolution on the order of fractions of a nanometer, more than 1000 times better than the optical diffraction limit. The AFM consists of a cantilever with a sharp tip (probe) at its end that is used to scan the specimen surface. When the tip is brought into proximity of a sample surface, forces between the tip and the sample lead to a deflection of the cantilever according to Hooke's law. An advantage of AFM over the scanning electron microscope (SEM) is that the AFM can produce 3-dimensional surface profiles where as the SEM provides a 2-D image. Additionally, samples viewed by AFM do not require any special treatments (such as metal/carbon coatings) that would irreversibly change or damage the sample, or mask surface effects that you are attempting to discern. (Giessibl 2003)

Physical characteristics of exposure effects

Each sample from pre- and post-exposure testing was weighed on a mass scale calibrated to 0.5 mg accuracy. Outgassing and re-absorbtion of water was mitigated as the samples to be weighed were allowed to acclimate to the local atmospheric environment during re-pressurization of the chambers.

Performance evidence of exposure effects

Representative samples from the UV exposure test were placed into an MTS G200 Nano Indenter apparatus to determine their hardness and modulus values as a function of surface depth using a continuous scan method (CSM).

Nanoindenters are a class of instrumented indentation testing (IIT) machines. Since the early 1990's, IIT has been developed to probe the mechanical properties of very small volumes of materials. At an elementary level, IIT uses a high resolution actuator to force an indenter tip into a test surface, and a high resolution sensor to continuously monitor the resulting penetration. Hardness and elastic modulus are the properties most frequently measured. These are calculated using the following equations:

$$Hardness\ (H) = P / A$$

Where:
P is the load applied
A is the projected contact area at that load

$$(1/E_r) = [(1-\nu^2) / E] + [(1-\nu_i^2)/E_i]$$

Where:
E is the elastic modulus of the test material
ν is the Poisson's ratio of the test material
E_r is the reduced modulus which is dependent on the geometry of the indenter and elastic contact stiffness
E_i is the elastic modulus of the indenter material
ν_i is the Poisson's ratio of the indenter material

While it may seem counterintuitive to need to know the Poisson's ratio of the test material in order to calculate its modulus, a 4% error in estimating the Poisson's ratio will only result in a 5% uncertainty in calculated modulus value. (Agilent Technologies 2009) Utilizing an Oliver-Pharr methodology, the nanoindenter software records the elastic contact stiffness by loading and unloading the indenter until penetration is realized. This is then fed to a calculation for unloading stiffness which is then used to calculate the reduced modulus. The reduced modulus value changes dynamically through the penetration depth and this provides a measurement of the elastic modulus of the test material as a function of depth.

When taking samples, a fused silica control sample is also measured for the same properties following the intended sample’s test series. This allows the operator to verify that the nanoindenter is working properly and for a reference standard to be available to use for calibration of the individual test samples if taken at different times.

Space radiation testing (high energy electrons)

The standard SCEPTRE high energy electron gun was targeted at the same exposure apparatus as the UV test. The electron source will be at one side of the sample apparatus so that as the apparatus is rotated, the samples will receive nearly equal exposure levels and times. A Faraday cup was used to record the electron flux passing in the chamber. Electron radiation utilized two identical flood guns: one at 1-keV and the other at 10-keV.

Atomic oxygen exposure

For the AO test, a custom AO exposure chamber was built and used. The chamber

Figure 13. Photo of atomic oxygen exposure chamber

consisted of an approximately 15-cm diameter vacuum rated central chamber connected on the bottom to cryogenic vacuum pumps and on the top to an AO source made of a silver oxide filament (see Figure 13). The exposure samples were placed on an aluminum tray that slid into the central chamber. The illite and metakaolin samples were butted against each other and then half their area was masked with a Kapton tape. A second mask made of sheet metal with a 2.5-cm diameter view port was then placed on top of the samples so that a circular exposure area was exposed to the AO source consisting of exposed illite, Kapton-masked illite, exposed metakaolin, and Kapton-masked metakaolin, each one-fourth specimen in size.

The chamber was pumped to 3.5×10^{-9} torr local pressure and the AO source was set to output a constant flux. A measurement of current collected as a result of electrons reacting with the AgO surface releasing atomic oxygen was measured at 25-30 mA. Typically the AO flux is measured by erosion of a control Kapton sample, however in this experiment the Kapton sample was shifted as a result of an anomaly and AFM inspection of the Kapton was unable to resolve a definitive erosion measurement. However, considering the electrical current through the silver filament, the basic chemical stoichiometry of the AO release reaction, and the time in chamber, it is estimated that the AO exposed samples in this test received about 1.2 years equivalent LEO mission time, more than enough to judge the material's worthiness with respect to AO since a 1-yr design lifetime allows for most "birth defect" satellite failures to be mitigated. (Tao 2008) During the test, the temperature of the mounting plate was monitored via thermocouple and the samples were visually checked on a periodic basis via viewing through a side mounted window port.

Summary of Methodology

This chapter presented the test methodology utilized for the experimental portion of the research campaign. Testing for Objective 1 would vary temperature and pressure as key variables in determining curing shrinkage dependencies. Testing for Objective 2 would utilize existing hardware and widely accepted best practices for determination of outgassing. Objective 3 testing would use two separate chambers to expose samples to both a radiation and AO exposure environment, then subject representative samples to evaluation testing for evidence of material changes due to the exposure regimes. The evaluation testing would involve techniques to explore mechanical as well as chemical properties.

IV. Analysis and Results

Chapter Overview

This chapter will present the analysis and results performed to achieve the three objectives stated previously: determining curing shrinkage dependencies (Objective 1), determining outgassing performance (Objective 2), and determining the performance of geopolymers with respect to exposure to a simulated space environment (Objective 3).

Objective 1- Curing Shrinkage

One result that quickly came to the forefront was that the material of the casting mold was extremely important. Initially, we had used simple polystyrene boxes but after the first samples, the buckling of the post-cure geopolymers and the residue on the molds

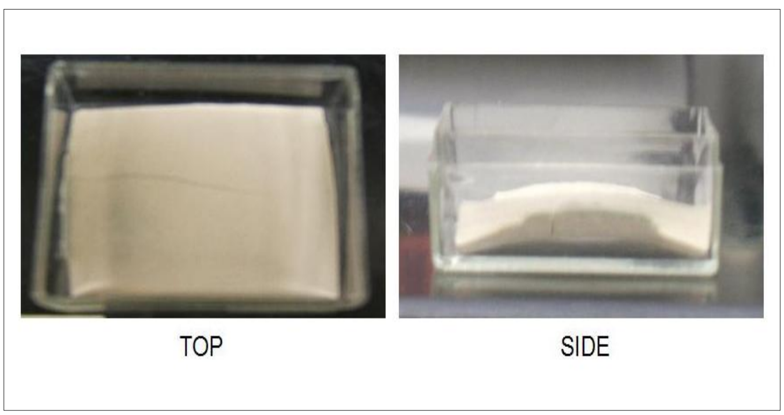

Figure 14. Evidence of bonding to polystyrene containers

themselves after sample extraction suggested that significant adhesion was taking place between the polystyrene and the geopolymer. This is seen in Figure 14, a photo of one of the samples from the first batch of tests. Because of the adhesion taking place, residual stresses were developing in the cured geopolymer causing the sample to bend that would make it difficult to accurately measure the curing shrinkage, in addition to causing cracks to develop in the geopolymer itself as well.

A quick review of materials revealed that nitrile rubber would be a good replacement for the polystyrene due to its anticipated inertness with the geopolymer. A set of blue nitrile rubber molds for use in subsequent experiments was constructed. Each sample chamber of the mold measured 25.23 x 25.23 x 6.32 mm within 0.01 mm of variation in each dimension. These square molds are seen in Figure 15 on the left side of the photograph. For times when a circular specimen was needed, Teflon rings with a 2.54-cm diameter hole were placed on a solid blue rubber nitrile mold (seen in Figure 15), the slurry was poured into the holes in the rings and after initial setting, the entire block and ring mold was placed into a vacuum bag and sealed. Once cured, the geopolymer samples easily separated from the molds by simply flexing the mold until a geopolymer corner was exposed, and extracting them by hand. There was no evidence of adhesion between the mold and geopolymer. For the ring samples, the cured geopolymer was solidly in the ring void, so the ring and joined specimen were placed in a 60 deg C oven to allow the Teflon ring to expand just enough that the geopolymer specimen could be pushed out easily without damaging the specimen.

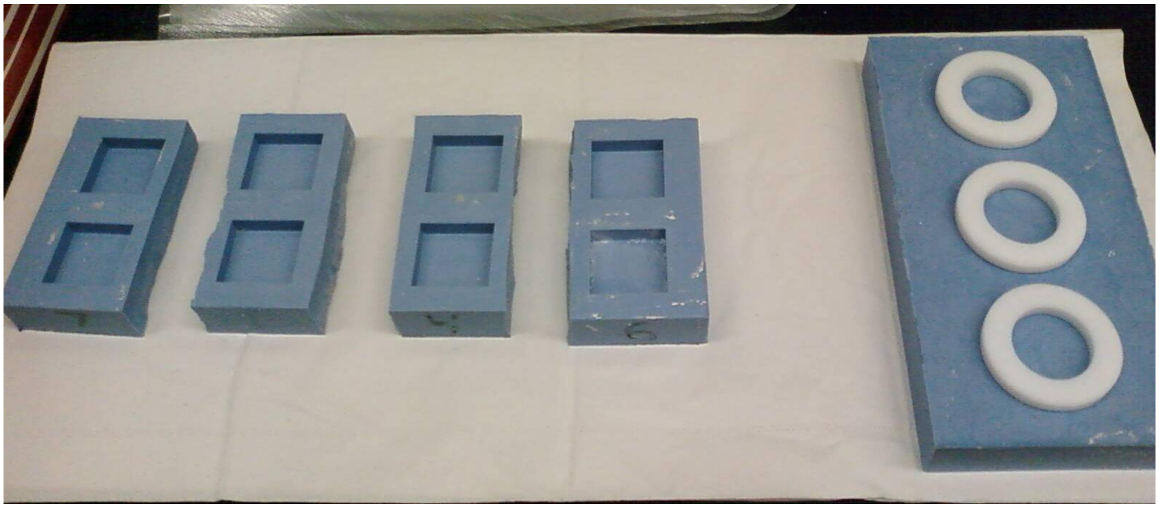

Figure 15. Blue rubber nitrile molds

Some interesting observations were noted during the curing process. First, in the vacuum bagged samples, there was a significant color change that occurred after the exposure from the vacuum bags where the illite samples changed from various shades of dark green to the expected grey tone. The color change occurring is due to an unfinished curing process where the water particles formed during the polymerization reaction had no chance to diffuse out of the polymer matrix resulting a hydrate form of the solid polymer. The change to the non-glossy gray color of the illite samples indicates the easiest path free water had escaped the polymer matrix to equalize with the ambient humidity level. The metakaolin samples from vacuum bags experienced a color change as well but not nearly as pronounced as the illite samples.

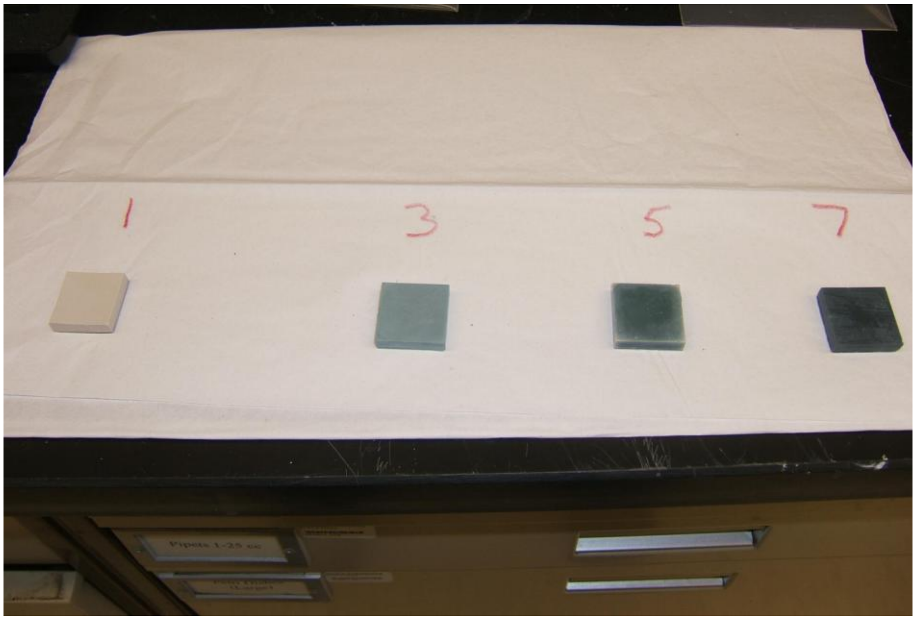

Figure 16. Color change of illite samples from ambient cure (1) to vacuum cure (7)

Second, little mass change was noted from the time the vacuum bagged samples were opened to after the ambient atmosphere acclimation time was complete. The maximum recorded mass gain was of +0.1 g on a 7.1 g specimen of illite after two days of exposure. This was an indication that although some water had equalized with the humidity in the local environment, there was still significant water by-product trapped in the pores of the polymer matrix and the specimen was highly hydrated, evidence by color change (Figure 16).

A final observation was noted on the illite and metakaolin samples that were left exposed to the room temperature and ambient atmosphere. Both of these samples showed significant buckling and flaking on the exposed surface and numerous surface cracks were apparent as well. This was a clear indication that a simple room temperature and ambient atmosphere curing process would not be sufficient for any application. Indeed, Perera, et al found that curing in sealed containers of different relative humidity provided crack free curing. However in my research, curing in an oven with same relative humidity offered no advantages-- this is taken as evidence of pressure as a key variable. (Perera 2007)

Analyzing the net change in linear dimensions showed that pressure was a dominant effect, although temperature was a contributor to controlling curing shrinkage. In Table 6, the largest linear shrinkage noted was for both open air cures of the two geopolymers (~ 5% for illite and ~3% for metakaolin). The elevated temperature and pressurized curing produced the smallest curing shrinkage for both illite and metakaolin. All the pressurized samples showed better performance in curing shrinkage than the open air samples (76-98% reduction in curing shrinkage) indicating pressure was a dominant variable. The variations in temperature effect were much less pronounced (0.7% in linear shrinkage difference for the two extreme illite cases of 60 deg C and -17 deg C), but still after pressurizing, going from room temperature to a heated cured gains an additional 5% improvement in curing shrinkage performance over the non-pressurized cure condition.

Table 6. Curing shrinkage experimental results

Material	Cure Conditions	Linear shrinkage
Illite	Room T, open air	5.08 %
Illite	60 deg C, vacuum bagged	0.49%
Illite	Room T, vacuum bagged	0.72%
Illite	-17 deg C, vacuum bagged	1.17%
Metakaolin	Room T, open air	3.32%
Metakaolin	Room T, vacuum bagged	0.25%
Metakaolin	60 deg C, vacuum bagged	0.04%

Observations & summary

It is clear from the experimental data that in order to control curing shrinkage in geopolymers, a pressurized environment is key, even one as mundane as vacuum bagging the molds. A higher temperature cure can also contribute to controlling the curing shrinkage. Comparing to other common polymers as shown in Table 7, it is seen that geopolymers perform favorably, as the geopolymers volume shrinkage is between 0.2-1.2% and the other organic polymers have a curing shrinkage range of 4-14%.

Additionally, the presence of "mudcracks" was noted after all cure periods. These small cracks in the surface appear in almost all polymers and cement formations as a natural effect of water leaving surface layers. The cracks do not typically penetrate deep as evidenced that after a short polishing procedure following initial cure that reduces the depth dimension by less than 1 mm, the mudcrack layer was eliminated easily.

Table 7. Comparison of geopolymer to common organic polymer curing shrinkage

Polymer	Volume Shrinkage
Illite (best experimental performance)	1.2 %
Metakaolin (best experimental performance)	0.2 %
Epoxy	4-5 %
Acrylic	6-9 %
Polyester	9-14 %

Objective 2- Outgassing

High water release value

The results from the two sets of outgassing tests at NASA Goddard are presented in Table 8. This data taken from the NASA GSFC data sheets following the first outgassing test in Jan 2008, shows that in both Total Mass Loss (TML- water + other materials) and Net Mass Loss (NML- excluding the water effect) the material fails the NASA standard for both TML and NML (NASA standard is < 1% TML for most materials and < 1% NML for hydrogopic materials). Additionally trace amounts of condensed volatiles (CVCM) deposits were recorded, although the amounts were small enough that neither geopolymer failed that metric (NASA requires < 0.1% CVCM). In the second test in April 2008, the TML and NML were significantly reduced, and the NML to a level that would meet standards acceptable for a NASA waiver of approval even though the TML still shows significant outgassing, mostly from water.

Table 8. Outgassing test results

Sample	TML	WVR	NML	CVCM
Jan 08 Illite	19.26 %	9.39 %	9.87 %	trace
Jan 08 MK	20.7 %	8.98 %	11.72 %	trace
Apr 08 Illite	6.15 %	5.61 %	0.54 %	none
Apr 08 MK	8.35 %	7.63 %	0.72 %	none

The poor outgassing performance of the Jan 08 samples from a TML point of view was due to the fact that the samples initially sent to NASA were not “pre-baked” (or annealed) to release the free water still trapped in the polymer matrix. The free water was then released in the outgassing testing chamber when heat treated to 140 deg C under vacuum conditions. This is not unexpected. As the geopolymer cures, water molecules are the effluent reaction products. If water is evolved in the polymer, then the individual water molecules bunch together into clusters that then get trapped in the geopolymer matrix internals. If water is formed at or near the external surface, it likely evaporates away at the first application of heating. The heating under vacuum that occurred during the outgassing test at NASA GSFC in January 2008 drove the rest of the water molecules internal to the geopolymer to diffuse to the surface and evaporate, leaving a dehydrated geopolymer. This inadvertent test failure actually spawned the idea on how to improve the geopolymer process as discussed later.

Modification to geopolymer preparation

The outgassing issues were fixed by changing the preparation procedure. The geopolymer samples were baked out (annealed) in a heated low vacuum chamber, then at a room temperature high vacuum chamber (10^{-8} torr) as a final step in the curing process. After that, the samples were sealed in vacuum bags for shipment to GSFC. By doing this set of steps before the formal outgassing testing, it allowed the non-surface water on the geopolymer to be evaporated, this change accounts for the difference in TML and NML values seen in Table 8 in the April 2008 data set. The TML value was reduced significantly from the January test to the April test indicating that a lot of the water that had outgassed in the previous test had been eliminated pre-test by our change in production procedure.

More importantly, the NML value changed from nearly 10% to less than 1% (Table 8). This means two things. First, this indicates that most of the material from the January test that contributed to the high NML was internal water trapped in the geopolymer matrix. Second, this means that the polymer itself is not outgassing. This is important as it can now be asserted with confidence that the geopolymer itself is not a concern to outgas and deposit material on a spacecraft surface or destructively breakdown due to vacuum and heating. A < 1% NML value can be used as the basis for a material waiver from NASA since you can assure that only effluent is water vapor absorbed during storage and launch preparations from the local humid environment.

However, post-heat & vacuum treatment exposure to ambient atmosphere still causes re-absorption of water to occur at the pore surfaces. Depending on the length of time the treated geopolymer is allowed to rest in ambient atmosphere, significant amounts of water vapor will be re-introduced not just onto the surface of the geopolymer, but into the internal pore structure of the matrix through diffusion mechanisms. In order to control this phenomenon, one of three methodologies must be adopted. First, the samples could be stored in vacuum bag like conditions, however, if used in a space application, there will be time that the geopolymer is exposed to high humidity atmosphere while waiting for a launch vehicle opportunity, like at Cape Canaveral in Florida or Vandenberg Air Force Base in California. Second, the geopolymer structure could be kept in a nitrogen only atmosphere, but the use of a nitrogen purged launch fairing on a space launch vehicle during the complete preparation and wait time before launch occurs is an expensive and labor intensive process. Third, the geopolymer structure once "baked out" could immediately be coated by a hydrophobic sealant to prevent water absorption. This however presents challenges as well since a coating would likely have CTE mismatches between the geopolymer and the other mirror materials it is supposed to bond to, in addition to ensuring the coating is not damaged during follow-on instrument or spacecraft processing. These preparation changes have been noted for future application work.

One additional interesting observation was seen during the outgassing specimen preparation at AFRL/RX. After the geopolymers were subjected to vacuum oven preparation the first time following curing, the samples were immediately removed from the oven to be weighed once the pressure had equalized. The shock of going from a 125 deg C local temperature to a 70 deg C local temperature caused thermal stresses to be introduced in the material and surface fissures to form on the geopolymers. These propagated to the point that the samples cracked into small fragments. This result caused a revision in preparation procedure to include a slow cool down time of 6-8 hours following the conclusion of vacuum oven heating with the cooling mechanism inside the oven governed by the entrance of air into the oven through a valve opening and natural cooling to occur.

Observations & summary

For Objective 2, the outgassing performance of the geopolymers was characterized and although the materials failed in terms of the TML standard ($< 1\%$), the NML performance is likely good enough to warrant a waiver. In terms of solving the problems seen in the outgassing testing, the solution was a simple change in preparation procedures. A vacuum bake at 125 deg C after initial cure eliminated much of the water from the geopolymer hydrate. The results from our outgassing tests have shown that geopolymers will meet the minimal standards for surviving the initial space environment exposure, namely exposure to vacuum and heating.

However, the reabsorbing issue during pre-launch storage is a major concern. The hydrogopic nature of geopolymers means that re-absorption of water from the local humidity is inevitable without expensive storage procedures or sealants being applied to the geopolymer surface. If the sealant option is selected, a major advantage of the geopolymer, the CTE tailorability may be lost since the sealant will form the contacting surface, not the geopolymer. The water gain and rapid release in orbit may be a concern for those applications where water deposition is hazardous or mass margins are particularly contentious.

Objective 3- Space Radiation and LEO Environment Exposure

UV & high energy particle exposure results

The UV and high energy particle exposure tests were done in parallel on the same samples, so their results will be presented together.

Samples from the SCEPTRE run were measured for mass change before and after the test. The samples were weighed attached to the mounting holders for the SCEPTRE chamber wheel. The values are listed in Table 9. For illite samples, the mass loss was remarkably consistent, with 1.1% being the average mass loss. For metakaolin samples, there was a slight bit more variation with a range of mass loss percentage from 0.4-1.0%, but still the mass loss was minimal.

In both pre- and post-test weigh-ins, the samples were left exposed to the room atmosphere for over 24 hours. This means that water absorption was present both before and after vacuum exposure. The mass changes are consistent in percentage value with those seen in the outgassing tests, signifying that the UV and high energy particle exposure tests did not react enough with the specimens to cause reactions that liberated species from the geopolymers. The results show that the mass loss from all of the samples was minimal; indicating that UV exposure with high energy particle exposure did not erode away any surface from the bulk materials.

Table 9. Mass change on geopolymers following SCEPTRE chamber exposure test

Mass Loss Data, SCEPTRE Test on Geopolymers, 2009				
Specimen	**Pretest Specimen & Holder Mass (g)**	**Post-test Specimen & Holder Mass (g)**	**Mass Change (g)**	**% Change**
Illite Sample 1	24.32	24.12	0.20	0.8
Illite Sample 2	24.71	24.44	0.27	1.1
Illite Sample 3	24.22	23.95	0.27	1.1
Illite Sample 4	25.18	24.92	0.27	1.1
Illite Sample 5	24.62	24.35	0.27	1.1
Illite Sample 6	24.97	24.69	0.28	1.1
Metakaolin Sample 1	22.51	22.32	0.19	0.8
Metakaolin Sample 2	21.72	21.60	0.12	0.5
Metakaolin Sample 3	22.54	22.45	0.09	0.4
Metakaolin Sample 4	22.82	22.58	0.24	1.0

From visual inspection as shown in Figure 17, all samples of illite and metakaolin showed a darkening in surface color as early as after exposure to only ~200 equivalent solar hours, or about 2 weeks on orbit in LEO. This is potentially indicative of UV induced aging effects seen in other polymers. However in this case, the oxide layers on the surface of the geopolymers darkened in accordance with well understood oxide darkening mechanisms. As is seen in the subsequent series of photographs in Figure 17,

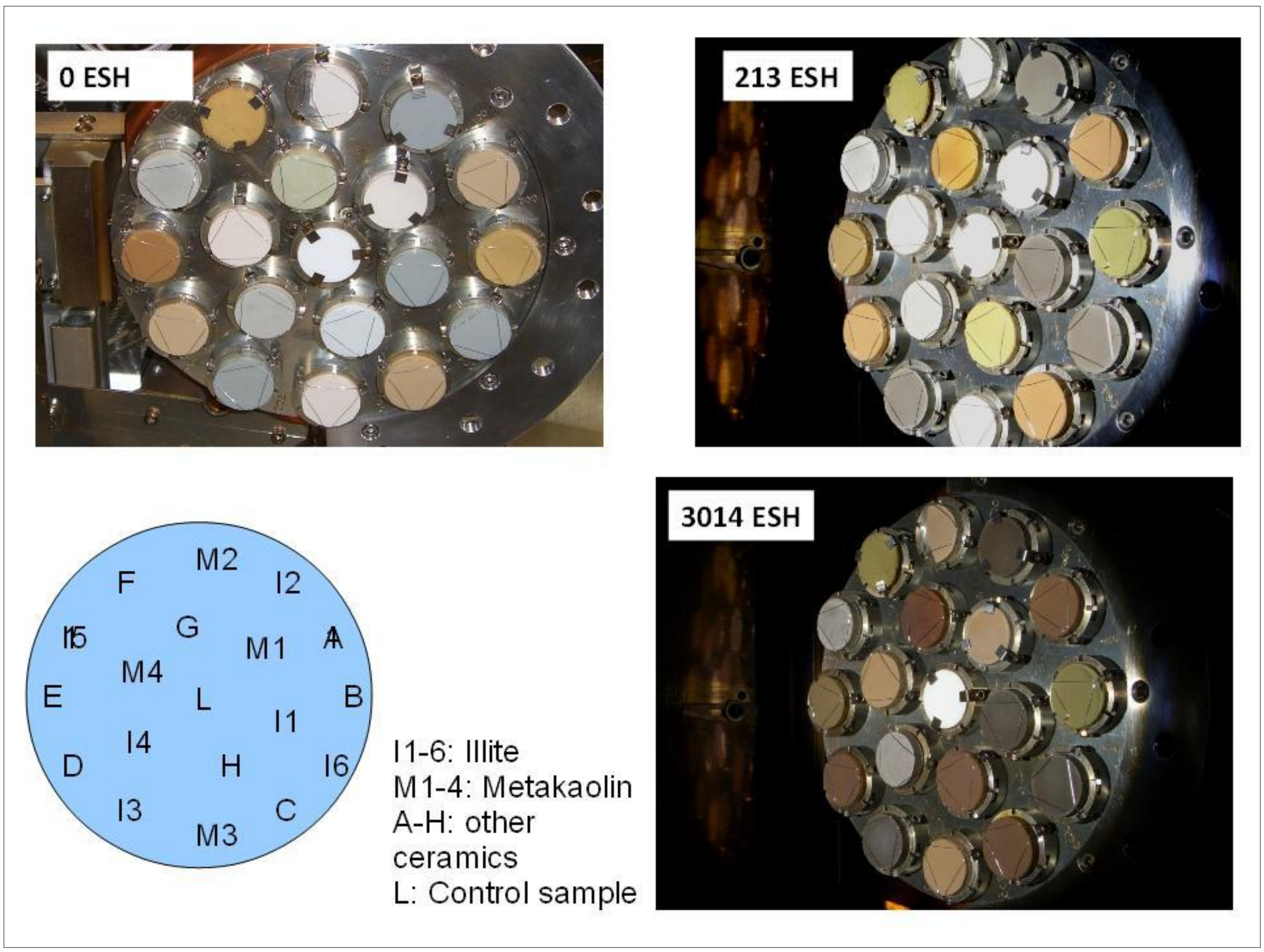

Figure 17. Time series of photos of geopolymers during SCEPTRE chamber exposure

the illite and metakaolin samples continue to darken over time. While the darkening was pronounced, it was not unexpected. Figure 18 shows a photograph of an illite sample from the UV exposure test after the test was over. The distinct discolorations on the photograph are in areas where metal clamps were used to hold the specimen in the metal puck. This clearly shows that the UV induced some darkening.

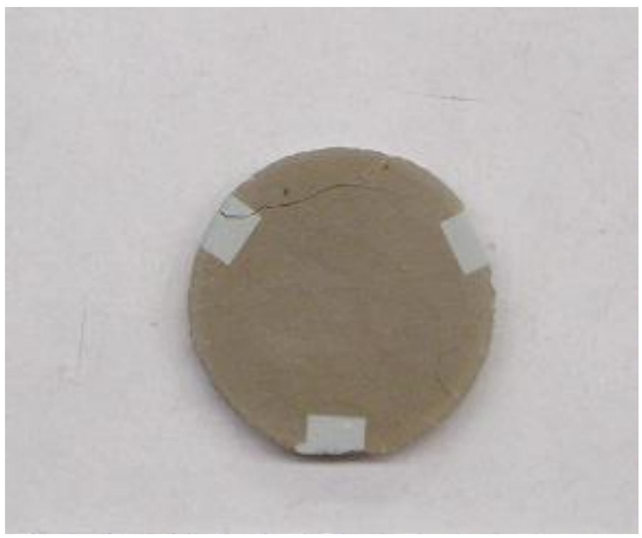

Figure 18. Illite sample post-UV exposure. The areas where the metal holding clamps prevented UV exposure darkening are clearly seen

Since the samples were not polished to an optical flatness, they did not fit exactly flat against the spectrometer sensor port. A sub-millimeter difference in distance from the spectrometer source can affect the reflectivity amplitudes by significant amounts. Consequently, absolute amplitudes of the reflectivity, as seen in Figure 19, cannot be used with high confidence.

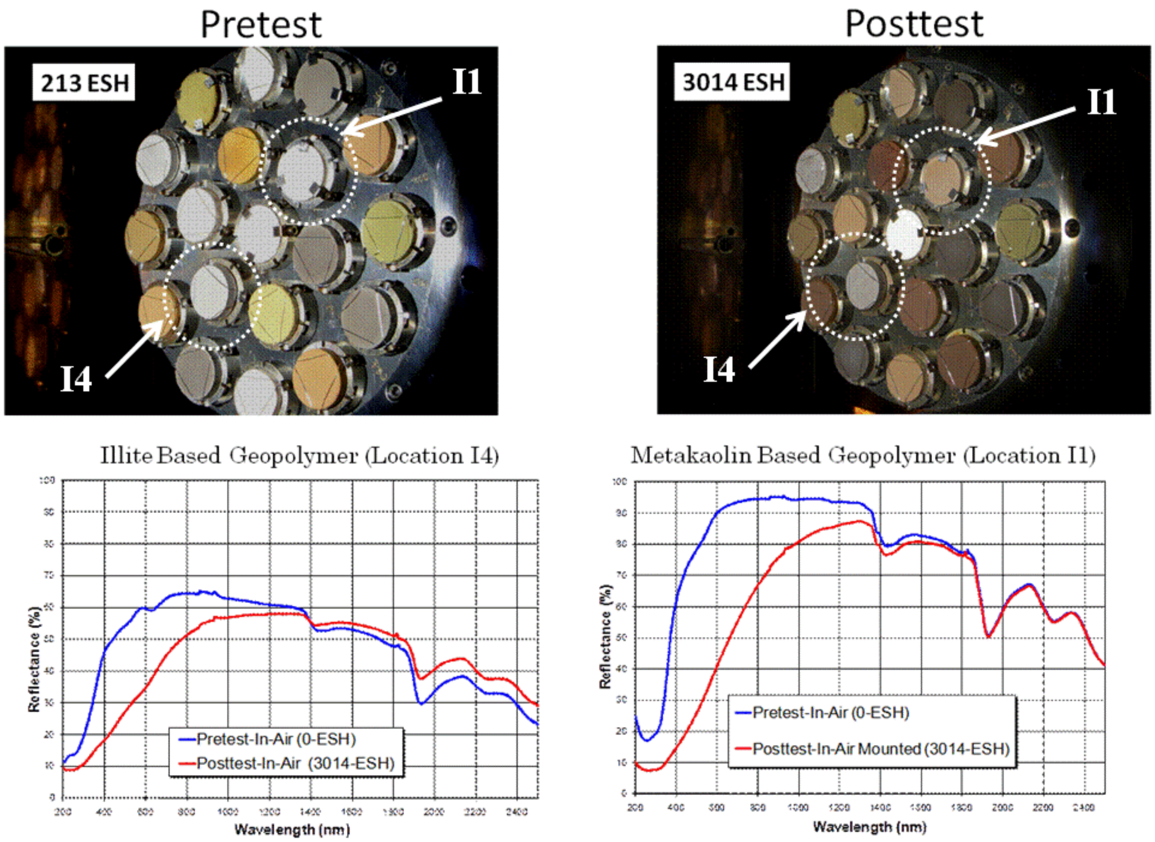

Figure 19. Pre- and Post-test photos and spectra of geopolymers following UV exposure

However, a normalization routine was used in order to compare like material samples. The maximum amplitude recorded for an individual photometric signature was used as the normalizing value for the rest of the samples. So in presenting the data, the curves in Figure 20 and Figure 21 are shown with reflectivity as a percentage of the maximum reflectivity value for that signature. Since the concern is whether the general behavior of the specimen changed with respect to its spectral signature, this technique allows general behavior changes to be analyzed. The amplitude of the signature may change as its distance to the sensor changes consistent with a $1/r^2$ optical attenuation, but the relative behavior of the individual spectral lines associated with that material will not. For each material, illite or metakaolin, the multiple samples spectral signatures are averaged for all samples. In the normalized reflectivity graphs, three lines are seen. The “Pre, normlzd, avg” line is the average spectral signature of the pre-UV exposed specimens, normalized for its maximum amplitude signature value. The “Post, mntd, normalized, avg” line is the average spectral signal of the post-UV exposed specimens while still mounted to the SCEPTRE holding puck with fine metal wire, normalized for its maximum amplitude signature value. The “Post, unmntd, normalized, avg” line is the average spectral signal of the post-UV exposed specimens unmounted (i.e. just the specimen against the sensor port), normalized for its maximum amplitude signature value. The difference between the two post-UV exposure values is attributed to the additional reflectivity added by the highly reflective metal wire holding the specimen in the holding puck. While the values are not significantly different between the wire and not wire post-UV exposure test signatures, both results are presented for completeness.

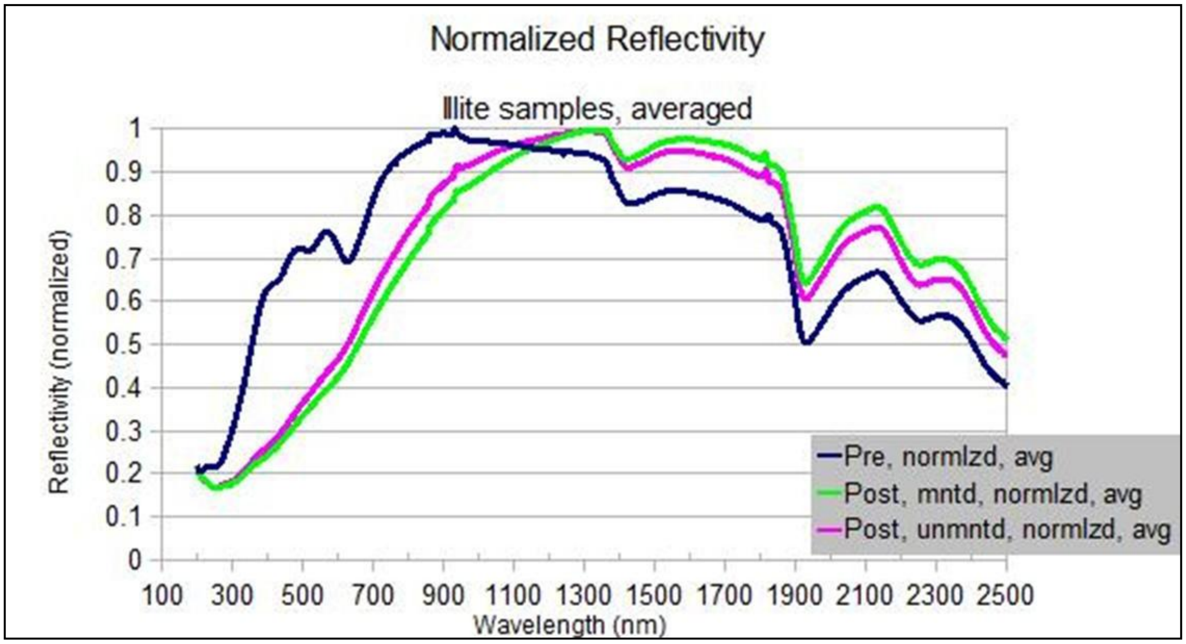

Figure 20. Normalized reflectivity of illite, pre- and post-UV exposure

The first result that jumps out in the illite analysis as shown in Figure 20 is that there is significant change in UV (200-400 nm) and IR (1100-2500 nm) reflectivity. The UV region shows that after UV exposure, the illite samples become much less reflective to UV, indicating a change that the samples go from net UV reflectors (> 50% reflectivity) to net UV absorbers (< 50% reflectivity).

In the IR region on Figure 20, a clear transition occurs. In the non-exposed illite, the material begins to lose reflectivity after 900 nm. In the post-exposed illite, the reflectivity loss transition point happens at around 1300 nm. The general behavior in terms of peaks is the same following that transition point, but the shifting to the right of that IR loss transition point and the increase in reflectivity in IR wavelengths following UV exposure of illite may indicate that the illite becomes more of a heat reflector as it ages. It may also be that in the process of UV exposure and high energy particle bombardment, erosion of large peaks (greater than IR wavelengths) occurred causing the surface to become more smooth, and hence more reflective in the IR. This may complicate heat management design on the spacecraft. If the geopolymer operates cooler after six months on-orbit than it did at launch, this may require a greater use of on-board heaters, which will then lead to a greater load on the power generation and storage subsystem of the spacecraft.

The reduction in reflectivity in the visible wavelengths (400-700 nm) is consistent with the darkening of the samples as seen in the visible light photographs due to additional oxidation occurring on the surface, typical of many oxide compounds. Reflectance spectroscopy is sensitive to subtle changes in crystal structure or chemistry, and these results seem to confirm a surface chemistry or polymeric structure change following UV and high energy electron exposure. It is also important to note however, that oxides (which geopolymers are) darken when oxygen atoms are knocked out of the polymer matrix due to UV exposure. This causes vacancies to form in the matrix and these vacancies will refill once exposed to ambient atmosphere with supply of oxygen atoms at room temperature.

The metakaolin results shown in Figure 21 demonstrate the same general behavior as the illite. This was expected since they are from the same mineral family. A significant reduction in reflectance in the 200-700 nm bandwidth (UV through visible) followed by an increased reflectivity in the IR wavelengths indicates the metakaolin was similarly affected by UV and high energy electron exposure as the illite. The spectroscopic results raise the question as to how far the changes penetrated in the bulk material.

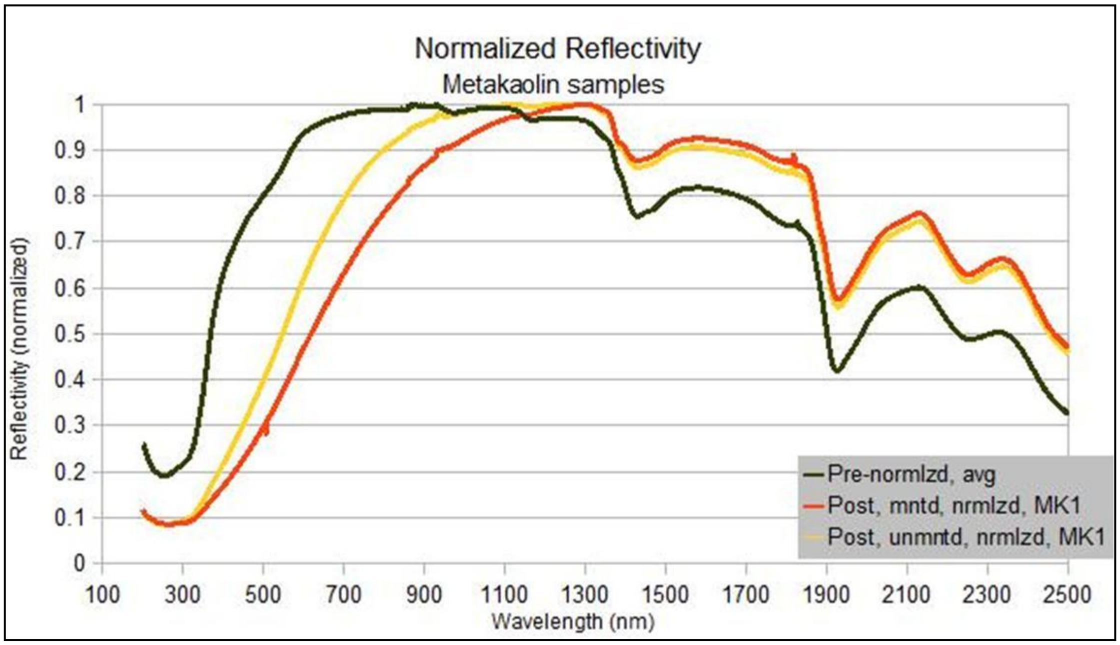

Figure 21. Normalized reflectivity of metakaolin, pre-and post-UV exposure

Additionally, one of the geopolymer samples, the metakaolin specimen shown in Figure 22, exhibited significant cracking following the UV exposure period. The metakaolin cracking caused flaking of surface layers that were exposed to the UV. Upon removal from the chamber, the outer edges of the specimen broke off into smaller pieces. This may be due to the already established thermal shock issues associated with geopolymers as seen in the outgassing experiments. Alternatively, it may be a result of forces impinging on the sample from the metal wire holding the geopolymer disk to the mounting puck. Theses stresses are then amplified during the heating process in exposure, and cause the wires to dig into the sample.

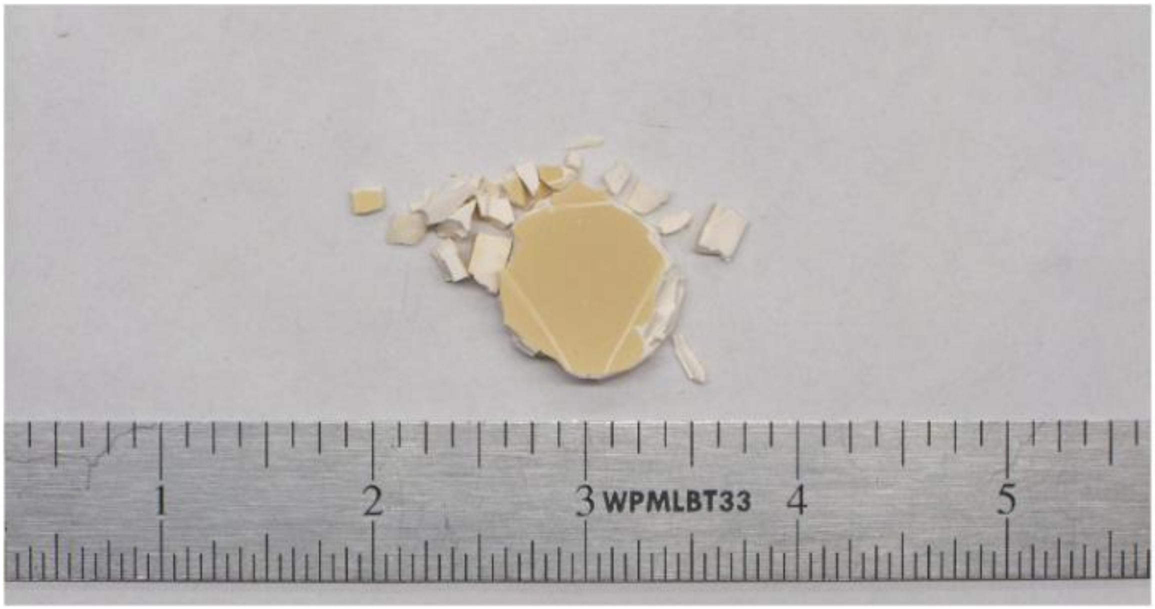

Figure 22. Post-UV metakaolin sample fracturing

Because of the thickness of the samples and the unique mounting techniques used, the samples were not adequately dissipating heat to the back metal cooling plate in the SCEPTRE chamber, and as such specimen temperatures were higher than desired during the exposure. Temperatures as monitored during the test reached as high as 135 deg C on the illite and metakaolin sample surfaces during exposure to the UV main beam. It is thought that in the rapid cool down period between lamp on and off times, the temperature gradient was too high and much like common glass, the geopolymers fractured under the stress. An active feedback loop thermal control system and better heat sink method would alleviate this problem in the future.

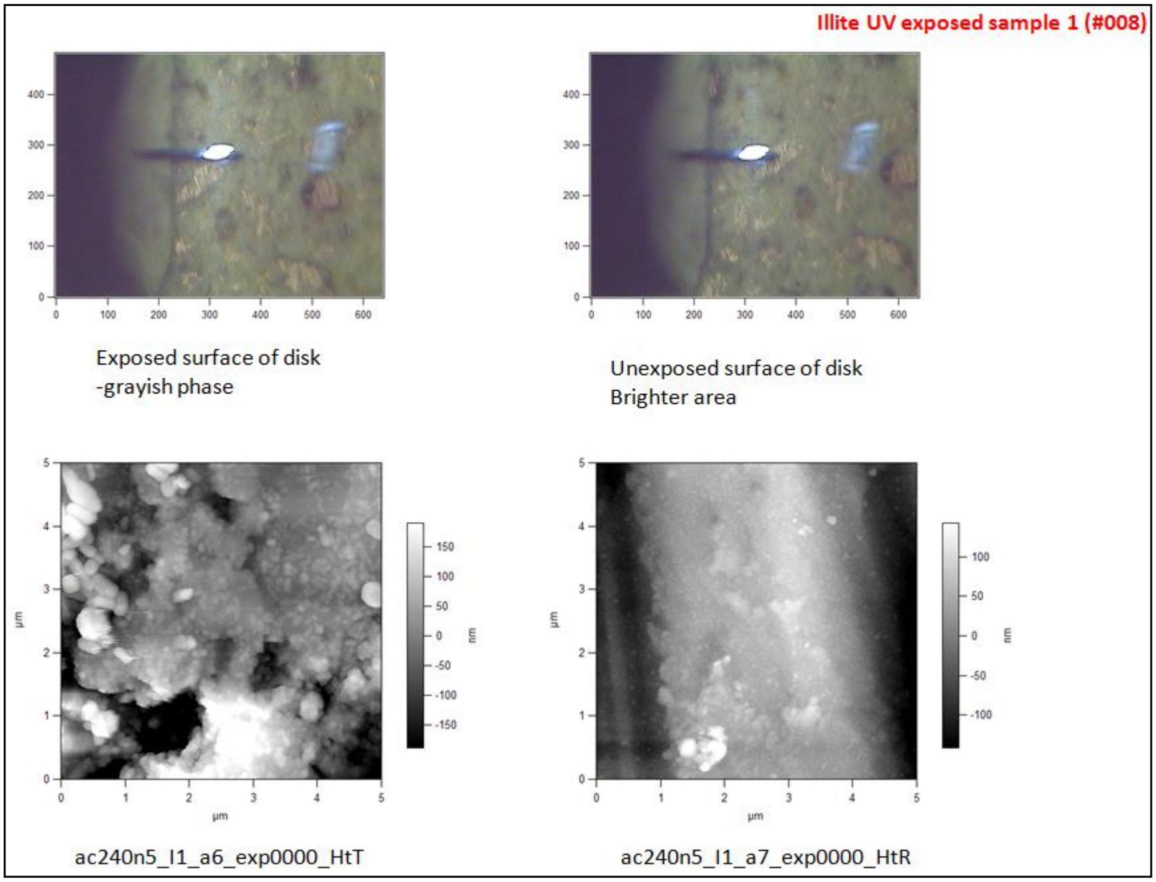

Figure 23. Comparison AFM scans of UV exposed and non-exposed illite surface

AFM testing was also performed on the UV exposed illite and metakaolin. Sample images of the illite UV exposed samples at the same scale obtained with AFM show a clear difference between the exposed and non-exposed sample, as seen in Figure 23. The surface morphologies are clearly different. The UV exposed illite shows a pitted surface consistent with particle impact and erosion while the non-exposed surface is more consistent and without the impact cratering. However, when analyzing the root mean square (RMS) surface roughness, the unexposed sample shows a higher value (1.081 um mean image value vs. 0.628 um mean image value), in the data from Figure 24. This may

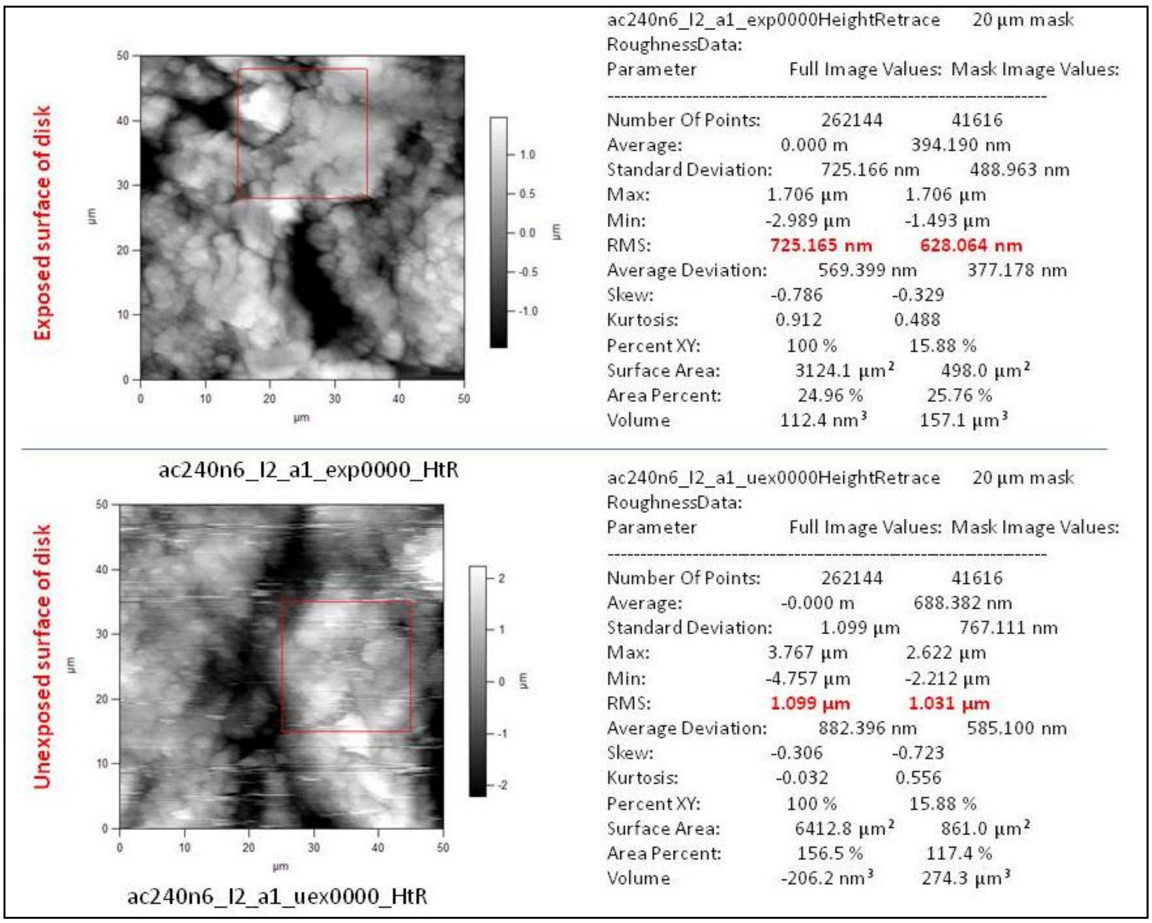

Figure 24. AFM comparison of illite UV exposed and non-exposed samples with statistical analysis

be because when the UV exposure at the surface activates the response mechanism in the geopolymer, the polymer matrix bonds schism and collapse to a more stable, compact energy state, similar to organic polymer behavior. Hence, the variation in surface roughness decreases (by 41% as shown in the example in Figure 24) as the geopolymer surface collapses down on itself due to the rearrangement of the polymer matrix. But this

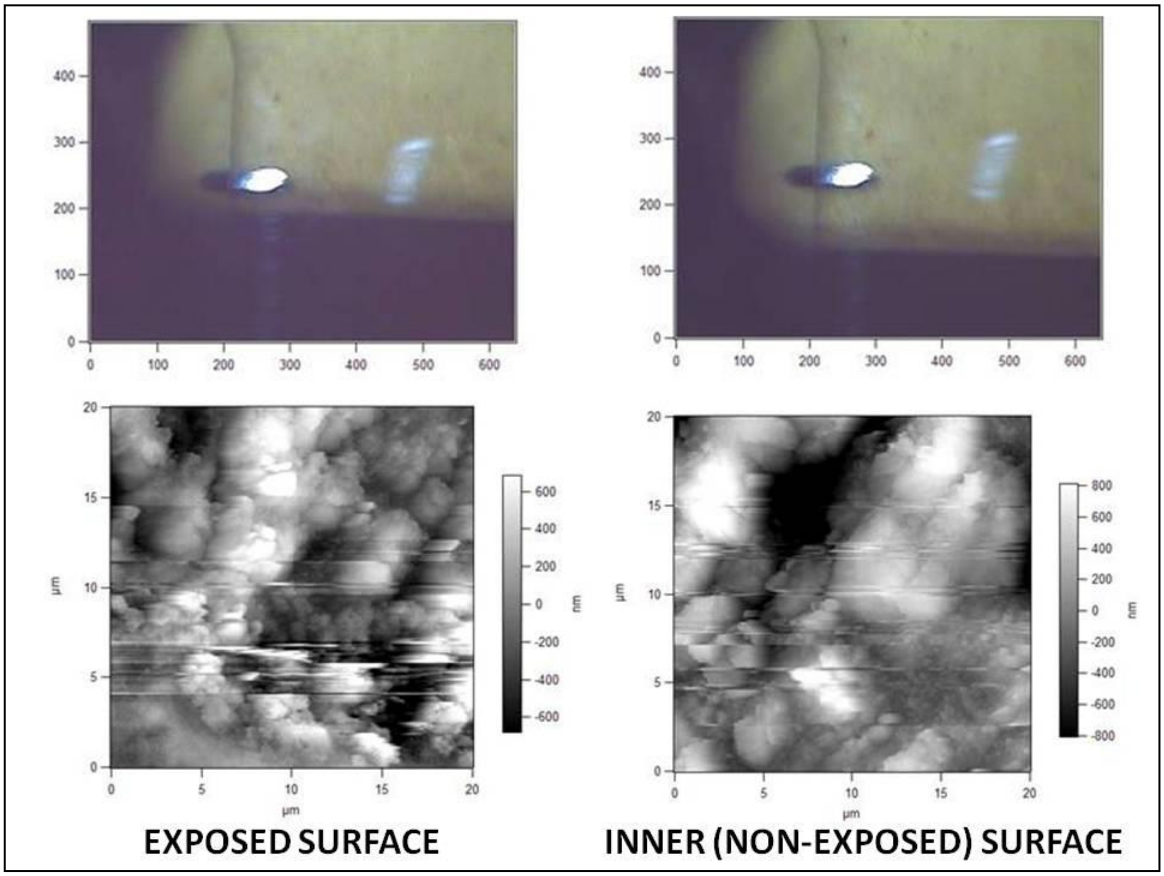

Figure 25. AFM side profile scan of UV exposed illite progressing toward inner (non-exposed) material

effect was only limited to the surface. When an AFM scan was done along a cross-section depth profile (Figure 25), there was not a clear boundary which could be identified between the exposed surface and inner layers of material. This leads to the conclusion that the exposure effects were limited to being only present at the surface.

Even on the surface, with differences on the order of 2 microns from peak to valley (see Figure 24), this has to be taken into effect when considering surface polishing. If a reflecting surface is attached, the adhesive chosen must fill in the cracks and provide a smoother surface, otherwise print through can be an issue. Print through is a complication in adhering nanolaminates to mirror substrates. If the surface roughness of the mirror substrate is rough, the nanolaminate can actually settle into the "valleys" of the mirror substrate surface. This introduces areas of non-flatness which can introduce aberrations into the optical system. If the print through is at wavelength or larger size, this can affect the optical quality of the reflecting surface.

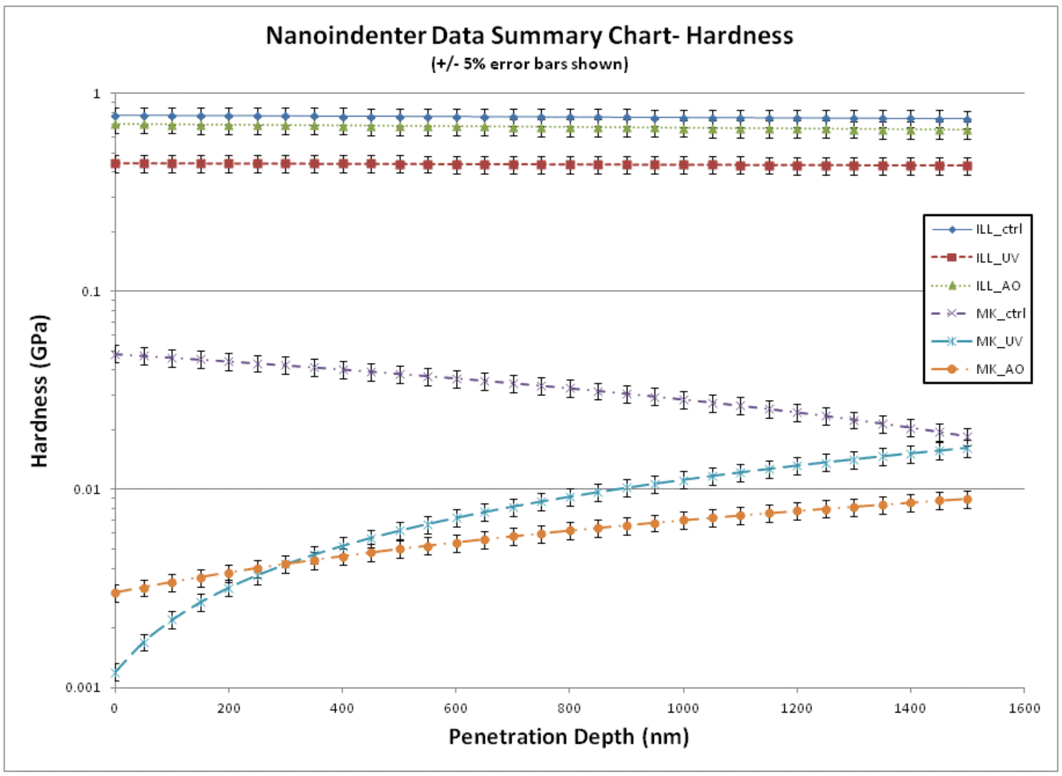

Figure 26. Nanoindenter data summary chart, trendlines, hardness

Mechanical testing of the UV exposed samples was performed on the nanoindenter mentioned previously. A continuous scan method (CSM) was performed which allowed a depth profile to be determined. Data was collected on calculating both hardness and Young's modulus and plots of hardness and modulus are shown in figures below grouped

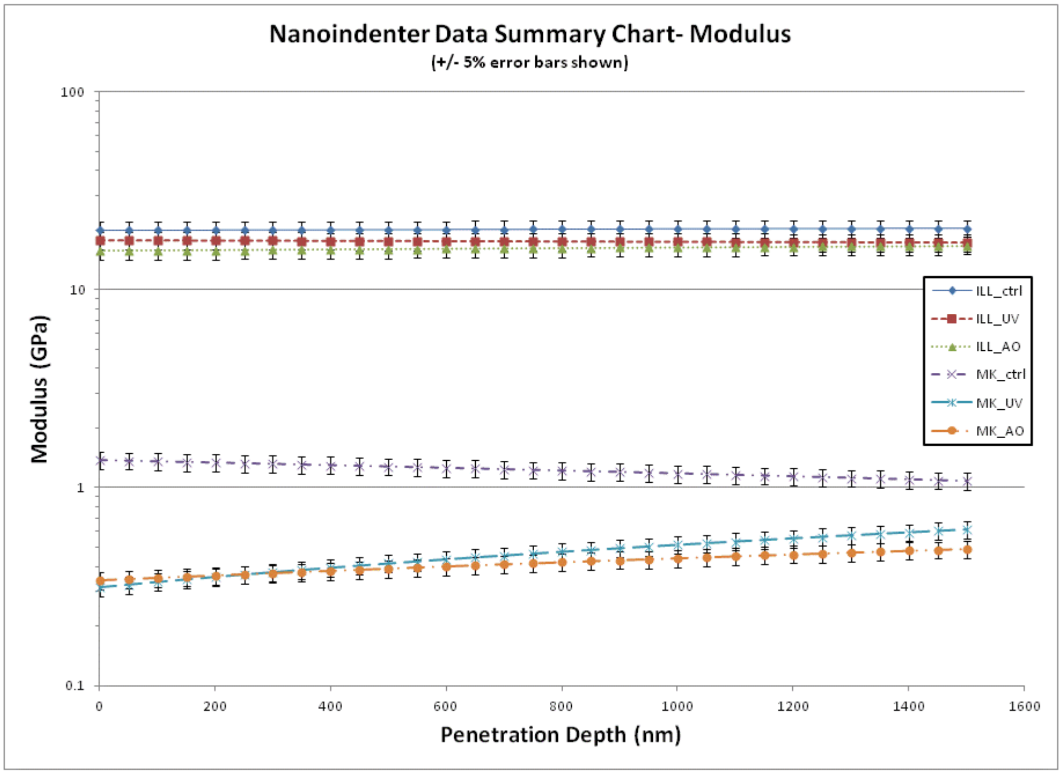

Figure 27. Nanoindenter data summary chart, trendlines, modulus

by test type and material. While one of the UV exposed metakaolin samples fractured during exposure testing, there was sufficient UV exposed metakaolin material remaining to use for nanoindenter testing. The test value (hardness or modulus) is plotted on the y-axis with probe displacement from the surface (i.e. penetration depth) is on the x-axis.

The combined trendline data accumulated through multiple test runs on the nanoindenter apparatus is seen in Figure 26 and Figure 27. In the graph, the trendlines for each type of test were calculated by combining the nanoindenter for all runs of a similar sample, then using a linear fit to “average” all the runs on a similar sample. Also shown are +/- 5% error bars to represent the inherent 5% error calculated by the nanoindenter as a result of

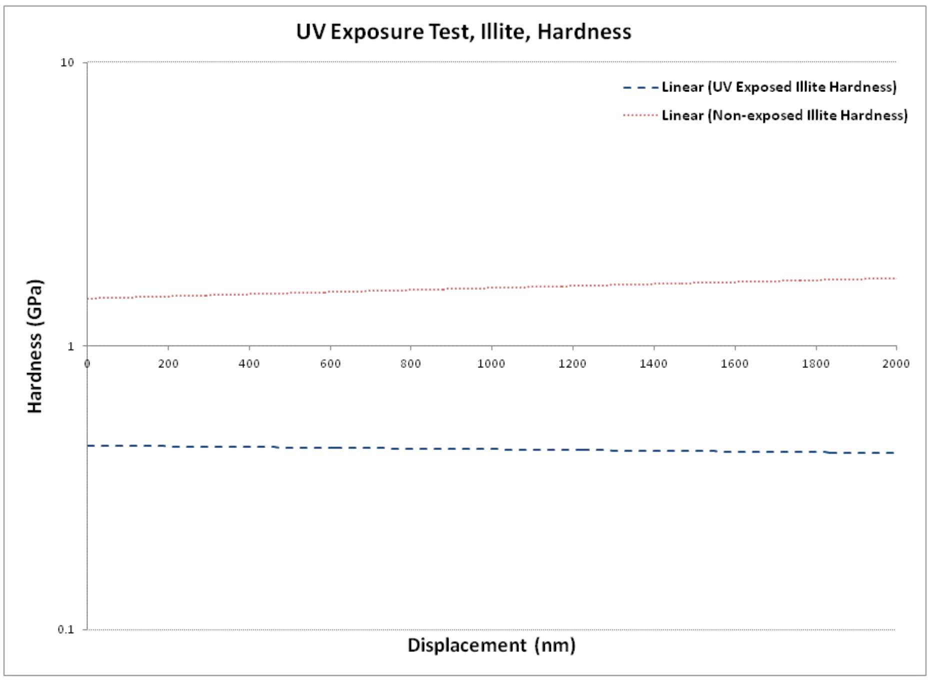

Figure 28. Nanoindenter data trendline, hardness, UV exposed illite

the CSM method with an estimate of Poisson’s ratio as discussed earlier. Contained in the legend on the graph are explanations of each data set: “ILL_ctrl” is the unexposed illite sample, “ILL_UV” is the ultraviolet and high energy particle exposed illite sample, “ILL_AO” is the atomic oxygen exposed illite sample, “MK_ctrl” is the unexposed metakaolin sample, “MK_UV” is the ultraviolet and high energy particle exposed metakaolin sample, and “MK_AO” is the atomic oxygen exposed metakaolin sample. A brief inspection of the graph shows that the illite samples converge to similar values the deeper into the material the probe travels, signifying that the bulk illite material is unaffected by the exposure regimes. While the metakaolin samples at the surface are more divergent than the illite samples at a similar depth, the values for both hardness and modulus begin to converge later in the material. This also shows a general trend of the

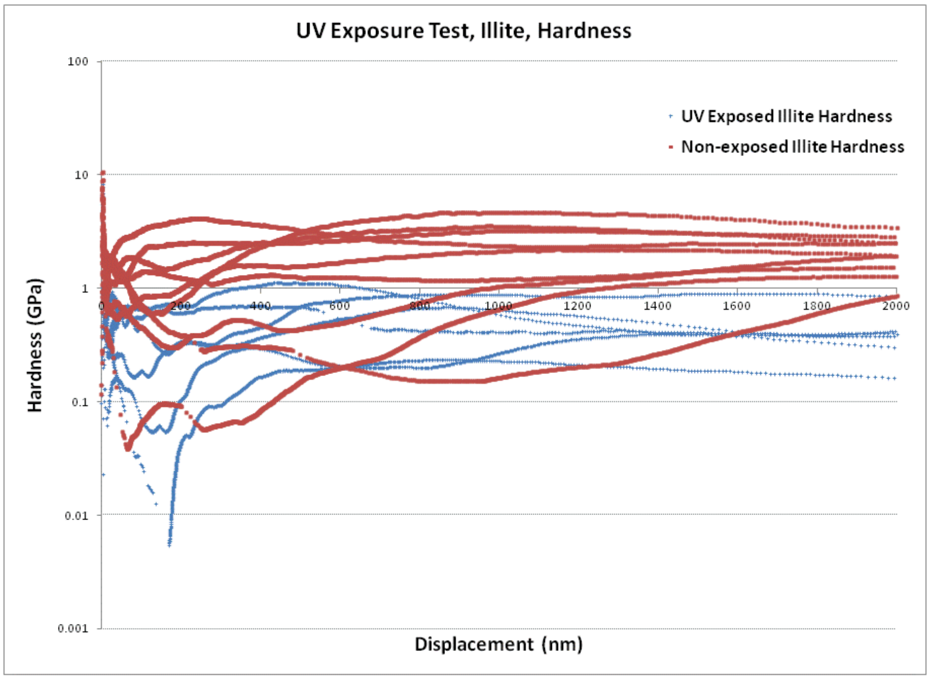

Figure 29. Nanoindenter data, hardness, UV exposed illite

material being affected on the surface by the exposure regimes, but that the bulk material remains unaffected. These results are expanded upon in the sections to follow.

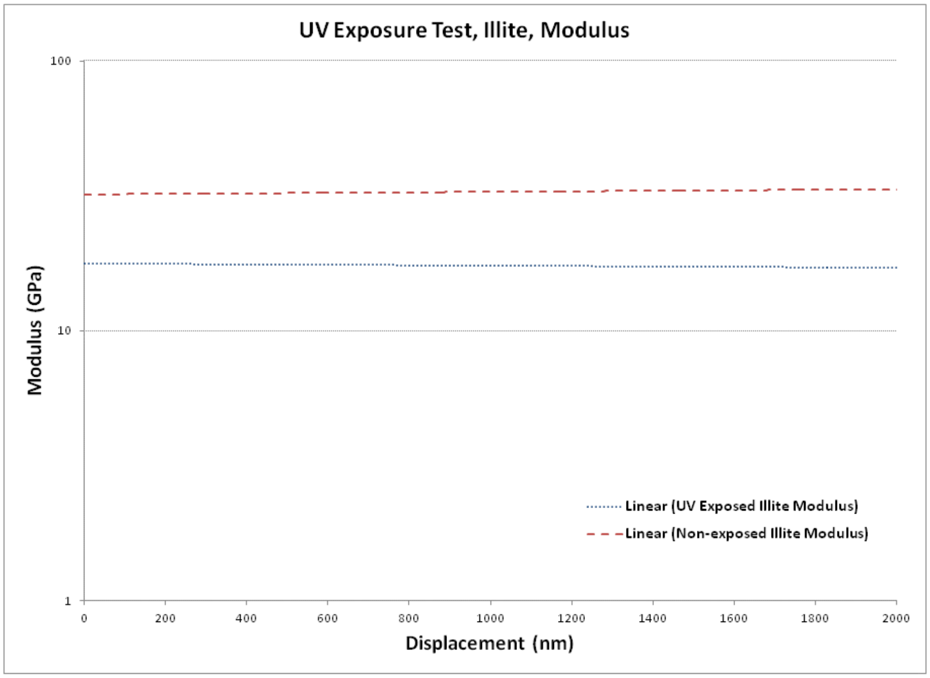

Figure 30. Nanoindenter data trendline, modulus, UV exposed illite

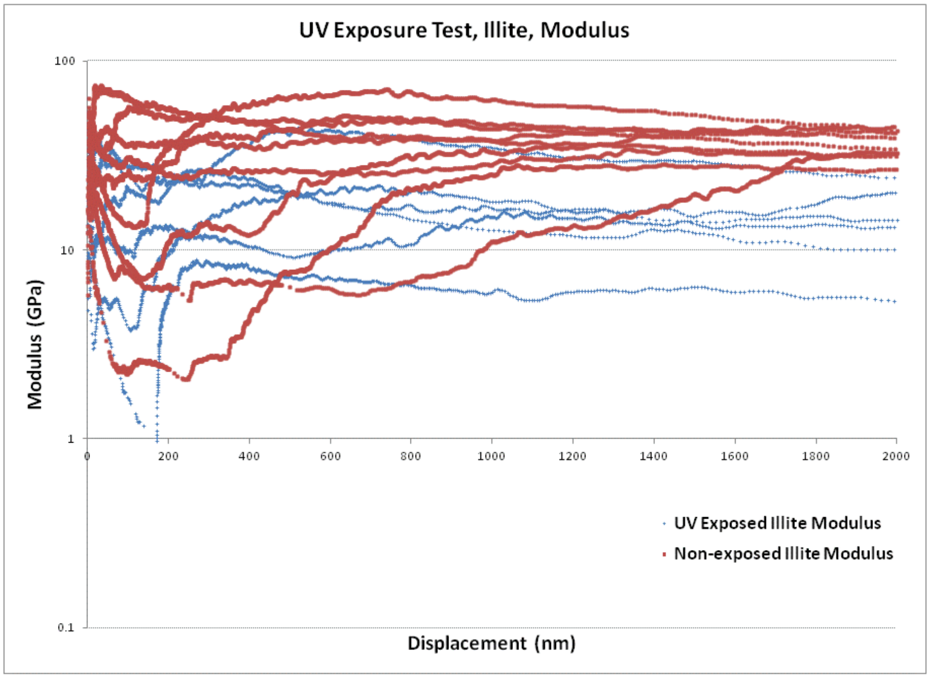

Figure 31. Nanoindenter data, modulus, UV exposed illite

The UV exposed illite data is shown in Figure 28 - 31. For each measurement of hardness and modulus, a corresponding trendline has been calculated for that data set using a linear regression fit. Figure 28 & 29 shows that for hardness in UV exposed illite, hardness is slightly lower overall than the non-exposed sample (~ 0.5 GPa for exposed vs. 1.5 GPa for non-exposed). This means that the UV exposed material is "softer" than the non-

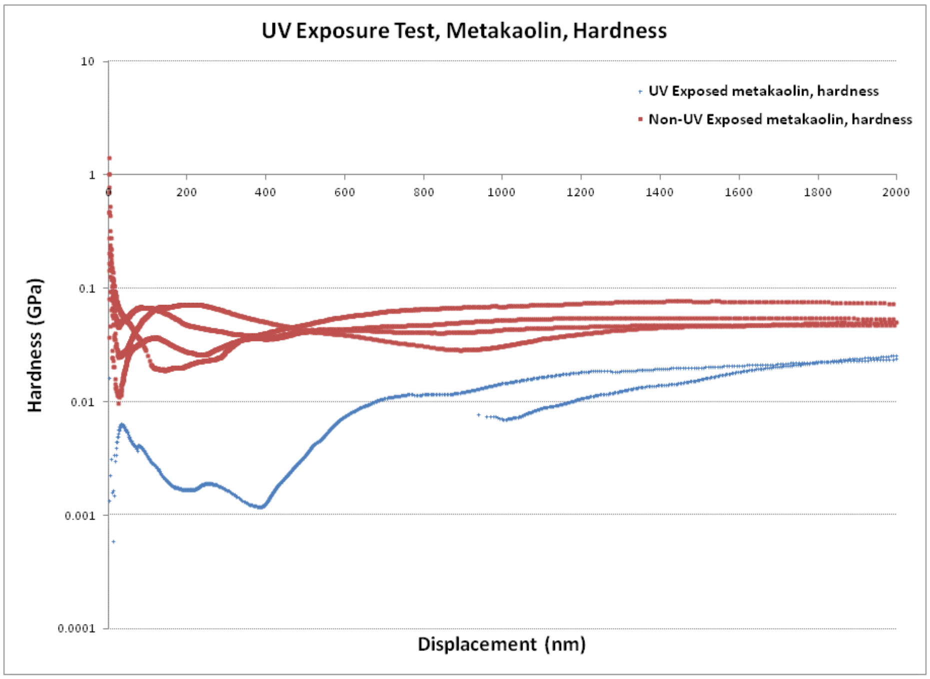

Figure 32. Nanoindenter data, hardness, UV exposed metakaolin

exposed sample. The modulus data in Figure 30 and Figure 31 also show a decrease in measured value between the non-exposed and exposed illite samples. This behavior is not consistent with typical organic polymer behavior where hardness increases after UV exposure due to separation of polymer chains and reformation into more compact polymer matrices.

However, this effect has been seen in some organic polymers when exposed to UV radiation and when noting a significant temperature increase (like with happened with the geopolymer samples on the SCEPTRE mounting plate), the modulus and hardness actually decrease after UV exposure. (Wallace 1990) This has been traced to heat induced softening of polymers which actually counteracts the UV exposure effects. It is believed that this is what happened with the illite samples during their UV exposure.

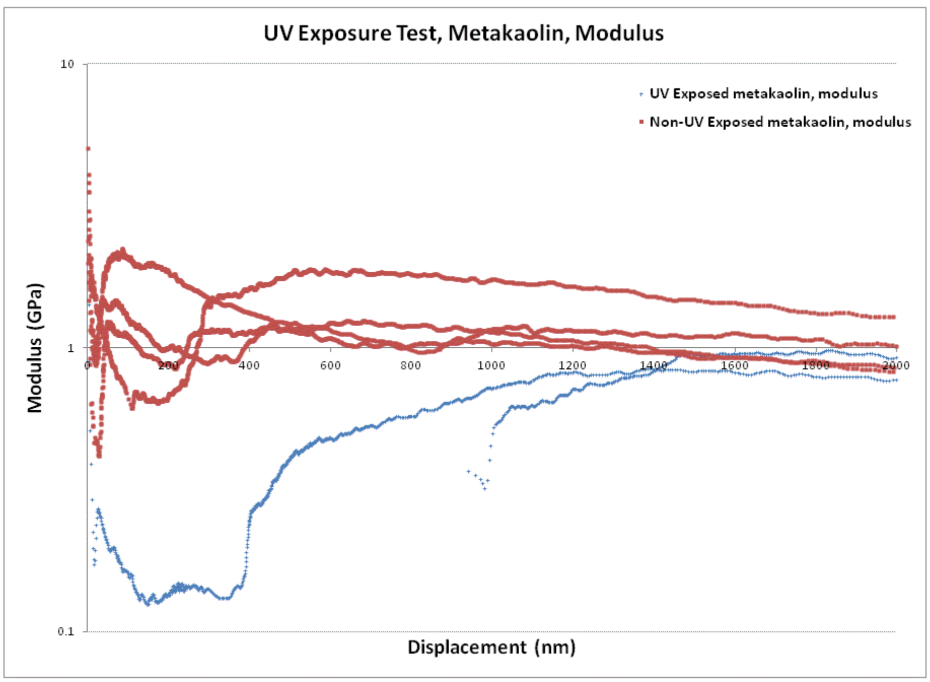

Figure 33. Nanoindenter data, modulus, UV exposed metakaolin

Variations in hardness and modulus of the illite samples with respect to depth over the first 1000 nm penetrated depth of exposed material are also seen, but between 1000 - 1200 nm, the effect is seen to level off. This is consistent with surface effects where additional hydrate or oxide layers are present, transitioning to a more homogenous bulk material on the interior. These variations are not unexpected and are not an indication of significant effects by the exposure itself.

The UV exposed metakaolin data is shown in Figure 32 - 35. In Figure 32 and Figure 33, data from one UV exposed test series below 1000 nm was discarded due to a calibration

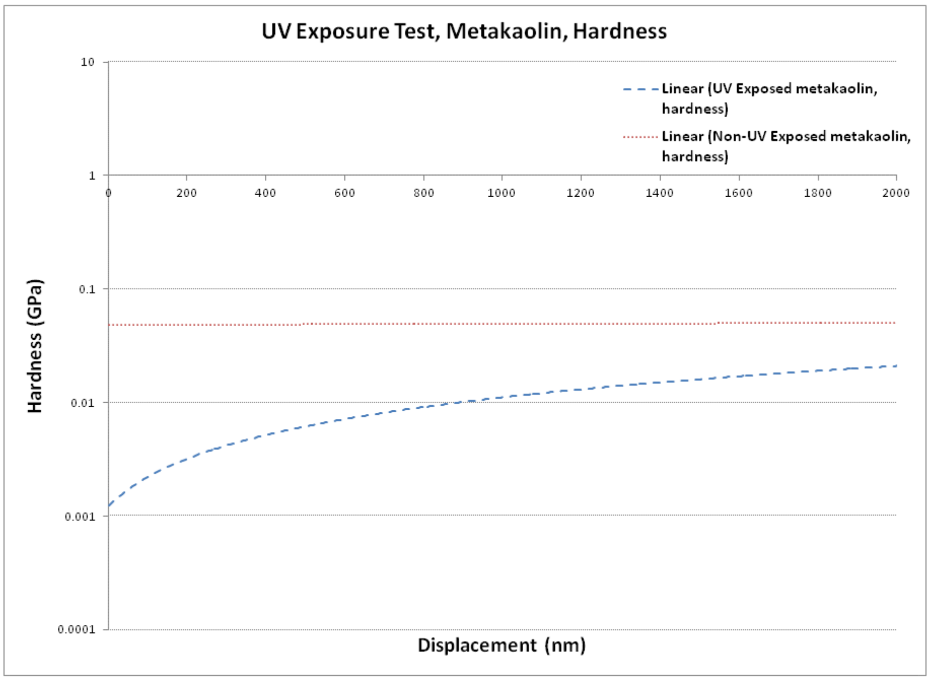

Figure 34. Nanoindenter data trendline, hardness, UV exposed metakaolin

error on the nanoindenter associated with an unexpected but significant laboratory vibration disturbance. For each measurement of hardness and modulus, a corresponding trendline has been calculated for that data set using a linear regression fit. Figure 32 & Figure 34 show that for hardness in UV exposed metakaolin, hardness is slightly lower overall than the non-exposed sample (~ 0.02 GPa for exposed vs. ~0.08 GPa for non-exposed according to the trendlines plotted in Figure 33). This means that the UV exposed material is "softer" than the non-exposed sample. Even with this difference in hardness value at the surface layers however, the hardness values for both exposed and non-exposed samples begin to converge within an order of magnitude the deeper in the material the data is recorded.

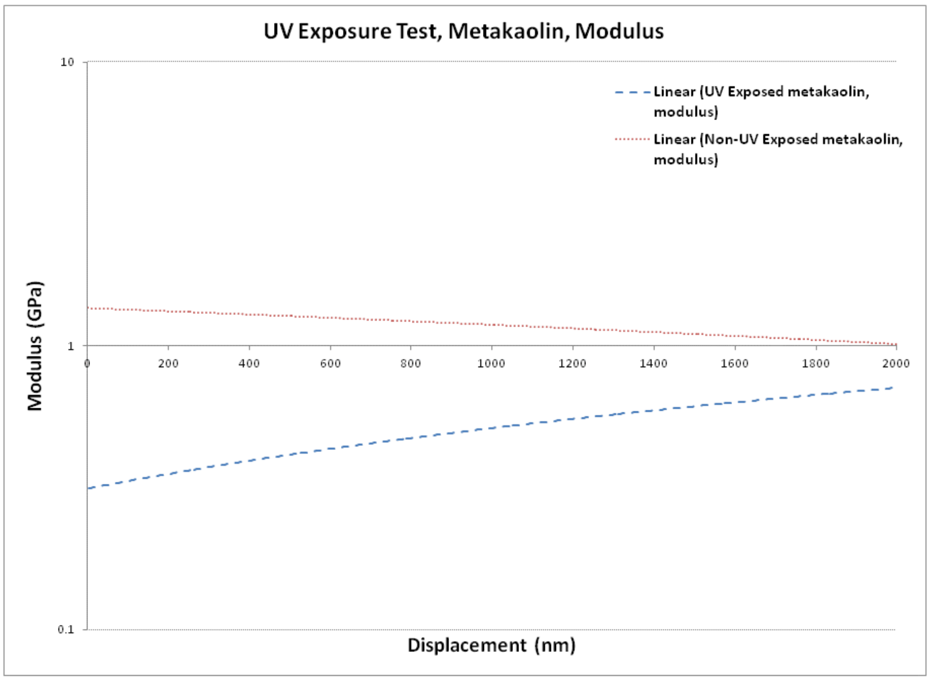

Figure 35. Nanoindenter data trendline, modulus, UV exposed metakaolin

The modulus data in Figure 33 and Figure 35 also show a decrease in measured value between the non-exposed and exposed metakaolin samples. However, the trendlines plotted in Figure 35 show that again, the average modulus value for both exposed and non-exposed samples begin to converge around 1 GPa the deeper in the material the data is taken. This shows that interior material on the exposed sample was not affected by the UV exposure since its behavior is indistinguishable from the bulk material of the non-exposed sample. This also suggests that UV exposure is limited to effects contained within approximately the first micron of surface depth. Both the hardness and modulus data for metakaolin show similar trends and behaviors to the illite samples, thus suggesting that this behavior is a geopolymer behavior.

.

Observations & summary- UV & high energy testing

While the UV & high energy particle exposed samples did exhibit fracturing following the SCEPTRE chamber exposure, analysis of the samples surface and mechanical parameters lead us to believe that the cause of the fracturing was due to thermal effects associated with the mounting and heat management subsystem of the SCEPTRE chamber mounting apparatus, and not directly related to the UV or high energy exposure itself.

This means that after use in a space environment, the geopolymer will not soften and weaken (as seen in the hardness and modulus data) due to UV exposure alone. With an active thermal control system, the materials should only exhibit minimal surface deformations in physical performance. The differences between material morphology as exhibited in the AFM data and the limited penetration of hardness change in the geopolymers all suggest superficial surface layer effects that can be easily mitigated with good systems engineering that limits the external exposure of the material to direct illumination conditions (i.e. used in internal structures, as an adhesive between two materials, or coated with a protective laminate layer).

The spectrograph data is important for two reasons. First, since the illite and metakaolin had similar behavior changes, it can be assumed that they were impacted similarly by the combination of UV and high energy electron exposure. Second, a change in infrared reflectivity toward higher values means that the material will have less thermal capacitance. This is important as thermal properties need to be stable over the lifetime of satellite missions as the thermal control subsystems on spacecraft are delicately balanced. If thermal properties of materials change on orbit, thermal stresses can be introduced on joints and connection points, possibly introducing optical distortions if that stress is at an optical payload interface.

Atomic oxygen exposure testing

Before discussing the AO exposure results from the evaluation test sequence, an anomaly during the AO exposure in the chamber must be noted for the record. When the samples were extracted from the AO chamber it was noticed that the metakaolin sample had fractured and shifted in the holding plate. There still was a stable exposed portion of the sample present underneath the aluminum mask and the experiments as planned were valid. The illite sample was seen to be seemingly intact. While no definitive explanation is present at this time, it is believed that a heat buildup occurred in the aluminum mask which caused the aluminum mask to buckle over the metakaolin sample and put pressure on the metakaolin to the point that the metakaolin sample fractured and shifted. That fracturing allowed a stress relief for the aluminum plate and there was no further anomalies noted during the exposure testing. Photos of the anomaly with an explanation at each step are presented in Figure 36. The two exposure areas on the metakaolin sample that occurred when the metakaolin block shifted are clearly seen.

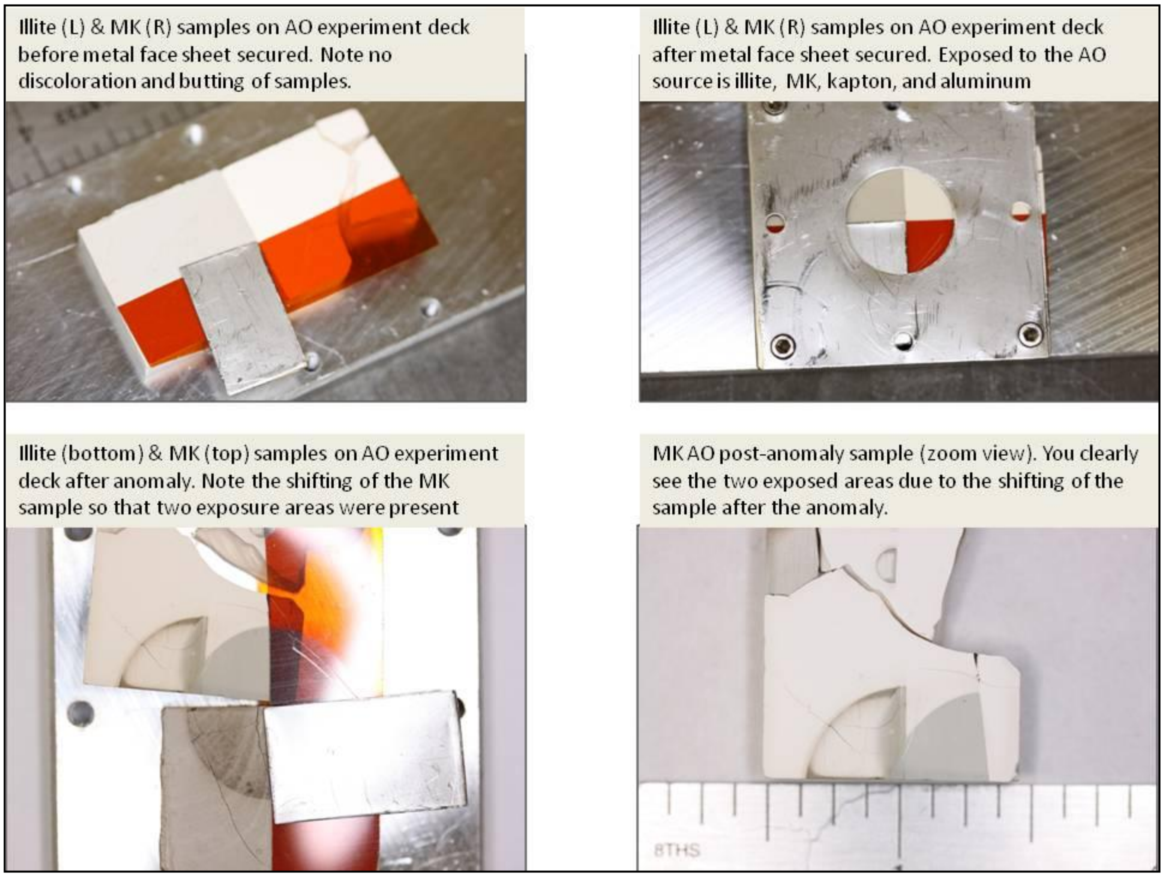

Figure 36. AO anomaly photographs and explanation of the event

AO Exposure results

Upon visual inspection, it is obvious where the exposed and masked surfaces were on the samples. The exposed surfaces on both illite and metakaolin showed a definitive color change indicating that some effect was present. The question is to what extent did the AO exposure change the surface of the material and if there are significant erosion markers present.

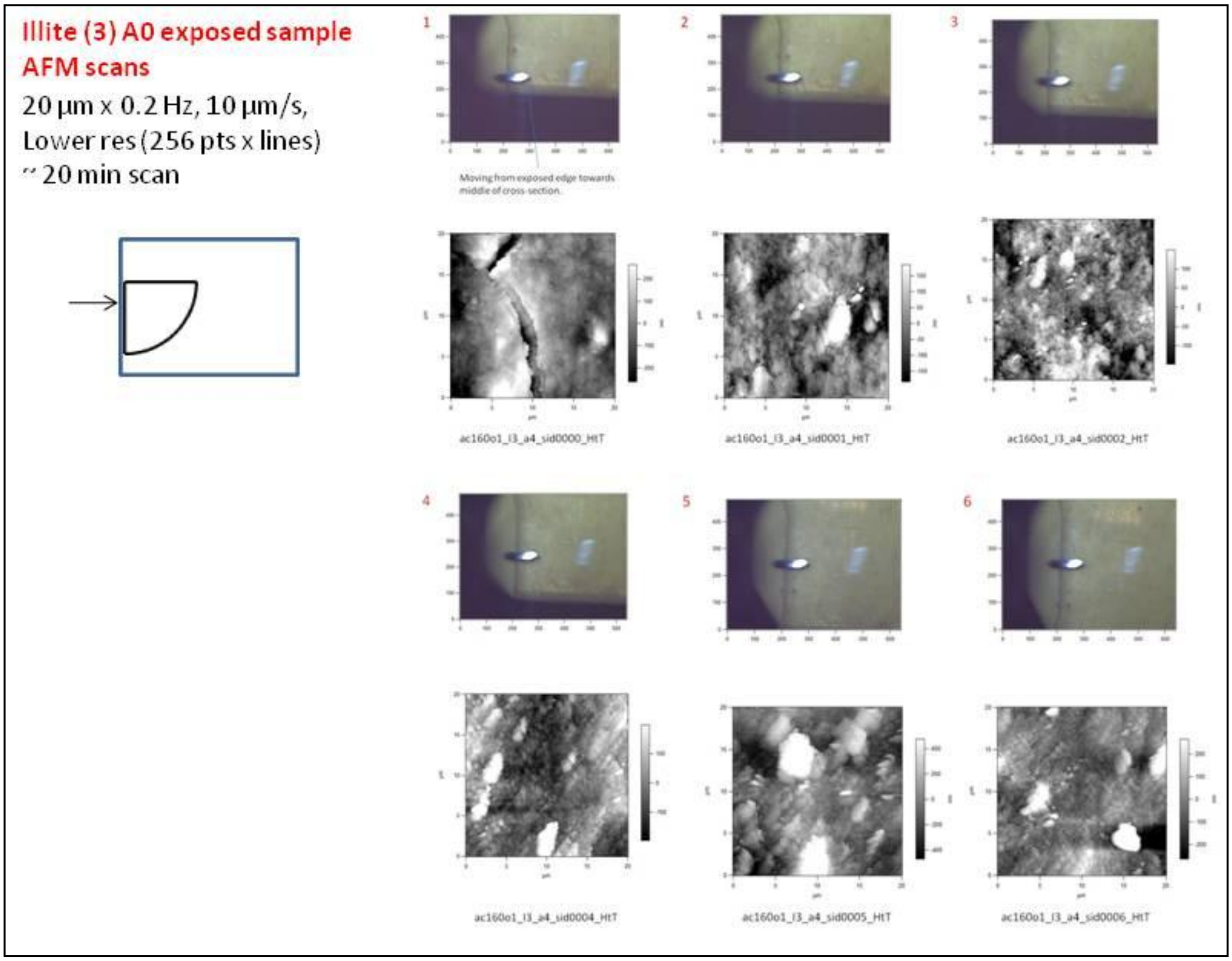

Figure 37. AFM scans of illite after AO exposure, side profile

The illite and metakaolin samples were scanned with AFM to record surface changes as a result of AO bombardment. Analysis showed interesting results. Qualitatively, the AFM images couldn't consistently be used to define the border region between the exposed and non-exposed sides of the same samples, as in Figure 37. AFM scans across the surface of the exposed samples. Additionally, depth profile scans where the probe started at the exposed surface and scanned down a side of the sample in terms of depth were performed, as seen in Figure 37. Neither style of AFM scan was able to define a transition state either on the surface or in depth between exposed and non-exposed portions of the samples.

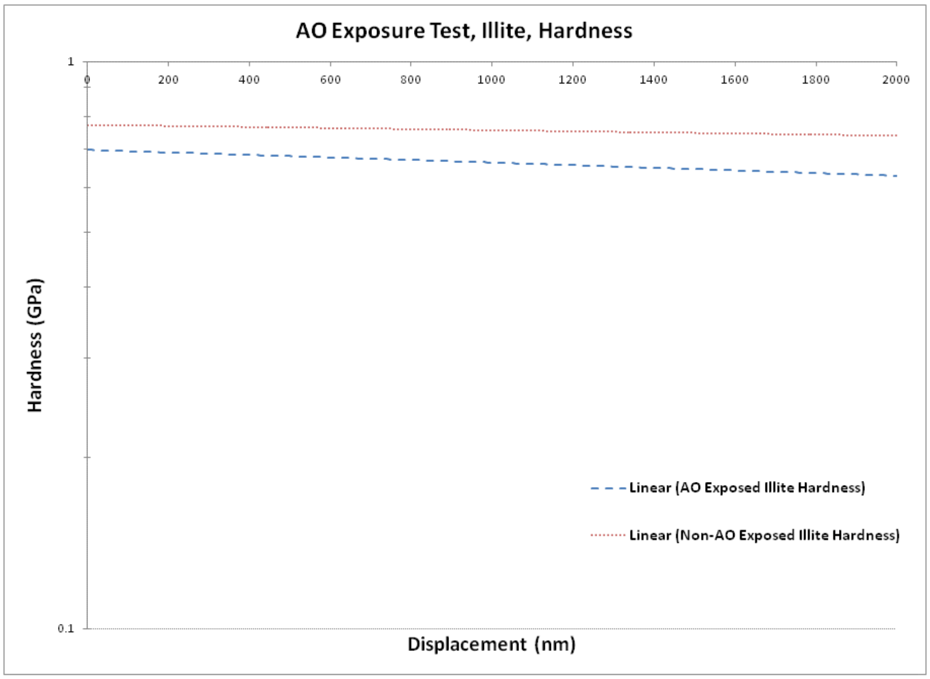

Figure 38. Nanoindenter data trendline, hardness, AO exposed illite

The surface roughness of the AO exposed illite measured 1.03 microns RMS. The metakaolin measured approximately 200 nm RMS in surface roughness. One other issue apparent on the AFM scans is that some of the surface features are showing differentials from peak to valley as over 2 microns in masked areas. This means that if used as a structural mirror substrate, an adhesive used in bonding reflective surfaces to the substrate must fill in the valley cracks, otherwise print-through of those cracks may propagate to the optical surface. Because this print-through would be on the order of wavelengths for near IR and below wavelengths, these features would not allow this

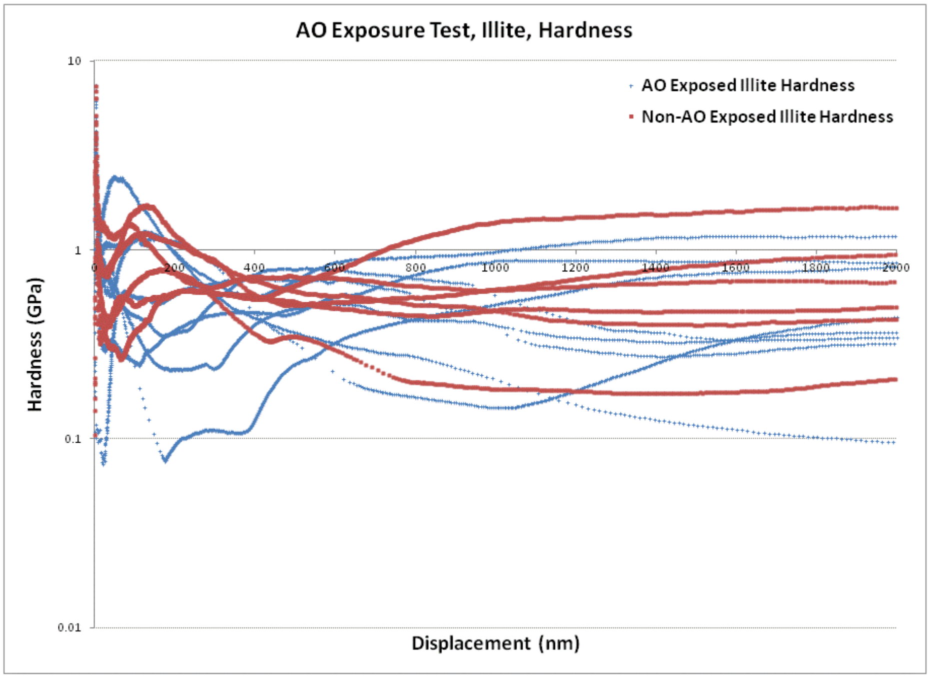

Figure 39. Nanoindenter data, hardness, AO exposed illite

material to be used as mirror reflecting surfaces of wavelength similar to and below the peak to valley size of the surface feature. An alternative would be to polish the adhering surface to an appropriate optical flatness.

Mechanical testing of the AO exposed samples was performed on the nanoindenter mentioned previously. Hardness and modulus data are calculated using the CSM test and the graphs display the individual data points and trendlines as a function of probe depth. This data is presented in Figure 38, Figure 39, Figure 40, and Figure 41 for the AO exposed illite samples. AO exposed metakaolin sample data is shown in Figure 42, Figure 43, Figure 44, and Figure 45. Each trendline was calculated based on a second order polynomial regression fit.

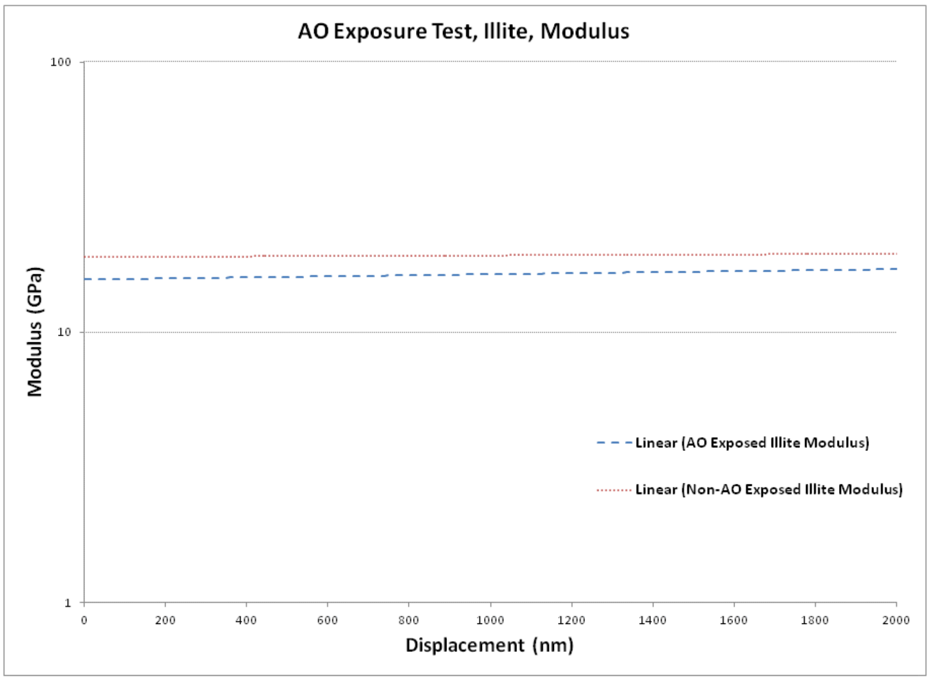

Figure 40. Nanoindenter data trendline, modulus, AO exposed illite

The AO exposure showed similar behavior to the UV exposure test series. For the AO exposed illite, Figure 39 shows that the individual hardness tests of AO exposed illite and non-exposed illite are smeared together with no discernable difference. The trendline for both the AO exposed and non-exposed illite from Figure 38 shows minimal differences in the average values as depth is increased (~0.8 GPa at the surface for both samples, decreasing to 0.5 – 0.75 GPa at the 2000 nm penetration depth limit). Both these results show that for hardness, illite is not affected by AO exposed in a statistically significant way.

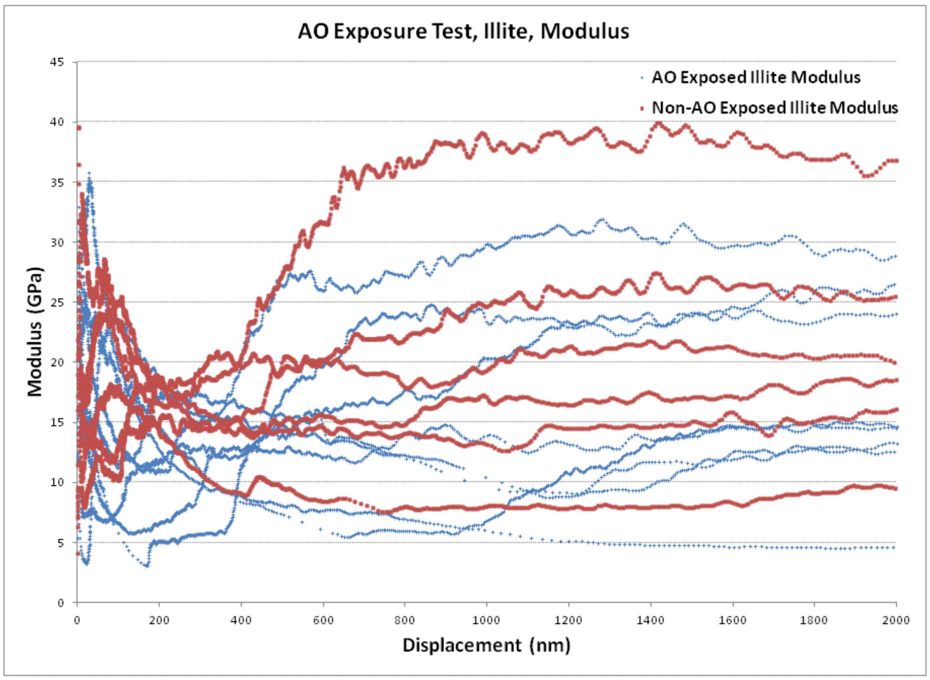

Figure 41. Nanoindenter data, modulus, AO exposed illite

Modulus data in Figure 40 and Figure 41 also shows the same behavior—no discernable difference between the two samples over the entire depth profile. The average value of modulus changes over the 2000 nm penetration depth from approximately 18 GPa to 20 GPa for non-exposed illite, while the exposed illite changes from about 15 GPa to 17.5-18 GPa.

Both hardness and modulus data show an inflection point in behavior around 200 nm. Since it is seen in both AO exposed and non-exposed samples and the data trends continue consistently between samples as penetration is increased regardless of the exposure regime, this is assumed to be a surface effect of a slight difference in chemical composition (i.e. a hydrate or oxide layer due to exposure with the atmosphere) than an effect generated by the AO exposure.

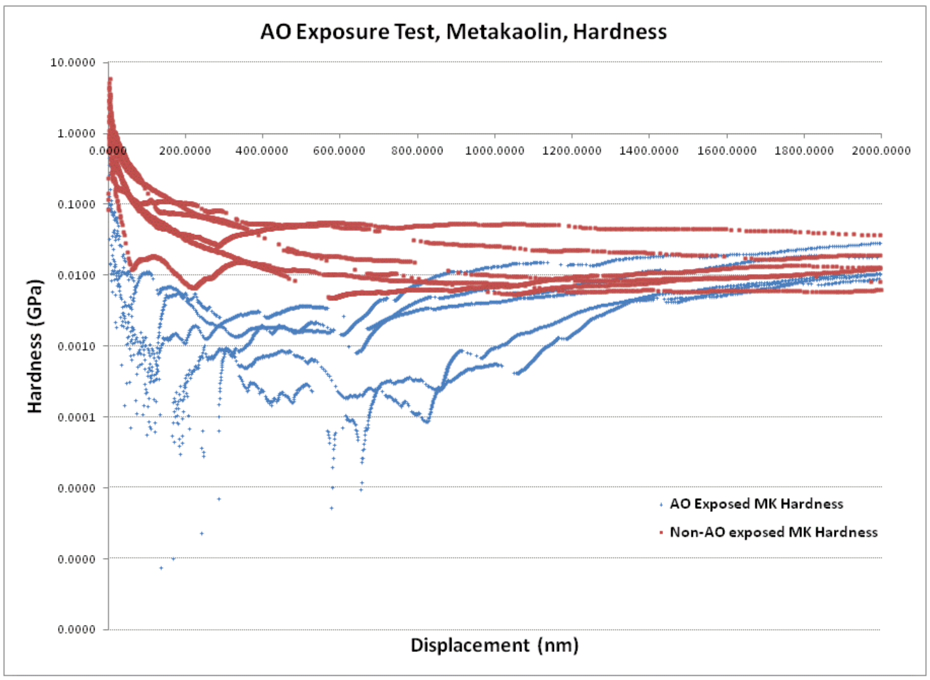

Figure 42. Nanoindenter data, hardness, AO exposed metakaolin

Metakaolin samples for the AO test show a similar absence of significant differences between the AO exposed and non-exposed samples. In Figure 42, the AO exposed metakaolin has a lower hardness value than the non-exposed sample. Modulus data comparisons in Figure 43 also show the same general behavior. However, since the metakaolin sample was the one of the two samples that was most impacted by the AO test anomaly, it is reasoned that this decreased can be explained away by the same thermal softening theory from the UV exposure tests. To restate, when some polymers were subjected to significantly increased temperature while exposed to a “brittle-ing” agent (UV or AO exposure in this case), the hardness and modulus both decreased in opposition to expected behavior from the exposure alone.

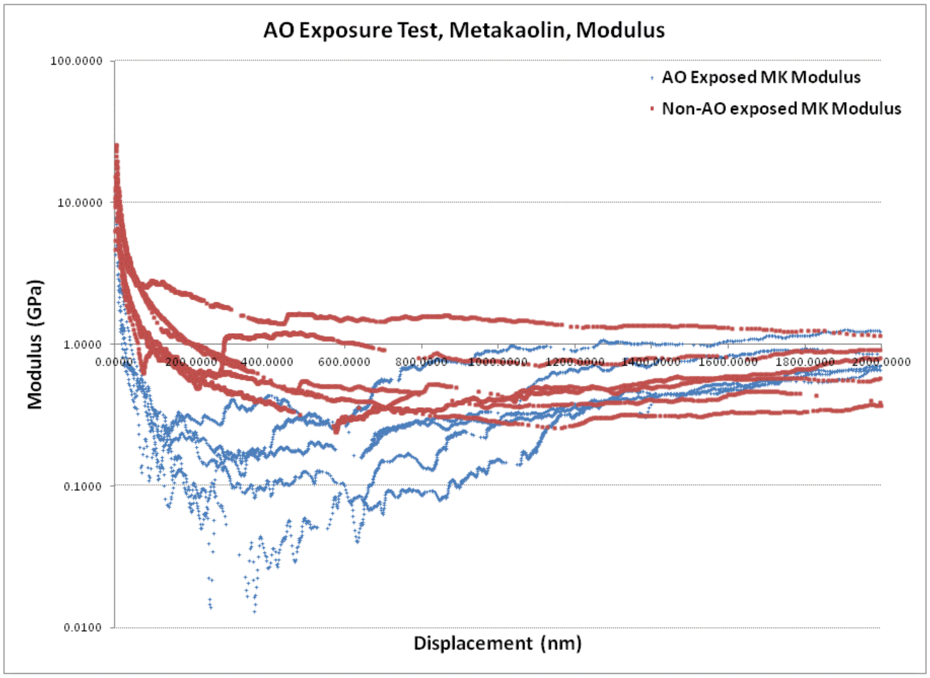

Figure 43. Nanoindenter data, modulus, AO exposed metakaolin

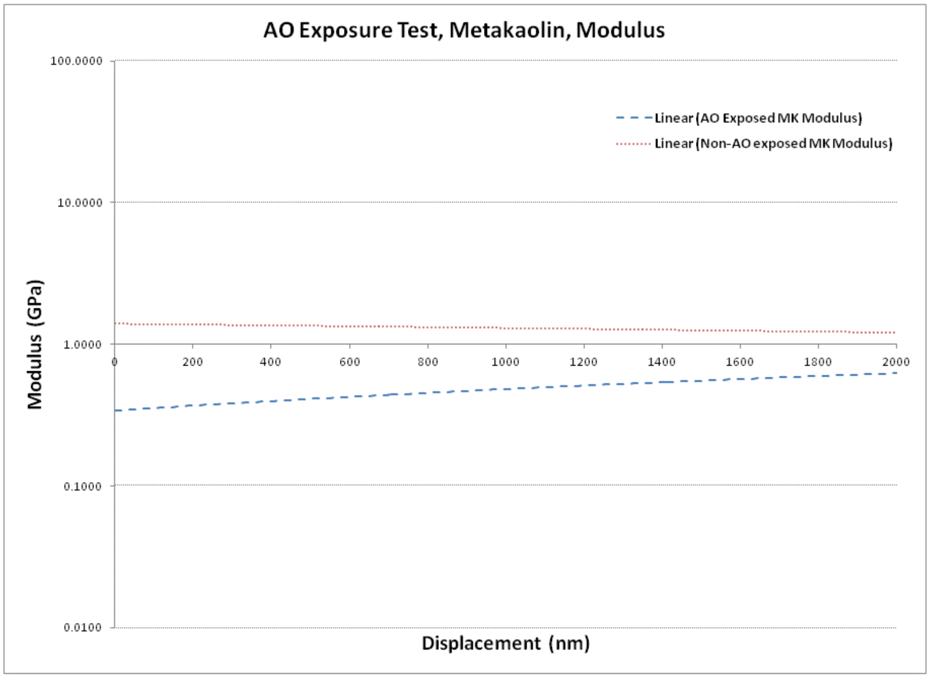

Figure 44. Nanoindenter data trendline, modulus, AO exposed metakaolin

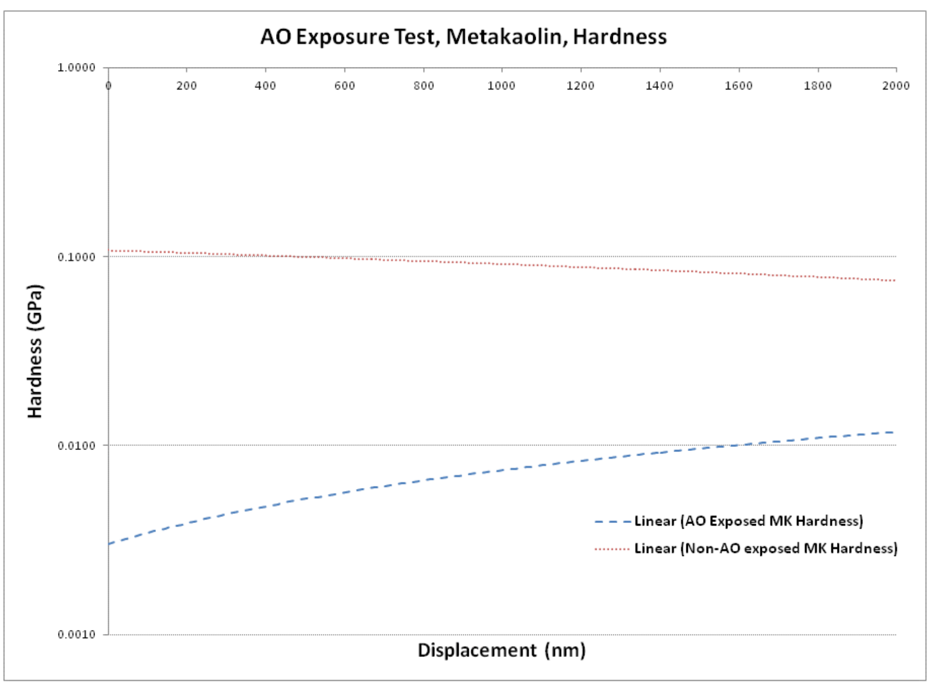

Figure 45. Nanoindenter data trendline, hardness, AO exposed metakaolin

XPS data was also gathered for the AO exposed samples to look for evidence of chemical reactions on the surface due to the atomic oxygen exposure. Each AO exposed sample was placed in the XPS unit and irradiated for testing on the exposed side and the non-exposed side of the sample. This allowed for a direct comparison between the two surfaces.

Data was taken in the form of binding energy spectra measured in eV. This corresponds to the bond energies of the various constituents on the sample being measured. The top (red) lines represent the AO exposed surface and the lower (blue) lines represent the non-exposed surface representing the “bulk material”. Plots are shown for the entire bond energy spectrum, and then magnified plots are shown for key peaks representing points for further discussion. Of significance in the plots is not necessarily the change in amplitude, but whether the same peaks appear in both the surface and bulk material. This signifies if the same chemical constituents are present. Additional plots are shown for each surface independent of the other showing percentage composition of the chemical constituents present.

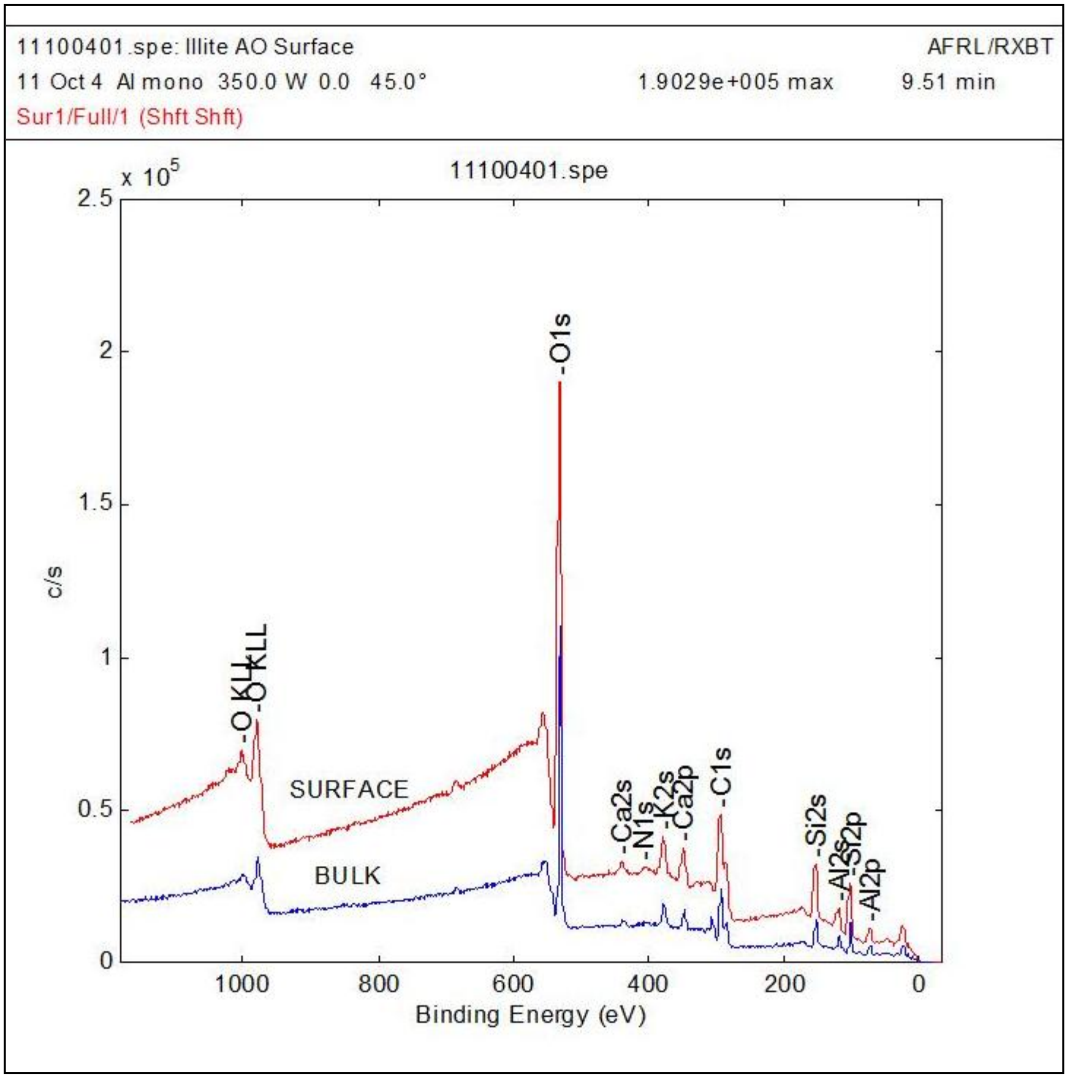

Figure 46. XPS data for illite, AO exposed sample. The top signature (red) is the XPS reading at the exposed surface. The lower signature (blue) is the XPS reading at the non-exposed surface.

The AO exposed illite sample shown in Figure 46 has similar peaks between the surface and bulk material, and at a macro qualitative level, there seems to be little difference between the chemical compositions of the exposed and non-exposed illite surfaces.

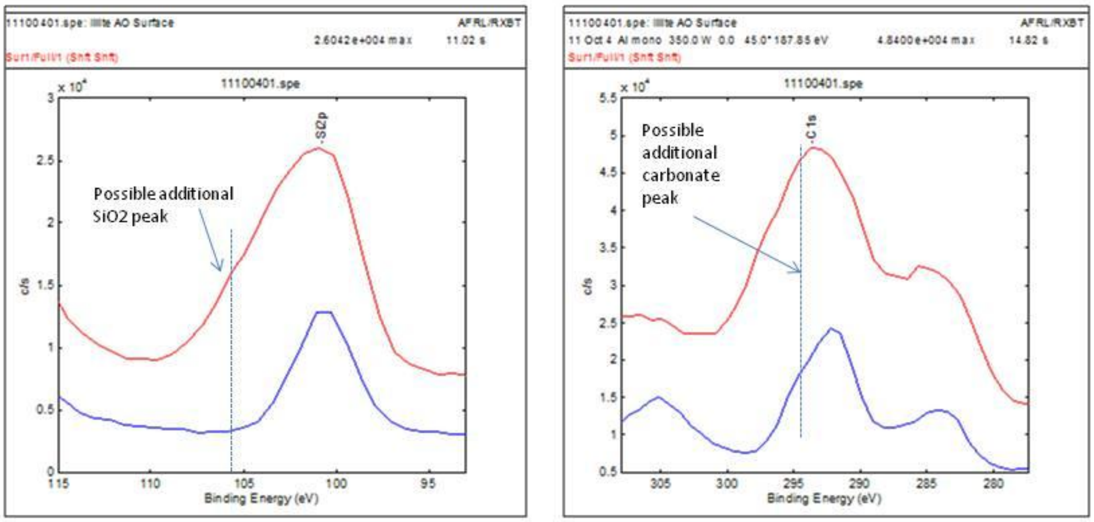

Figure 47. XPS data on AO exposed illite, Si & C peaks

A closer inspection of the peaks around the silicon and carbon bond areas (Figure 47) reveals a few minor changes. The Si 2p atomic orbital peak for the exposed surface shows a potential additional peak around 105 eV. This corresponds to energy associated with a silicon oxide bond, meaning that the exposed sample may have picked up additional SiO bonds-- not unexpected for a silicon based polymer just subjected to bombardment by atomic oxygen. (Casa Software 2011) However, the contribution of this potential peak is extremely small. The carbon peak around 294 eV on the non-exposed surface also may have a slight carbonate peak to it, but this is routinely seen with materials that may have been in contact with biological matter in the preparatory stage for placement in the XPS chamber.

Table 10. Illite XPS relative chemical constituents, AO exposure series

	Illite AO-exposed				Illite non-exposed			
	Test 1	Test 2	Test 3	Avg	Test 1	Test 2	Test 3	Avg
O1s	63.2	63.2	64.6	63.7	60.8	59.8	60.5	60.4
Si2p	16.3	17.2	16.7	16.7	13.3	13.9	13.6	13.6
K2s	7.9	5.4	6.8	6.7	6.8	7	5.1	6.3
Al2p	6	5.9	4.8	5.6	6.6	6.4	6.5	6.5
C1s	4.1	5.9	4.6	4.9	6.5	6.1	7.7	6.8
Ca2p	2.4	2.4	2.2	2.3	2.3	2.4	2.7	2.5
Trace	0	0	0.3	0.1	3.7	4.4	3.9	4.0

Looking at the relative percentages of chemical constituents in the XPS measurements (see Table 10), the primary difference in non-exposed to exposed chemical constituents is the loss of trace materials (N, F, Na) from the non-exposed side to the exposed side. This is likely due to the AO reacting with and eroding away the compounds where those trace elements were located. This part of the material was compensated for on the exposed side by higher oxygen concentrations, suggesting that additional oxide layers were formed by the reaction of the atomic oxygen impacting surface metallic and semi-metallic elements present in the geopolymer matrix, raising the overall concentration of oxygen on the exposed surface. This small difference in composition between the exposed and non-exposed surfaces suggests the AO exposure had minimal impact on the geopolymer.

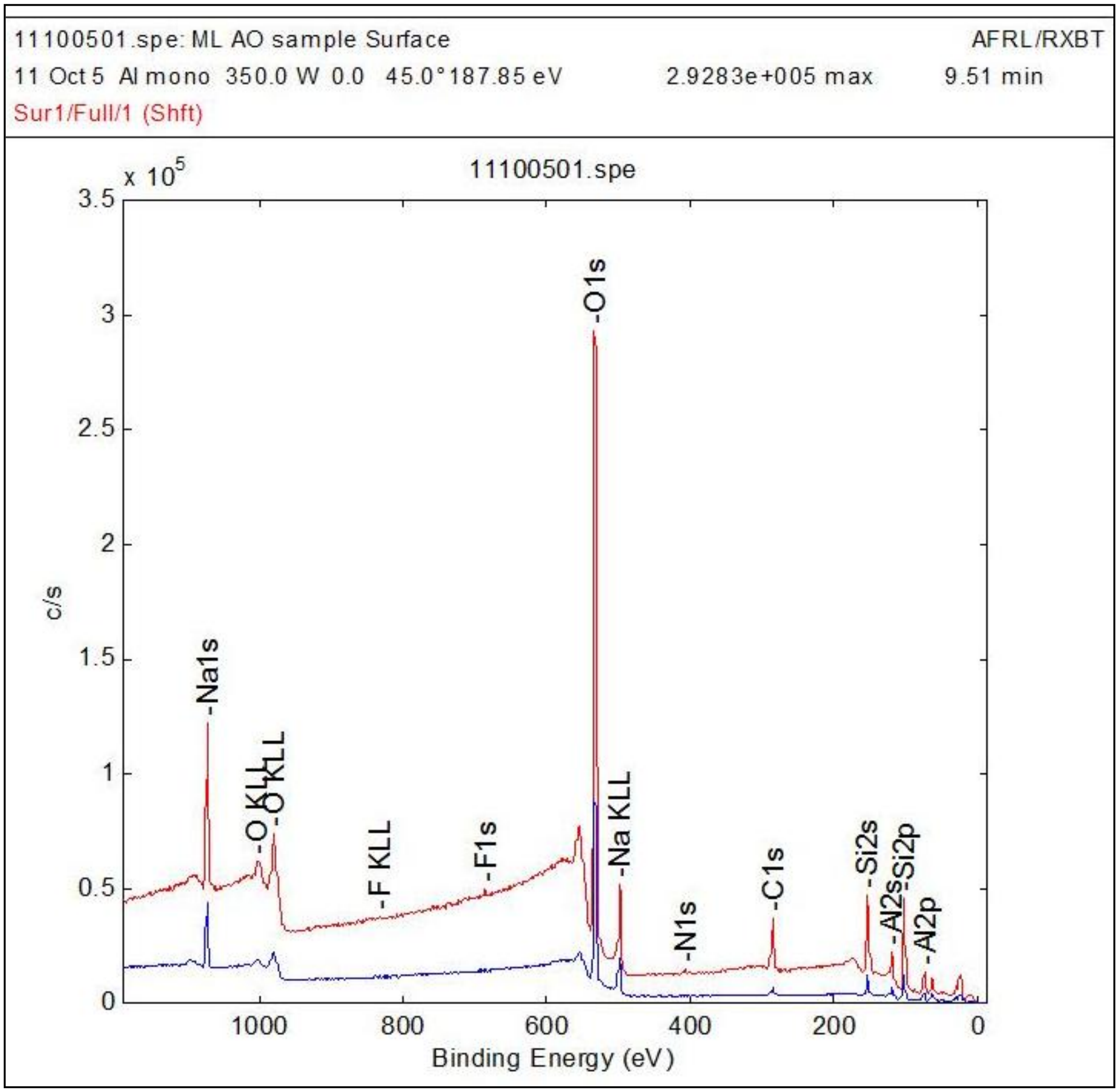

Figure 48. XPS data for metakaolin, AO exposed sample

The AO exposed metakaolin sample shown in Figure 48 has similar peaks between the surface and bulk material again, and at a macro qualitative level, there seems to be little difference between the chemical compositions of the exposed and non-exposed surfaces. Additional peaks for nitrogen and fluorine 1s bonds are present in the non-exposed surface (blue) data set, similar to how they appeared as trace constituents in the illite sample.

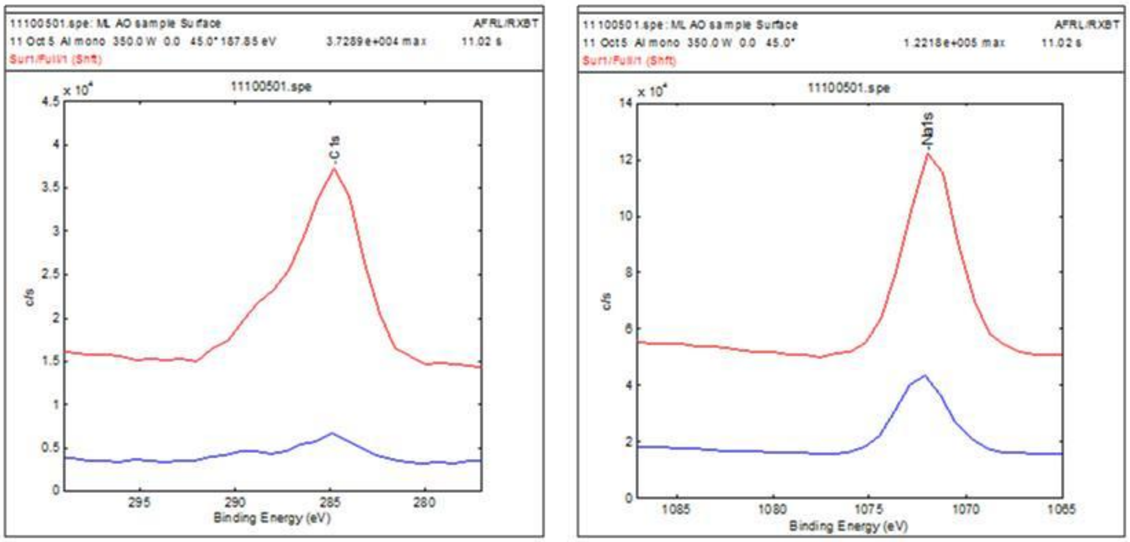

Figure 49. XPS data on AO exposed metakaolin, C & Na peaks

Closer examination of individual peaks for the metakaolin sample (see Figure 49) was focused on peaks for C and Na elements. The C peak again showed a potential carbonate peak on the non-exposed side suggesting likely a minor biological contamination, and the Na peak was more pronounced than in the illite sample. This is due to the presence of Na in the metakaolin trigger solution and so it is expected.

Looking at the relative percentages of chemical constituents in the XPS measurements for metakaolin (Table 11), the primary difference in non-exposed to exposed chemical constituents of metakaolin is the loss of trace materials (N, F) from the non-exposed side to the exposed side as seen in the illite series. This again is likely due to the AO reacting with and eroding away the compounds where those trace elements were located. This percentage of the material was once again seen to be compensated for on the exposed side by higher oxygen concentrations, suggesting that additional oxide layers were formed by the reaction of the atomic oxygen impacting surface metallic and semi-metallic elements present in the geopolymer matrix, raising the overall concentration of oxygen on the exposed surface.

Table 11. Metakaolin XPS relative chemical constituents, AO exposure series

	Metakaolin AO-exposed				Metakaolin non-exposed			
	Test 1	Test 2	Test 3	Avg	Test 1	Test 2	Test 3	Avg
O1s	57	56	55.6	56.2	53	54.2	54.2	53.8
Si2p	15.8	16.5	17.2	16.5	18	17.3	17.2	17.5
Al2p	7.2	7.2	7.9	7.4	6.1	6.1	6.1	6.1
C1s	7.5	6.7	6.6	6.9	13.2	12.5	12.6	12.8
Na1s	12.6	13.6	12.6	12.9	8.6	9	8.8	8.8
Trace	0	0	0	0.0	1.1	0.9	1	1.0

Observations & summary- Atomic oxygen exposure testing

From the results of the post-exposure evaluation, it can be summarized that while there is obvious evidence of AO exposure on the surface of the samples (the color change), there appears to be minimal impact on the actual performance of the samples from a mechanical sense. The hardness and modulus differences as a function of depth appear to be limited to superficial surface effects only as they approach similar values as those of the bulk material. Erosion of the geopolymer surfaces is recorded to be minimal over time via examination of surface roughness using AFM scans. No flaking of material and only minimal mass loss was noted from the intact materials. Therefore, it is believed AO exposure is not a threat to performance of the geopolymers over time in the space environment.

Summary of Chapter

This chapter presented the results and analysis of the experimental work described in Chapter III. For Objective 1, it was shown that while pressure and temperature contributed to curing shrinkage variability, pressure was the dominant variable, and an increased pressurized environment is best for minimizing curing shrinkage. For Objective 2, it was shown that while room temperature and pressure cured geopolymers could not pass the NASA outgassing standard for TML, the CVCM value was well within acceptable levels, and the NML level for the cured and annealed samples was low enough to likely warrant a TML waiver for use on spacecraft. For Objective 3, it was shown that UV exposure and AO exposure did affect the geopolymer samples, but these effects were limited to superficial surface effects and did not change the bulk material's performance in a mechanical sense. Therefore, all three objectives were completed satisfactorily.

V. Summary

Chapter Overview

This chapter will summarize the results of the experiments and answer the objective questions stated in Chapter I. In the context of this research, the term geopolymer in this section will refer to the illite and metakaolin formulations used in this experiment set.

Conclusions of Research

Objective 1- Is there a curing variable (pressure and temperature) that impacts curing shrinkage greater than others, or is curing shrinkage a result of coupled curing variables? In addition, how do simply optimized geopolymers compare to other space qualified polymers quantitatively in terms of curing shrinkage?

It has been shown that pressure and temperature impact the extent of curing shrinkage on geopolymers. Per the results in Chapter IV, pressure and temperature both have a positive effect on reducing the curing shrinkage of the geopolymer; however, pressure is seen as the dominant variable. When compared to other like materials in terms of general chemical character and application use for space missions, geopolymers are better in terms of curing shrinkage. The best performance by a geopolymer during this research work was 76% better for illite and 96% better in terms of volumetric shrinkage over a standard epoxy. This clear difference in performance, in addition to the geopolymer advantage in curing at room temperature or slightly elevated temperature makes it superior in comparison to other like application space materials for controlling curing shrinkage.

Objective 2. Following the subjection of the geopolymer samples standard outgassing tests as defined by NASA, can we quantify their outgassing performance in comparison to accepted metrics?

The outgassing performances of cured and rehydrated, as well as cured and annealed geopolymers have been quantified in the context of qualification for space usage against a NASA standard. Based on the standard for Total Mass Loss (TML), neither processed geopolymer would normally qualify for use as a space material since both are above the acceptable value of < 1% TML. However, both materials did not emit measurable levels of Collected Volatile Condensable Materials (CVCM) - a NASA qualification standard- and both materials had < 1% of Net Mass Loss (NML). It has been shown that since the outgassed material consisted of almost exclusively water vapor and the NML is < 1%, it is likely a waiver would be approved for geopolymer use.

Two additional items must be noted though. First, the TML and NML levels achieved in the end were accomplished by changing the preparation procedure so that a post-cure vacuum baking was used to reduce the releasable water vapor trapped in the geopolymer matrix after initial setting or curing. Without this change in procedure, the NML value for both geopolymers would have been prohibitively high.

Second, because of the chemical nature of geopolymer materials, surface re-absorption of water on geopolymer surfaces is an issue the spacecraft engineer must take into account. If the geopolymer is used in an application where surface exposure to the pre-launch terrestrial environment is non-existent (like as an adhesive between two solid materials), surface water re-absorption should not be an issue. If used as a structural material, the unmodified geopolymer will need to not be placed next to water sensitive components. Otherwise, the geopolymer component will have to be launched in a nitrogen purged space launch vehicle (SLV) fairing, which has happened with some past launch operations. In a practical matter though, the water evaporated from a geopolymer surface will pale in comparison by volume to the amount of water outgassed from various SLV components and structure members. The primary systems engineering concern with outgassing is the unavoidable additional mass of re-absorbed water that may impact early satellite operations in SLV deployment, pointing accuracy, or propulsive maneuvers due to changes in center of mass of the spacecraft. After a few orbits with sun exposure and vacuum conditions, the geopolymer will stabilize with respect to mass and should not be an issue.

Objective 3. After the exposure periods to UV, high energy particle, and atomic oxygen have been completed, are there significant deviations in performance with respect to standard mechanical performance values between exposed and non-exposed samples? Are there additional signs of failure mechanisms visible through other inspection methodologies?

The answers to this Objective will be separated into two parts, the first dealing with the UV and high energy particle exposure experiments, and the second dealing with the atomic oxygen exposure experiments.

The UV and high energy particle exposure evaluations showed in terms of modulus and hardness values, that both materials saw a decrease in performance following UV exposure. However, since there was an unusually high heat load applied to the samples as they were not sufficiently thermally stabilized during the exposure period, it is thought that this is actually similar to other polymers' behaviors under high heat loads similar to a phenomenon known as thermal softening, and not related to the UV or high energy particle exposure itself. Analysis of the differences in mechanical performance also showed that the majority of the decreases noted were limited to the first 1000 nm of penetration off the surface, essentially surface effects. Looking past that penetration depth into the bulk material, there does not appear to be a change to the mechanical properties.

Other inspection methodologies showed some differences between the exposed and non-exposed geopolymer samples, but no failure mechanisms. Photographic inspection and spectroscopic measurements of both samples showed a visible darkening of both materials related to understood oxidation processes, and the spectroscopic measurements also revealed an IR reflectivity increase. AFM analysis on both samples did not show significant changes in surface morphologies to suggest radical damage by the UV and high energy particle exposure periods.

Following the atomic oxygen exposure, superficial surface effects (discoloration) were seen on the illite and metakaolin samples, but an analysis of mechanical properties (hardness and Young's modulus) and chemical composition testing through XPS showed that any differences between the surface noticeable areas and the bulk material depth were inconsequential. Both exposed and non-exposed hardness and modulus data coalesced to similar values in the bulk material interior, at a distance of just over 1 micron (1000 nm). Surface erosion was seen to be minimal according to analysis from AFM imaging.

Systems Engineering Issues

This research primarily dealt with addressing the qualification of geopolymers at a bulk material level. Ultimately, the approval of geopolymers for spacecraft usage needs to be evaluated at the systems engineering level. Caveats for their use have been determined from this research study at a systems engineering level, and are listed below:

- Structural components made of geopolymers will outgas in orbit due to the water re-absorption during pre-launch storage activities. Plans need to be made to account for the change in mass of the spacecraft from initial deployment to stable orbital position because of the water outgassing. This mass loss may be as much as 30% of the geopolymer storage mass. Unless the geopolymer component is stored in a nitrogen purged atmosphere through launch deployment or sealed with a water-phobic material coating, outgassing absorbed water in the pore structure of the geopolymer will happen.

- Thermal shock of the geopolymers is a real concern. Successful systems engineering designs incorporating geopolymers on spacecraft need to make efforts to keep the geopolymers in a stable thermal environment. This includes minimizing the thermal shock going from eclipse to sunlit and back conditions. Sun synchronous orbits where constant sunlight conditions are available are probably the optimal operating condition for geopolymer spacecraft components; internal spacecraft sections where the temperature can be actively controlled (like in optical train primary mirrors) are also optimal. Some work has been accomplished in inserting carbon nanotube fibers into the geopolymer matrix to reduce the effects of thermal shock, but the resulting bulk material has not been adequately evaluated on its own as of this time.

Additional issues related to applications and potential future research paths outside the scope of this study are discussed in Appendix D.

Significance of Research

Prior to this research, geopolymers had not been evaluated for use as space qualified materials. This research established the first rigorous evaluation of geopolymers for use in the space environment by quantifying their performance with respect to curing shrinkage, outgassing, and reaction to exposure by key components of the space environment. A baseline empirical characterization of geopolymers has now been created allowing for further evaluation of these materials in application specific contexts.

Final Summary

To be used on spacecraft applications, geopolymers (namely the illite and metakaolin formulations used in this research) must in the least be able to survive basic exposure to elementary components of the space environment. The research performed for this dissertation has shown that geopolymers should be able to survive the vacuum environment but there are water absorption concerns that require systems engineering caveats to be applied based on the exact application. UV, high energy particle, and AO exposure are a minimal concern but superficial surface effects will be present.

One key processing difficulty, the minimization of curing shrinkage, has been addressed through control of atmospheric temperature and pressure during curing phases. Specifically, compression should be applied to the geopolymer to force the polymer matrix to form as many cross links as possible and lock in the 3-D structure.

In the end, the space environment provides some, but not insurmountable, hurdles to the use of geopolymers on spacecraft applications. These restrict the unlimited use of raw, unmodified geopolymers for spacecraft applications, but solutions to mitigate these issues are not out of reach with smart systems engineering and / or additional materials science modifications to a geopolymer composite.

Appendix A

Photos of the geopolymer samples and testing

Geopolymer preparation molds, blue nitrile rubber and nylon circles

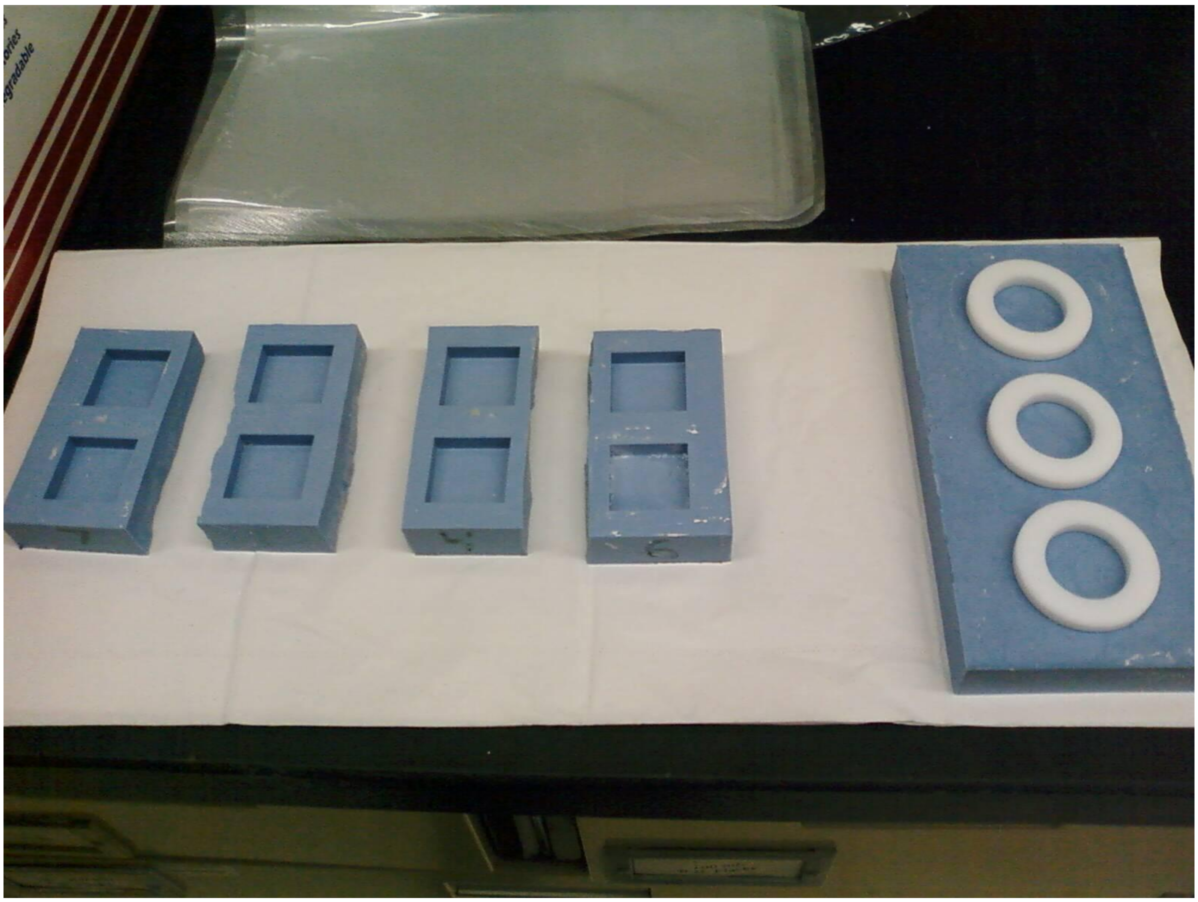

Curing shrinkage testing samples, Aug 2008, polystyrene molds (right- before cure; left-post cure)

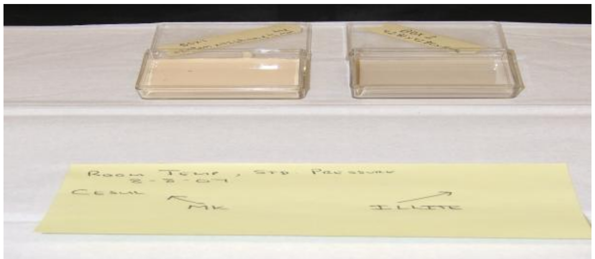

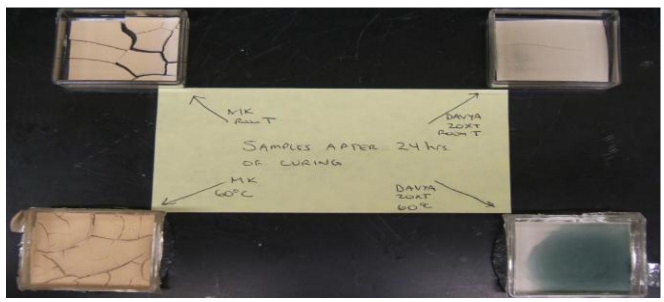

Illite samples prepared pre-cure and post cure, Jun 2008

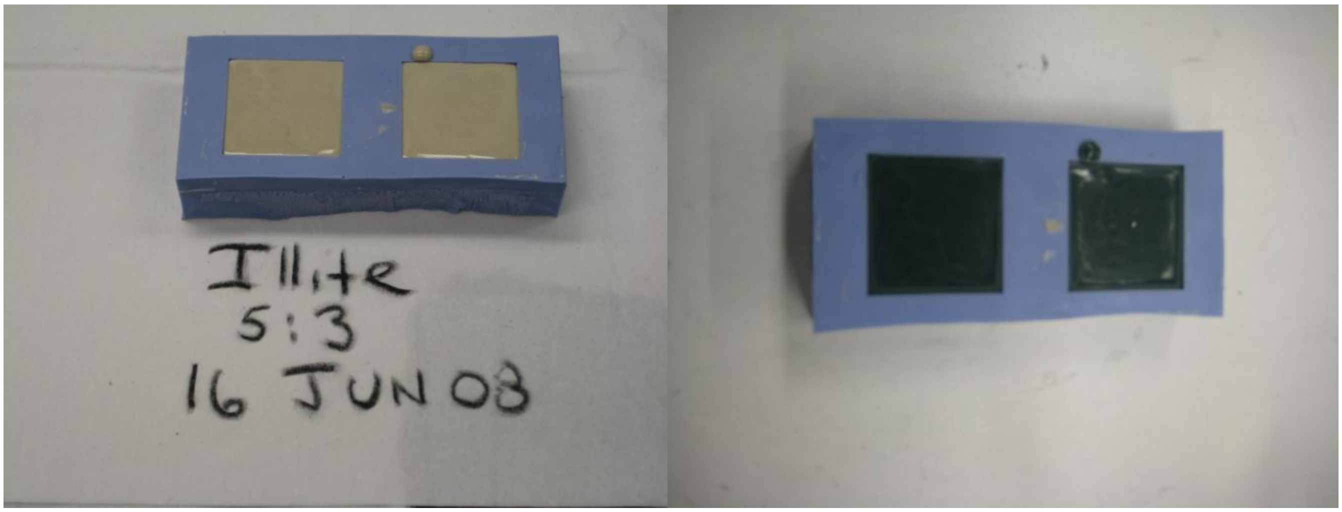

Metakaolin samples prepared pre-cure and post cure, Jun 2008

Illite samples prepared for MISSE-7 mission, pre-cured, June 2008

Illite samples prepared for MISSE-7 mission, vacuum bagged during cure, June 2008

Illite samples prepared for MISSE-7 mission, post-cure, June 2008

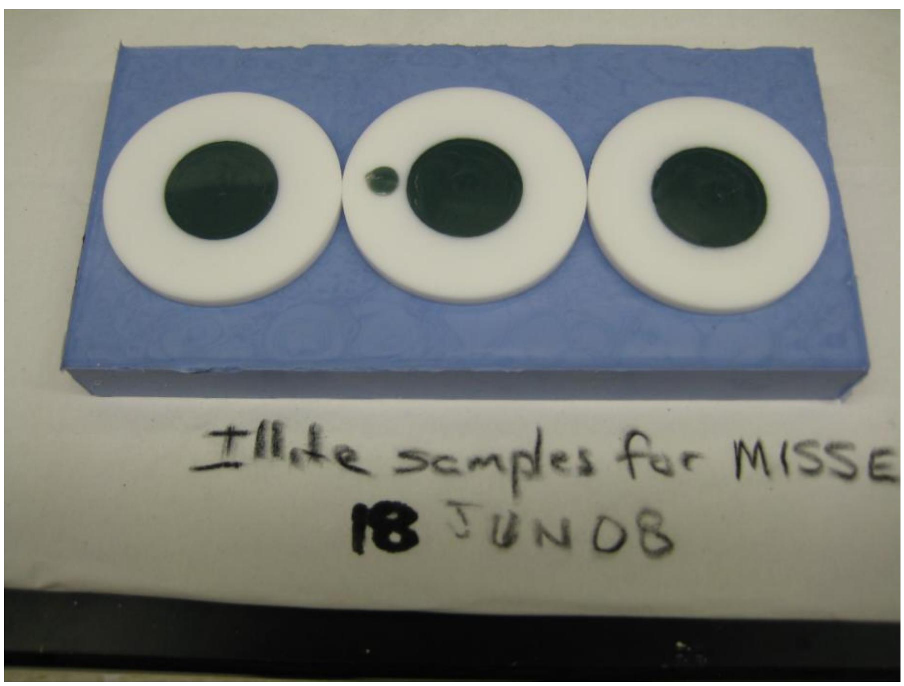

Illite samples prepared for MISSE-7 mission, post-vacuum bake out, June 2008

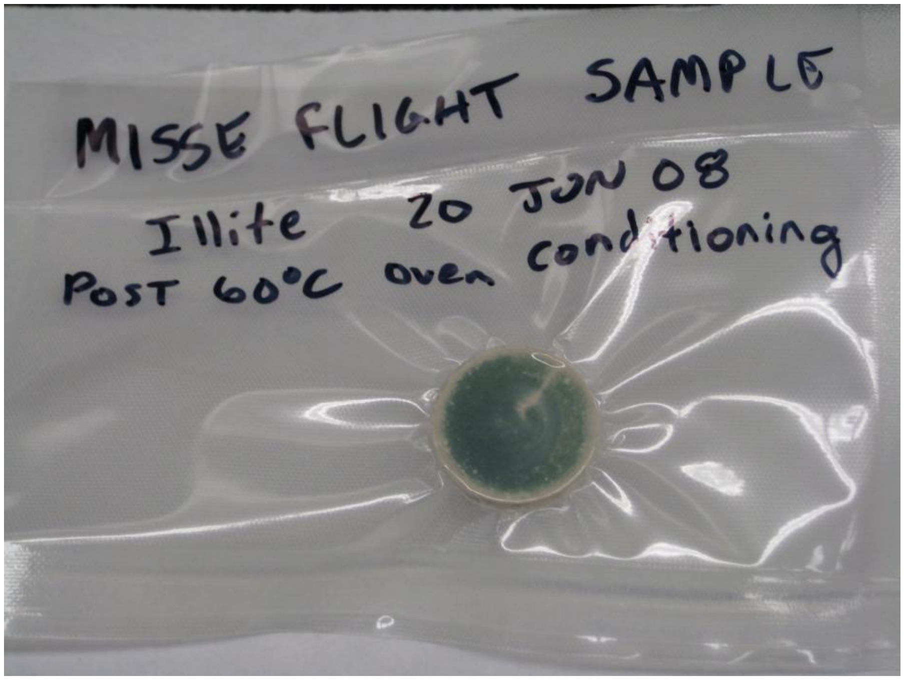

Example of post-vacuum bake thermal shock effects, fracturing the sample

Appendix B

NASA GSFC Outgassing Test Data Sheets

MICRO VCM TEST REQUEST AND DATA SHEET PER ASTM E-595-93
(Requestor please read, then furnish all information above asterisks.)

Requested by: **Brandon Cesul** Phone: **937-522-4239** Date: **4/8/08**
Material Identification (product name, number, description, classification, etc.)
Davya 20XT geopolymer

Manufacturer of Material (Name, City and State Address): **USAF AFR:/RXM, Wright Patterson AFB, OH**

Material application (general usage, i.e. adhesive, coating, potting, etc.):
J. O. Number/Project Name: Request Infra-Red Spectra? ☐YES ☐NO
Originator Source/Code (other than Code 541): **USAF/AFIT/ENY**

Indicate processing required by GSFC Materials personnel. Include the recipe, cure(s), and special instructions to be performed.

If material is to be tested in the "as received" condition, without further processing required, indicate in full the past history, recipe, cure(s), post cure(s), nomenclature of components, etc.

Sample was made from a mixture of commercial Davya 20XT (Illite) powder and curing agent in a 5:3 ratio (powder:liquid). Cure was at room temperature in a sealed vacuum bag following initial setting time of 45 minutes in a nitrile rubber mold. Sample was kept in vacuum bag for 1 day. Sample was then baked at 60C overnight and subjected to 24 hour vacuum bake at 140C for 24 hours prior to shipping (25C for 45 min, 60C for 8 hours, 140C for 24 hours).

****
****

CVCM test specimen preparation and description: **Cut up and Placed in boats**

Bar Position-CVCM Test Number	**30793 (22)**	**30794 (23)**	**30792 (24)**
Initial mass, holder and specimen, gm	0.280382	0.276945	0.279806
Mass of holder, gm	0.032917	0.032377	0.031686
Initial specimen mass @ 50 %RH, gm	0.247465	0.244568	0.248120
Final mass, holder & specimen, gm	0.264885	0.261975	0.264769
Total mass loss, specimen, gm	0.015497	0.014970	0.015037
Percent TML, specimen	6.26%	6.12%	6.06%
Average value TML	*****************	**6.15%**	******************

	*****		
Mass after 50 %RH re-soak, 23 C, 24hr, gm	0.279107	0.275537	0.278496
Total mass, water vapor regain, gm	0.014222	0.013562	0.013727
Percent water vapor regain	5.75%	5.55%	5.53%
Average value WVR @ 50 %RH	*********************	**5.61%**	******************
Initial mass, collector, gm	1.784702	1.817558	1.894232
Final mass, collector, gm	1.784709	1.817562	1.894232
Collected mass – CVCM, gm	0.000007	0.000004	0.000000
Percent CVCM	0.00%	0.00%	0.00%
Average Value CVCM	*******************	**0.00%**	******************

Remarks: CVCM (unweighable) on separator plate to_____ mm diameter. CVCM appearance as follows: **X** is not detectable on collector plates.
☐ thin; ☐ heavy; _____ color; ☐ transparent; _____ colored liquid;
☐opaque; ☐ matte; ☐ interference fringes; ☐ foggy; ☐ distorts eye reflection; ☐ smooth; ☐ smoky; ☐ splotchy; ☐ partially opaque;
☐ clear liquid; ☐ liquid runs in excess; Deposit covers _____ % of collector disc.

Specimen appearance after test:
No Visible Change

Test started **4/29/08** Test completed: **4/30/08** Period **24** Hrs. Pressure **$1.4X10^{-5}$ Torr**
Specimen Temp. **124.8** °C Collector Temp. **24.8**°C **Analyst Dewey Dove and Debbie Thomas**

VCM REV 1425 JAN 2001

MICRO VCM TEST REQUEST AND DATA SHEET PER ASTM E-595-93

(Requestor please read, then furnish all information above asterisks.)

Requested by: **Brandon Cesul** Phone: **937-522-4239** Date: **4/8/08**

Material Identification (product name, number, description, classification, etc.)

Meatakaolin geopolymer

Manufacturer of Material (Name, City and State Address): **USAF AFR:/RXM, Wright Patterson AFB, OH**

Material application (general usage, i.e. adhesive, coating, potting, etc.): **structure**

J. O. Number/Project Name: Request Infra-Red Spectra? ☐YES ☐NO

Originator Source/Code (other than Code 541): **USAF/AFIT/ENY**

Indicate processing required by GSFC Materials personnel. Include the recipe, cure(s), and special instructions to be performed.

If material is to be tested in the "as received" condition, without further processing required, indicate in full the past history, recipe, cure(s), post cure(s), nomenclature of components, etc.

Sample was made from a mixture of metakaolin powder and a KOH/SiO2/H2O solution. Cure was at room temperature in a sealed vacuum bag following initial setting time of 90 minutes in a nylon mold. Sample was then placed in high pressure autoclave for 1 hour. Sample was then baked at 60 C overnight and then 24 hour vacuum bakeout at 140 C prior to shipment. (25C for 90 min, 60C for 8 hours, 140C for 24 hours)

****

CVCM test specimen preparation and description: **Cut up and Placed in boats**

Bar Position-CVCM Test Number	**30790 (19)**	**30791 (20)**	**30792 (21)**
Initial mass, holder and specimen, gm	0.263309	0.266701	0.284715
Mass of holder, gm	0.030157	0.031826	0.031393
Initial specimen mass @ 50 %RH, gm	0.233152	0.234875	0.253322
Final mass, holder & specimen, gm	0.246072	0.250628	0.257340
Total mass loss, specimen, gm	0.017237	0.016073	0.027375
Percent TML, specimen	7.39%	6.84%	10.81%
Average value TML	**********************	**8.35%**	******************
Mass after 50 %RH re-soak, 23 C, 24hr, gm	0.261477	0.264979	0.283084
Total mass, water vapor regain, gm	0.015405	0.014351	0.025744
Percent water vapor regain	6.61%	6.11%	10.16%
Average value WVR @ 50 %RH	*********************	**7.63%**	******************
Initial mass, collector, gm	1.763995	1.774315	1.779690
Final mass, collector, gm	1.763999	1.774322	1.779699
Collected mass – CVCM, gm	0.000004	0.000007	0.000009
Percent CVCM	0.00%	0.00%	0.00%
Average Value CVCM	*******************	**0.00%**	******************

Remarks: CVCM (unweighable) on separator plate to_____ mm diameter. CVCM appearance as follows: **X** is not detectable on collector plates.

☐ thin; ☐ heavy; _____ color; ☐ transparent; _____ colored liquid;

☐ opaque; ☐ matte; ☐ interference fringes; ☐ foggy; ☐ distorts eye reflection; ☐ smooth; ☐ smoky; ☐ splotchy;
☐ partially opaque;

☐ clear liquid; ☐ liquid runs in excess; Deposit covers ______ % of collector disc.

Specimen appearance after test:

No Visible Change

Test started **4/29/08** Test completed: **4/30/08** Period **24** Hrs. Pressure **$1.4X10^{-5}$ Torr**

Specimen Temp. **124.8** °C Collector Temp. **24.8**°C **Analyst** **Dewey Dove and Debbie Thomas**

VCM REV 14 25 JAN 2001

MICRO VCM TEST REQUEST AND DATA SHEET PER ASTM E-595-93

(Requestor please read, then furnish all information above asterisks.)

Requested by: **Brandon Cesul** Phone: **937-522-4239** Date: **2/8/08**

Material Identification (product name, number, description, classification, etc.)

Davya 20XT geopolymer

Manufacturer of Material (Name, City and State Address): **USAF AFR:/RXM, Wright Patterson AFB, OH**

Material application (general usage, i.e. adhesive, coating, potting, etc.):

J. O. Number/Project Name: Request Infra-Red Spectra? ☐YES ☐NO

Originator Source/Code (other than Code 541): **USAF/AFIT/ENY**

Indicate processing required by GSFC Materials personnel. Include the recipe, cure(s), and special instructions to be performed.

If material is to be tested in the "as received" condition, without further processing required, indicate in full the past history, recipe, cure(s), post cure(s), nomenclature of components, etc.

1 in X 1 in X .25 in sample. Sample was made on 4 Jan 2008 from a mixture of commercial Davya 20XT (illite) powder and curing agent in a 5:3 ratio (powder:liquid). Cure was at room temperature in a sealed vacuum bag following initial setting time of 45 minutes in a nitrile rubber mold. Sample was kept in vacuum bag for 5 days. Sample was then exposed to ambient atmosphere in AFRL/RXM laboratory facilities prior to shipping

****

CVCM test specimen preparation and description: **Cut up and Placed in boats**

Bar Position-CVCM Test Number	**30664 (13)**	**30665 (14)**	**30666 (15)**
Initial mass, holder and specimen, gm	0.212365	0.236590	0.210682
Mass of holder, gm	0.033406	0.032014	0.032706
Initial specimen mass @ 50 %RH, gm	0.178959	0.204576	0.177976
Final mass, holder & specimen, gm	0.181035	0.192802	0.177113
Total mass loss, specimen, gm	0.031330	0.043788	0.033569
Percent TML, specimen	17.51%	21.40%	18.86%
Average value TML	**********************	**19.26%**	******************
Mass after 50 %RH re-soak, 23 C, 24hr, gm	0.197987	0.211743	0.193899
Total mass, water vapor regain, gm	0.016952	0.018941	0.016786
Percent water vapor regain	9.47%	9.26%	9.43%
Average value WVR @ 50 %RH	*********************	**9.39%**	******************
Initial mass, collector, gm	1.254769	1.754639	1.753996
Final mass, collector, gm	1.254772	1.754645	1.754000
Collected mass – CVCM, gm	0.000003	0.000006	0.000004
Percent CVCM	0.00%	0.00%	0.00%
Average Value CVCM	*******************	**0.00%**	******************

Remarks: CVCM (unweighable) on separator plate to______ mm diameter. CVCM appearance as follows: ______ is not detectable on collector plates.

☐ thin; ☐ heavy; **rainabow** color; ☐ transparent; ______ colored liquid;

☐ opaque; ☐ matte; ☐ interference fringes; ☐ foggy; ☐ distorts eye reflection; ☐ smooth; ☐ smoky; ☐ splotchy;
☐ partially opaque;

☐ clear liquid; ☐ liquid runs in excess; Deposit covers **50** % of collector disc.

Specimen appearance after test:

No Visible Change

Test started **3/11/08** Test completed: **3/12/08** Period **24** Hrs. Pressure **$1.5X10^{-5}$** **Torr**

Specimen Temp. **125.2** °C Collector Temp. **23.8**°C **Analyst** **Dewey Dove and Debbie Thomas**

VCM REV 14 25 JAN 2001

MICRO VCM TEST REQUEST AND DATA SHEET PER ASTM E-595-93

(Requestor please read, then furnish all information above asterisks.)

Requested by: **Brandon Cesul** Phone: **937-522-4239** Date: **2/8/08**

Material Identification (product name, number, description, classification, etc.)

Meatakaolin geopolymer

Manufacturer of Material (Name, City and State Address): **USAF AFR:/RXM, Wright Patterson AFB, OH**

Material application (general usage, i.e. adhesive, coating, potting, etc.): **structure**

J. O. Number/Project Name: Request Infra-Red Spectra? ☐YES ☐NO

Originator Source/Code (other than Code 541): **USAF/AFIT/ENY**

Indicate processing required by GSFC Materials personnel. Include the recipe, cure(s), and special instructions to be performed.

If material is to be tested in the "as received" condition, without further processing required, indicate in full the past history, recipe, cure(s), post cure(s), nomenclature of components, etc.

1 in X 1 in X .25 in sample. Sample was made on 16 Jan 2008 from a mixture of metakaolin powder and sodium silicate in 1:2 ratio (powder:liquid). Cure was at room temperature in a sealed vacuum bag following initial setting time of 60 minutes in a nitrile rubber mold. Sample was kept in vacuum bag for 6 days. Sample was then exposed to ambient atmosphere in AFRL/RXM laboratory facilities prior to shipping

****
****

CVCM test specimen preparation and description: **Cut up and Placed in boats**

Bar Position-CVCM Test Number	**30667 (16)**	**30668 (17)**	**30669 (18)**
Initial mass, holder and specimen, gm	0.224338	0.264129	0.194076
Mass of holder, gm	0.030938	0.031904	0.033019
Initial specimen mass @ 50 %RH, gm	0.193400	0.232225	0.161057
Final mass, holder & specimen, gm	0.184690	0.209823	0.164723
Total mass loss, specimen, gm	0.039648	0.054306	0.029353
Percent TML, specimen	20.50%	23.39%	18.23%
Average value TML	**********************	**20.70%**	******************
Mass after 50 %RH re-soak, 23 C, 24hr, gm	0.202173	0.230048	0.179531
Total mass, water vapor regain, gm	0.017483	0.020225	0.014808
Percent water vapor regain	9.04%	8.71%	9.19%
Average value WVR @ 50 %RH	*********************	**8.98%**	******************
Initial mass, collector, gm	1.756001	2.383558	1.759560
Final mass, collector, gm	1.756007	2.383561	1.759569
Collected mass – CVCM, gm	0.000006	0.000003	0.000009
Percent CVCM	0.00%	0.00%	0.01%
Average Value CVCM	*******************	**0.00%**	******************

Remarks: CVCM (unweighable) on separator plate to______ mm diameter. CVCM appearance as follows: ______ is not detectable on collector plates.

☐ thin; ☐ heavy; **rainabow** color; ☐ transparent; ______ colored liquid;

☐ opaque; ☐ matte; ☐ interference fringes; ☐ foggy; ☐ distorts eye reflection; ☐ smooth; ☐ smoky; ☐ splotchy;
☐ partially opaque;

☐ clear liquid; ☐ liquid runs in excess; Deposit covers **50** % of collector disc.

Specimen appearance after test:

No Visible Change

Test started **3/11/08** Test completed: **3/12/08** Period **24** Hrs. Pressure **$1.5X10^{-5}$** **Torr**

Specimen Temp. **125.2** °C Collector Temp. **23.8**°C **Analyst** **Dewey Dove and Debbie Thomas**

VCM REV 14 25 JAN 2001

Appendix C

Commercial geopolymer data sheets

Espace Créatis, Av. Archimède
Z.A. Bois de la Chocque
F-02100 Saint-Quentin, France
tel:(+33) (0)323 67 8922
fax: (+33) (0)323 67 8949
web : www.geopolymer.org

TECHNICAL DATA
DAVYA™ 20XT CEMENT

Description:

The DAVYA™ 20XT cement is an early-high-strength binder. It is described as inorganic polymer cement (a polysialate) derived from natural geological materials silica and alumina, hence the name geopolymer.

Geopolymerization is a geosynthesis (a reaction that chemically integrates minerals) that involves naturally occurring silico-aluminates. The silicon (Si) and aluminium (Al) atoms react to form molecules that are chemically and structurally comparable to those binding natural rock.

For DAVYA 20XT the initial set is as short as 20 minutes starting from the mixing of the resin, followed by a setting time of 25 minutes, totalising 45 minutes from the initial mixing until the complete hardening of the resin.

The resulting DAVYA™ XT (geopolymeric) cements have the following assets:

A new kind of cement

We have the technology to make superior cement that uses no limestone at all, but instead uses natural silico-aluminate. This cement is clean and green. It emits up to 90% less CO2 than classical Portland cement.

It is a strong an resistant cement that:
- Contains no hydration water and cannot explode in a fire,
- Is an early-high-strength binder,
- Has two to three times the flexural/tensile strength of Portland cement,
- The world’s safest toxic and nuclear waste-containment material
- Since there is no alkali-aggregate reaction and very low shrinkage rate, it cannot crack (depending on the fillers used).

It is beautiful and versatile:
- Makes very beautiful reagglomerated stone,

 Suited to pressured pipes and pipe tunnels,
 Suited to emergency repair cement, especially for aircraft runways and highways,
 Good for marine uses because no salt cannot affect it and it goes hard underwater within 2 hours.
 Suited for extremely cold temperature (it sets at –20°C).

It is economic:
 You do not need to re-equip your factory,
 You save two thirds of your fuel,
 You can make cement outside limestone regions.

Information:

More information is available in our Web site www.geopolymer.org, where you can download additional papers and order the Géopolymère '99 Proceedings including numerous scientific articles with tests and data on selected materials.

Properties:

DAVYA™ XT Cement does not use limestone as a material. Instead, it uses special kaolinite-based clays. The calcining temperature for this cement is approximately 750°C. This means that two thirds of fuel normally used for Portland cement production can be saved.

This cement has many special properties that can resolve many long-standing problems which have plagued Portland cement-based concrete. Therefore, it has attracted increasing attention. The following diagrams illustrate some of the main properties of DAVYA™ XT (geopolymeric) cement.

1. High early strength

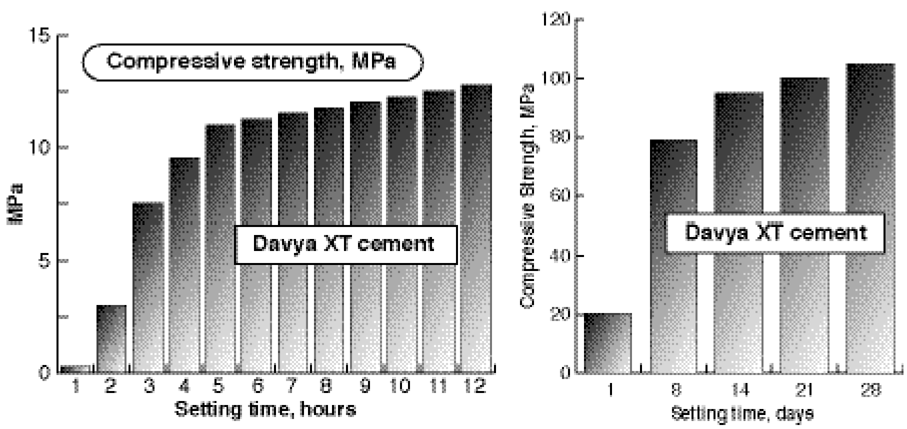

Figure 1. Compressive strength in MPa of the early high strength DAVYA™ XT cement

A plate of DAVYA XT (geopolymeric) cement of dimensions 1.6 meters on each side and 18 cm thick after 4 hours' setting can develop sufficient strength to withstand 12.2 tons of load added through a landing wheel of an F-4 fighter airplane.

2. Low shrinkage rate

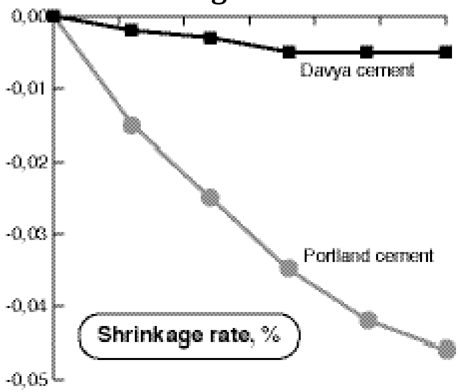

Figure 2. Comparison of shrinkage rate.

3. Resistance to corrosion

Since no limestone is used as a raw material, DAVYA XT cement has excellent properties within both acid and salt environments. It is especially suitable for tough environmental conditions. Sea water can be used for the blending of the cement rather than fresh water. This can be useful in marine environments and on islands short of fresh water. (It is impossible to make Portland cement with sea water).

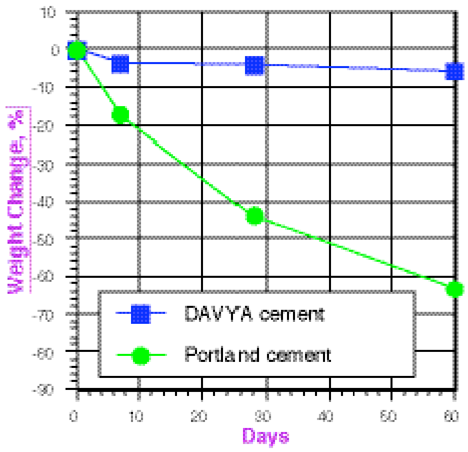

Figure 3. Comparison of resistance to corrosion between DAVYA cement and Portland cement. After 28 days' standard setting, samples were put into 5% sulfuric acid solution, and the weight loss was measured.

4. Very high fire-resistance properties

Since there is no hydratation water in DAVYA™ (geopolymeric) cement, it will not explode under high temperature. It can thus be used for tunnels and high-rise structures as a fire-prevention measure. For existing tunnels and high-rise structures, a 30 mm cladding of DAVYA cement will render them fire-resistant.

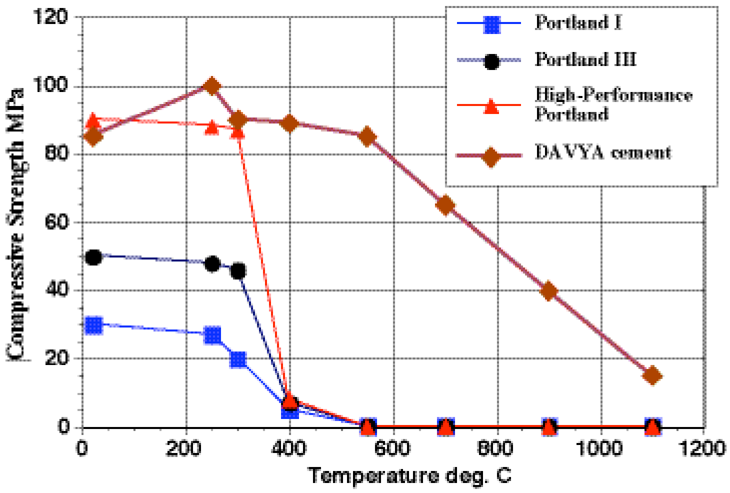

Figure 4. Comparison of strength of DAVYA cement-based concrete with high performance Portland cement-based concrete (Pyrament) and ordinary Portland cement-based concrete (type I and III) under high temperature.

The DAVYA cement-based concrete was kept at a temperature of 1000°C for three hours and still had a compressive strength of approximately 30 MPa. On the opposite, Portland cement-based concretes explode and deteriorate at 300°C.

5. High flexural strength

The ratio of compressive strength to flexural strength of normal Portland cement is about 10. The ratio for DAVYA XT is about 5. Some DAVYA XT (geopolymeric) cement can even reach 3.5. Therefore, for the same compressive strength, the flexural strength of DAVYA XT is two to three times higher than it is for Portland cement.

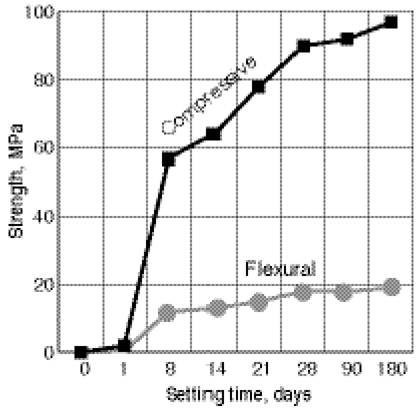

Figure 5. The comparison of compressive strength and flexural strength for DAVYA™ XT

6. No alkali-aggregate reaction

DAVYA cements even with alkali contents as high as 9.2% or higher do not generate any dangerous alkali-aggregate reaction. But in Portland cement, even alkali contents as low as 1.2% are dangerous.

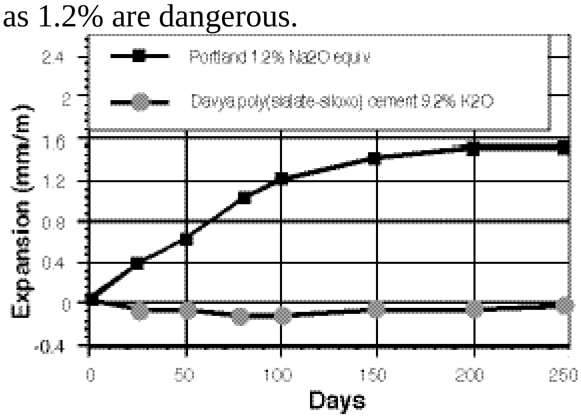

Figure 6. Alkali-aggregate reaction: ASTM C227 measures the linear expansion DAVYA cement and ordinary Portland cement.

7. Clean and green

Another reason for DAVYA attracting attention today is that during its production, the carbon dioxide emissions for the same weight of cement as Portland is only 15%-20% of that of Portland cement. The production of one ton of Portland cement emits one ton of carbon dioxide into the atmosphere. Huge quantities of cement production seriously threaten the world’s environment. Based on the continuity of development, especially in the developing countries, the use of DAVYA cement to reduce the burden on the atmosphere is highly necessary. Society benefits from cement production, but the cement industry has a responsibility to leave a sustainable atmosphere for future generation.

8. Technical Data Sheet for DAVYA™ geopolymeric cement type (Potassium, Calcium)- Poly(sialate-siloxo) / (K,Ca)-(Si-O-Al-O-Si-O-), Si:Al=2:1

These indicative data are only disclosed for a standard DAVYA binder, and may vary for more or less 25%, depending on the quality of the binder, its fillers, the manufacturing conditions of your sample.

Tested on standard sand mortar prisms:
- *setting:* 10 hours at -20°C to 20 minutes at +20°C.
- *shrinkage during setting:* <0,05%, not measurable.
- *compressive strength (uniaxial)*: > 105 MPa at 28 days.
- *flexural strength:* 20-22 MPa at 28 days (5 MPa after 24 hours).
- *Young Modulus:* > 2 GPa.
- *freeze-thaw:* mass loss < 0,1% (ASTM 4842), strength loss < 5% after 180 cycles.
- *wet-dry:* mass loss < 0,1% (ASTM 4843).
- *pH:* crushed and powdered, 11-11,5 after 5 minutes in deionized water (compared to Portland cement: 12 to 12,5, and granit: 11).
- *leaching in water*, after 180 days: K2O < 0,015%.
- *water absorption:* < 3%, not related to permeability.
- *hydraulic permeability:* 10-10 m/s.
- *Sulfuric acid*, 10%: mass loss 0,1% per day.
- *chlorhydric acid* 5%: mass loss 1% per day.
- *KOH* 50%: mass loss 0,02% per day.
- *ammoniac* solution: no mass loss.
- *sulfate solution:* shrinkage 0,02% at 28 days.
- *alkali-aggregate reaction*: no expansion after 250 days, -0,01% (compared to Portland Cement with 1% Na2O, +1,5%).
- *linear expansion*: < 5.10-6/K.
- *heat conductivity*: 0,2 to 0,4 W/Km.
- *specific hea*t: 0,7 to 1,0 kJ/kg.
- *electrical conductivity*: strongly dependent on humidity.
- *thermal stability*:

- mass loss < 5% up to 1000°C.
- strength loss < 20% at 600°C, < 60% at 1000°C

Other values:
- *D.T.A.*: endothermic at 250°C (zeolitic water).
- *MAS-NMR spectroscopy*:

- 29Si: SiQ4, major resonance at -94,5 ± 3ppm.
- 27Al: AlQ(4Si), major narrow resonance at 55 ± 3ppm.

- *Energy consumption*: SEC for cement 1230-1310 MJ/tonne (compared to Portland clinker 3500 MJ/tonne).
- *CO2 emission* during manufacture: 0,180 t/tonne of cement (compared to Portland clinker 1,0 t/tonne).

Directions for use DAVYA 20XT ™

This DAVYA 20XT user's manual describes the manufacture of an early-high-strength binder. We show here the easiest method to do it. It is obvious that the use of laboratory equipments makes the operation easier. The lab. Technician should use overall and gloves, and respect the safety and security rules that apply to his laboratory. He may be assisted by a second technician in charge of cleaning the tools, immediately in water, before the hardening of the binder. You can keep this DAVYA kit for 6 months.

For DAVYA 20XT the initial set is as short as 20 minutes (starting from the mixing of the binder as displayed in picture 3), followed by a setting time of 25 minutes, totalising 45 minutes from the initial mixing until the complete hardening of the binder at room temperature (20°C). The setting time depends on the room temperature. The initial set for DAVYA 20XT is measured at room temperature, namely 20°C. If your laboratory has a higher room temperature (for example in summer time, or you do not use any air conditioning system), the setting time will be shorter. At 25°C, the initial set for DAVYA 20XT may be 15 minutes. To slow down this setting time, we suggest that you carry out your experimentation early in the morning or you should store the powder, the hardener, and the fillers for 1 hour in a refrigerator.

Directions for use of DAVYA 20XT for simple applications:
1 – Prepare 5 parts by weight of powder (part A), 3 parts by weight of hardener (part B) and between 50% and 200% of fillers depending on its granulometry.
2 – Pour the hardener into the powder.
3 – Mix the whole with the mixer until obtaining a fluid resin. Then, add the fillers and mix again.
4 – **5** - Cast the mixture in a hermetically closed mould. Let it harden 24 hours long. To accelerate the setting, if necessary, let first set during 2 hours at ambiant temperature (this allows the chemical reaction to react completely), then place the mould in an oven at 60°C for 2 hours.
6 – You can very easily clean the equipment with water as long as the mixture has not yet hardened.
7 – Once it is set, place the sample in a plastic bag hermetically closed, or dip it in water, and store it so for at least 28 days at room temperature for full curing. Notice the black - green colour of the sample during the first day (it is a sign of good
geopolymerisation).
8 – After 28 days, take out the sample and notice that the colour has returned to normal. Now, you can carry out preliminary testing on this sample.

The use of fillers is mandatory, otherwise the DAVYA binder will crack. Unlike Portland cement which, when used without fillers, shrinks, DAVYA binder does not shrink but cracks. You will observe this characteristic on the top of your samples where some fillers have decanted. We always leave mechanically this fragile layer before carrying out our tests.

The Client agrees that Institut Géopolymère makes no warranties, express or implied, including without limitation the implied warranties of merchantability and fitness for a particular purpose, regarding the geopolymer chemistry or its use and operation alone or in combination with the Client products. In no event will Institut Géopolymère be liable for special, incidental or consequential damages arising from the use, sale or distribution of the Client products or any third party.

Safety Data Sheet

DAVYA 20XT

The present safety datasheet combines data for DAVYA 20XT (powder) and DAVYA 20XT Hardener

1. Identification of the substance/preparation and of the company

1.1 Identification of the substance or preparation :
Ingredient and trade material name :
DAVYA 20XT (powder) and DAVYA 20XT Hardener
Potassium silicate and amorphous silicate, aluminium oxide and calcium metasilicate solution in water.
1.2 Utilisation of the substance : Special hard cement used in civil engineering.

1.3 Company/undertaking identification :
Institut Géopolymère.
Espace Créatis, Av. Archimède, Z.A. Bois de la Chocque
F-02100 Saint-Quentin, France
1.4 Emergency telephone number : +33/ (0)3 23 67 89 22

2 Composition/information on ingredients (Preparation) :

Chemical names : CAS: 1312-76-1 (potassium silicate), 1344-28-1 (aluminium oxide), 7631-86-9 (amorphous silica), 13983-17-0 (calcium metasilicate) and 7732-18-5 (water)
Concentration or range of concentration that may be hazardous:
Hardener: Potassium silicate > 25%
Powder: N/A
EC Classification : *Hardener* : Xi -Irritant R36/38 - S24/25 S36/37/39
Powder : N/A S22 S25 S36/37/39

3. Hazards information (Security) :

Critical hazards to human : *Powder* : N/A
Hardener: Alkaline solution. Risk of serious damage to eyes. Irritant to skin.
Critical hazards to environment : *Powder* : N/D
Hardener : The alkalinity of this material will have a local effect on ecosystems sensitive to changes in pH.

4. First-aid measures :

Eye contact : Flush with large amounts of water for 15 minutes. Contact a physician
Skin contact : Wash with soap and water.
Ingestion : Do not induce vomiting. Wash out mouth with water. Contact a physician or regional Poison Control Centre immediately.
Inhalation : Long term overexposure to inhalation of mist or dust of dried down particles may cause tissue response in the lung (Pneumoconiosis).

5. Fire-fighting measures :

Suitable extinguishing media : In adaptation to materials stored in the immediate neighbourhood.
Extinguishing media which must not be used for safety reasons : none
Special exposure hazards arising in fire-fighting : Powder and Hardener are not flammable.
Special protective equipment for fire-fighters : Does not produce any known toxic fumes (water based mineral materials).

6. Accidental release measures :

Personal protection : *Powder* : Avoid generation of dusts; do not inhale dusts.
Hardener : Avoid contact to skin.
Necessity or not to alert neighbourhood: Dependant on local regulations with regard to pH controls.

Environmental protection : Discharge of this product to sewage treatment works is dependent on local regulations with regard to pH controls.
Methods for cleaning up, neutralising, absorbing, retrieving, throwing away (and what to avoid) :
Powder : Carefully take up dry. Forward for disposal. Clean up affected area. Avoid generation
of dusts.
Hardener : Neutralise excess with acid solution or dilute with plenty of water.
If Powder and Hardener are mixed : Use absorbent material or scrape up dried material and place into containers.

7. Handling and storage :

7.1 Handling : Material is stable at room temperature. Hazardous polymerisation will not occur.
7.2 Storage : Chemical incompatibilities: iron hydroxide, strong oxidisers and acids.
Conditions to avoid : Excessive heat.
Hazardous decomposition Product : None.
Materials to avoid : will react with aluminium, zinc, tin and their alloys evolving hydrogen.

8. Exposure controls/personal protection :

Maximum exposition value (V.M.E.) : N/A
Personal protective equipment :
Respiratory protection : *Powder* : required when dusts are generated.
Ventilation: normal room ventilation.
Skin protection : Protective gloves (latex or vinyl) required.
Eye protection : Safety glasses recommended.
Body protection : Blouse required.

9. Physical and chemical properties :

Appearance : *Powder* : very fine grey powder.
Hardener : liquid tinted in yellow or blue.
Odour : non
pH : *Powder* : pH: 7, neutral *Hardener* : pH: 14, strongly alkaline
Melting point temperature : *Powder* : > 1700 deg. C *Hardener* : N/D
Boiling point temperature : *Powder* : > 1700 deg C *Hardener* : 104 deg. C
Water solubility : *Powder* : insoluble *Hardener* : yes
Low explosive range : *Powder* : N/D *Hardener* : N/D
High explosive range : *Powder* : N/D *Hardener* : N/D
Flash Point : *Powder* : N/D *Hardener* : N/D

10. Stability and reactivity :

Stability : Material is stable at room temperature. Hazardous polymerisation will not occur.
Conditions to avoid : *Powder* : N/D. *Hardener* : Avoid excessive heat.

Materials to avoid : iron hydroxide, halogen oxides, ethylene oxide, fluorine, hydrogen halides, nitrates, vinyl acetate.
Powder and *Hardener* mixed : will react with aluminium, zinc, tin and their alloys evolving hydrogen.
Hazardous decomposition products : N/D

11. Toxicological information :

N/D
On the basis of the morphology of the product, no hazardous properties are to be expected when it is handled and used with appropriate care.
The product should be handled with the usual care when dealing with chemicals.

12. Ecological information :

Biologic degradation : Upon dilution, rapidly depolymerise into molecular species indistinguishable from natural dissolved silica.
Ecotoxic effects : N/D
Toxicity : The alkalinity of this material will have a local effect on ecosystems sensitive to changes in pH.
Further ecologic data : when it is handled and used with appropriate care, no harmful ecological effects are to be expected.

13. Disposal considerations :

Product : *Powder* : is not classified as hazardous waste under EEC Directive 91/689/EEC (European
Waste Classification code 01 04 09).
Hardener : is classified as hazardous waste under EEC Directive 91/689/EEC (Property H4, European Waste Classification code 06 02 05). Dispose of according to state or local standards.
Dilute it in water or neutralize it with an acid.
Powder and Hardener MIXED and DRIED: is not classified as hazardous waste under EEC Directive 91/689/EEC, (European Waste Classification code 01 04 08).
When *Powder and Hardener are DILUTED* in water to form a mud: is not classified as hazardous waste under EEC Directive 91/689/EEC, (European Waste Classification code 01 04 12).
Packaging : is recyclable after cleaning it with water.

14. Transport information :

Not subject to transport regulations.
Special transport care :
Avoid temperature above 80 deg. C.

15. Regulatory information :

EC Label Symbol : Xi (*Hardener*)
Risks sentences (R) : *Powder* : N/A
Hardener : R36/38 : Irritating to eyes and skin.

Security sentences (S) : *Powder* : S22 Do not breathe dust, S25 Avoid contact with eyes, S36/37/39
Wear suitable protective clothing, gloves and eye/face protection.
Hardener : S24/25 Avoid contact with skin and eyes., S36/37/39 Wear suitable protective clothing, gloves and eye/face protection.

16. Other information :

N/A : Not Applicable, N/D : Not Determined
This EC Safety Datasheet is written according to the directive 91/155/EEC, 93/112/EEC, 2001/59/EC, and has 3 pages.
The information contained herein is based on the present state of our knowledge. It characterizes the product with regard to the appropriate safety precautions. It does not represent a guarantee of the properties of the product. We believe that such information is accurate and reliable as of the date of this safety data sheet; but no representation, guarantee or warranty, express or implied, is made. We urge persons receiving this information to make their own determination about the product as to the information's suitability and completeness for their particular application. We further urge purchasers to determine compatibility of this product for their application prior to use by making their own tests, also with regard to possible applicational influences. The abidance of conditions or methods of handling, storage, use and disposal of the product by the client are beyond our control and may be beyond our knowledge. For this and other reasons we do not assume responsibility and expressly disclaim liability for loss, damage or expense arising out of or in any way with the handling, storage, use or disposal of the product.
May 2007

Appendix D

Additional Issues

There are other parts of the space environment that are concerns for the spacecraft material designer, such as electromagnetic interference, electrical conductivity, and resistance to certain counterspace attacks. These effects though can for the most part be mitigated by design choices and engineering work-arounds, as such they are application dependent. As a result, this study was only concerned with qualification independent of specific application. These additional tests were not conducted as part of this study, but are mentioned in the discussion for completeness and to provide suggestions for follow-on research.

Electromagnetic Interference (EMI)

The space environment, especially at LEO, is also an electrically active region. This is due to the fact that the ionosphere, the region of the Earth's upper atmosphere comprising much of LEO, is a mass of charged plasma species. As a result, spacecraft have to be electrically neutral and able to dissipate charges that build up on the surface of the spacecraft due to electrically active spacecraft components like antennas or electronics. While materials for spacecraft applications do not have to be electrically conductive, the conductivity properties must be known so as to account for EM potential differences that may arise during the mission. EM interference testing involves the material being used in an application and then that device or component being tested for electrical conductivity values. The bulk material can also be tested to establish what the material resistivity value is via a number of simple electrical tests.

As a consequence of the electrical and magnetic environments being interrelated according to Maxwell's Equations, an active electrical environment also impacts the magnetic environment. In space, the Earth's magnetic field can be approximated by a simple dipole with dynamo activity being on the millennial time scale. Many spacecraft utilize the nature of the Earth's magnetic field as a navigation source through the use of magnetometers to determine the time stamped magnetic vectors apparent at any time in an object's orbit. The spacecraft designer then must be fully aware of the magnetic reference the assembled spacecraft has in order to properly calibrate the on-board magnetometers. Therefore, the material magnetic properties must be known so that a highly magnetic material is not placed in the immediate vicinity of the magnetometers. Illite and metakaolin have not been extensively studied for their magnetic properties, although the chemistry suggests that neither should be magnetically active and simple bench top empirical testing with common magnets shows no attraction.

Exposure to counterspace attacks

Spacecraft have become invaluable to the modern military. Satellite communications, satellite navigation (GPS), and space-based intelligence, surveillance, and reconnaissance (ISR) assets are all seen as force multiplies that allow modern armed forces to engage in operations utilizing over-the-horizon strategies. Because of this, potential adversaries of space faring nations are developing counterspace, or anti-satellite, technologies to attack a spacecraft and provide effects ranging from denial of service to spacecraft destruction. (Air Force Doctrine 2004) Most notably in recent history, China has demonstrated this with a successful test of a direct ascent interceptor ASAT system in January 2007. (Covault 2007)

The range of counterspace options are varied and can attack the spacecraft itself or the support infrastructure to deny the spacecraft user access to the asset. Certain counterspace options target the degradation or outright destruction of materials used on the spacecraft so as to cause massive failures of the components those materials make-up. Specifically, the spacecraft material designer needs to be aware of the threat from ASAT laser attack.

Laser attack involves the direct lasing of a target satellite, typically from a ground based platform with either a low or high power beam. Low power laser ASAT systems usually target imaging spacecraft in LEO in order to saturate and blind the imaging sensor on the spacecraft. Low power laser ASAT systems have wavelengths in the band of the imaging sensor, usually in visible or near-IR wavelengths. (Butt 2009) For most structural materials, this is inconsequential as that wavelength of laser energy is either highly reflected or if absorbed, transformed into low heat loads that can be easily dissipated by on-board thermal control systems.

High power laser attack seeks to cause permanent damage on a spacecraft by using wavelengths of laser energy that would be absorbed and transformed into thermal energy at loads that cannot be dissipated easily by the spacecraft. This heat build-up would then cause rapid temperature increases in affected material, and depending on the material, would cause heat-related damage mechanisms such as phase changes or structural failure.

A common damage mechanism in this instance for traditionally space qualified polymers is that the increased heat load causes the material to expand rapidly and this then causes additional stresses on the mechanical or adhesive joints the polymer is involved in. In the case of solar array construction, this can cause the individual solar cells to then detach from the array backing structure. Geopolymers with their low initial CTE, are more resistant to this attack since they have high heat capacities, and would not change dimensions significantly upon the application of heat loads that would effect common organic polymers. As seen in the analysis of post UV exposure spectra, geopolymers may have an advantage of high reflectivity to IR bands post-space launch operations.

Bibliography

"Ablebond 84-1". Datasheet. Emerson Cuming Company. 2006.

Agilent Technologies. “User Manual: Testworks 4 Nanoindentation Software”. 2009.

Air Force Doctrine Document 2-2.1. Counterspace Operations, 2 August 2004. http://www.dtic.mil/doctrine/jel/service_ pubs/afdd2_2_l.pdf.

Air Force Research Laboratory, Materials and Manufacturing Directorate [AFRL/RX]. 2007. “SCEPTRE Facility: Materials Testing in a Simulated Space Environment”. Pamphlet. Available at http://www.ml.afrl.af.mil/publications/pdf/SEPTRE_brochure.pdf.

American Society for Testing and Materials. “E 349 – 06 Standard Terminology Relating to Space Simulation.” ASTM International Document #E349-06. (2006)

American Society for Testing and Materials, “E 384 – 08ae1 Standard Test Method for Microindentation Hardness of Materials.” ASTM International Document # E384-08ae1`. (2008)

American Society for Testing and Materials. “E 512 – 94 (Reapproved 2004) Standard Practice for Combined, Simulated Space Environment Testing of Thermal Control Materials with Electromagnetic and Particulate Radiation.” ASTM International Document # E512-94. (2004)

American Society for Testing and Materials, “E 490-00a Standard Solar Constant and Air Mass Zero Solar Spectral Irradiance Tables”, *2004 Annual Book of ASTM Standards*, Vol. 15.03 (2004).

American Society for Testing and Materials, “E 512-94 Standard Practice for Combined, Simulated Space Environment Testing of Thermal Control Materials with Electromagnetic and Particulate Radiation”, *2003 Annual Book of ASTM Standards*, Vol. 15.03 (2003).

American Society for Testing and Materials. “C 1161-02c Standard Test Method for Flexural Strength of Advanced Ceramics at Ambient Temperature”. ASTM International Document # C1161-02c. (2008)

American Society for Testing and Materials. “C 1424 – 04 Standard Test Method for Monotonic Compressive Strength of Advanced Ceramics at Ambient Temperature.” ASTM International Document # C1424-04. (2004)

Balaguru, P.N. & Arafa, M. “Geopolymer Coating Demonstration Project for Route I-295 Scenic Overlook” *New Jersey Department of Transportation.* Document # FHWA-NJ-2005-021. August 2006.

Balaguru, P.N., Nazier, M., Arafa, M. “Field Implementation of Geopolymer Coatings” *New Jersey Department of Transportation.* Document # FHWA-NJ-2002-11 . May 2008.

Banks, Bruce, et al. “Atomic Oxygen Effects on Spacecraft Materials”. NASA/TM—2003-212484. NASA Glenn Research Center. June 2003. Available from NASA Center for Aerospace Information, 7121 Standard Drive, Hanover, MD 21076

Banks, B. A., and Rutledge, S. K. “Low Earth Orbital Atomic Oxygen Simulation for Materials Durability Evaluation”, *Proc. Fourth European Symposium on Spacecraft Materials in Space Environment*, CERT, Toulouse, 6-9 September, 1988.

Bell, J; Gordon, M; Kriven, W. “Use of Geopolymeric Cements as a Refractory Adhesive for Metal and Ceramic Joints”. *ACERS Conference.* Cocoa Beach, FL. 2005.

Bellotto, M.; Gualtieri, A.; Artioli, G.; Clark, S.M. “Kinetic study of the kaolinite-mullite reaction sequence. Part I: kaolinite dehydroxylation.” *Phys. Chem. Minerals*. Vol 22, 207-214. 1995.

Boboev, T.B., Regel, V.R., Chernyi, N.N. “Comparison of the effect of ultraviolet radiation on polymer creep rate in a vacuum and in air.” *Mechanics of Composite Materials.* Vol. 5, No. 3. May 1969.

Butt, Y. “Effects of Chinese Laser Ranging on Imaging Satellites”. *Science and Global Security*. 17:20-35, 2009.

Campbell, W.A. and Scialdone, J.J. “Outgassing Data for Selecting Spacecraft Materials”. NASA Goddard Space Flight Center, Greenbelt, MD. September 1993.

Carlin, P.S. “Light weight mirror systems for spacecraft- An overview of materials and manufacturing needs,” Proceedings of IEEE Aerospace conference, 18-25 March, 2000, Big Sky Montana, Vol. 4, pg. 169-182. Available from Defense Technical Information Center, Fort Belvoir, VA.

Casa Software, “CasaXPS Manual- XPS Spectra”. Published 2011.Available at http://www.casaxps.com/help_manual/manual_updates/xps_spectra.pdf

Catanzaro, B. E.; et al. “C/SiC advanced mirror system demonstrator design.” *Proc. SPIE- UV, Optical, and IR Space Telescopes and Instruments*. Vol. 4013. July 2000. Pp. 672-680.

Cerbus, C. A. and P. S. Carlin, "SCEPTRE: The Air Force Combined Space Environment Facility," *1st Spacecraft Thermal Control Symposium Proceedings*, STCS '94, USAF Phillips Laboratory, Albuquerque, NM (1994).

Coulter, Daniel R. "Technology Development for the Next Generation Space Telescope: An Overview." *Proc. of SPIE-Space Telescopes & Instruments V.* Kona, Hawaii, USA. 20 Mar 1998.

Cordoba, S.S.F. "100-km altitude boundary for astronautics." http://www.fai.org/astronautics/100km.asp. Fédération Aéronautique Internationale. n.d. Web. 21 June 2004.

Covault, Craig. "China's Asat Test Will Intensify U.S.-Chinese Faceoff in Space". *Aviation Week*. 21 Jan 2007.

Davidovits, J. *Geopolymer Chemistry and Applications.* Saint-Quentin, France: Geopolymer Institute. 2008.

Davidovits, J. "Geopolymers: Inorganic Polymeric New Materials". *J. Thermal Analysis*. Vol. 37, 1991. pp. 1633-1656.

Davidovits, J. "30 Years of Geopolymers" *Geopolymer 2002 Conference*, Melbourne, Australia. October 28-29, 2002.

Decker, C. "Photodegradation of PVC". In *Degradation and Stabilization of PVC*, Owen, E.D. (ed.), London: Elsevier Applied Science Publishers, p. 81-136. 1984.

De Silva, P., Sagoe-Crenstil, K., Sirivivatnanon, A. (2007) "Kinetics of geopolymerization: Role of Al_2O_3 and SiO_2." *Cement and Concrete Research*. Vol 37, Issue 4, Apr. 2007. pp 512-518.

Dever, J. A., Banks, B. A., Yan., L., "Effects of Vacuum Ultraviolet Radiation on Dow Corning (DC) 93-500 Silicone," *Journal of Spacecraft and Rockets.* Vol. 43, No. 2, Pp. 386-392. Mar-Apr 2006.

Dobbs, L. *Space: The Next Business Frontier*. New York: iBooks, Inc. 2002. ISBN 0-7434-5260-7.

Dooling, D., Finckenor, M.M. "Material Selection Guidelines to Limit Atomic Oxygen Effects on Spacecraft Surfaces". *NASA Marshall Space Flight Center NASA document #* NASA/TP-1999-209260. June 1999.

Dressler, R.A. *Chemical Dynamics in Extreme Environments*. Singapore: World Scientific. 2001. ISBN 978-981-02-4177-3.

Duxson, P., et al. “Understanding the relationship between geopolymer composition, microstructure and mechanical properties”. *Colloids and Surfaces A: Physicochem. Eng. Aspects.* No. 269. Pp 47-58. 2005

Fisher, Aaron and Mermelstein, Benjamin, "A Compilation of Low Outgassing Polymeric Materials Normally Recommended for GSFC Cognizant Spacecraft," NASA TM X-65705, July 1971.

Giessibl, Franz J. "Advances in atomic force microscopy". *Reviews of Modern Physics.* No. 75. Pp 949. 2003.

Gilmore, D.G., et al. “11.5 Thermal.” In W.J. Larson & J.R. Wertz (Eds.) *Space Mission Analysis and Design, 3rd Edition*. Pp. 428 – 458. El Segundo: Microcosm Press. 2004.

“Graniterock: Technical Note: Plastic Shrinkage Control”. http://www.graniterock.com/technical_notes/plastic_shrinkage_cracking.html. Graniterock Company. n.d. Web. 1 Nov 2009.

Gross, F. “Room Temperature Curing Polymers for Aerospace Hardwware” *NASA Technical Information Page # 100*. Oct 2002.

Grossman, E., Gouzman, I. “Space environment effects on polymers in low earth orbit”. *Nuclear Instruments and Methods in Physics Research Section B: Beam Interactions with Materials and Atoms.* Vol. 208. Pp. 48-57. Aug 2003.

Gualtieri A F*, Journal of Applied Crystallography*, Vol. 33. 2000. p.267-278

Haener, C.; Colony, J.. “Effects of Low Earth Orbit on Spacecraft Materials”. *NASA Technical Information Page # 099*. Jan 2003.

Haffke, J.; Woolam, J. “Synergistic Degredation of CV-1144-O due to Ultraviolet Radiation and Heat”. *Proc of the International Conference on Protection of Materials and Structures from Space Environment, 6th annual (ICPMSE-6)*. Toronto, CAN. 1-3 May 2002. Pp.183-191.

Hecht, Eugene. *Optics*. 4th Edition. San Francisco: Addison Wesley, 2002. ISBN 0-8053-8566-5.

Hedin, A.E. “MSIS-86 Thermospheric Model.” *J. Geophys. Res.* Vol. 92, Pp. 4649-4662. 1986.

Kishner, S; Flynn, D.; Cox, C. “Reconnaissance Payloads for Responsive Space”. *Proc. of 4th AIAA Responsive Space Conference*. Los Angeles, CA. 24-27 Apr 2006.

Kopp, Carlo. “High Energy Laser Directed Energy Weapons”. Air Power Australia. Technical Report # APA-TR-2008-0501. 2008.

Kriven, W.M. Multiple publications found at <http://www.matse.illinois.edu/Faculty/kriven/publications.html>. 2009

Lee, Stuart. *Dictionary of Composite Materials Technology.* Lancaster: Technomic Publishing. 1989. ISBN 87762-600-6

Kumar, Sanjay (2008, July 31). “Geopolymers: New Generation Materials by Mimicking Rock Formation”. SciTopics. Retrieved March 26, 2010, from http://www.scitopics.com/Geopolymers_New_Generation_Materials_by_Mimicking_Rock_Formation.html

Licari, J.; Swanson, D. *Adhesive Technology for Electronic Applications*. Norwich, NY:William Andrew Publishing, 2005.

Liddle, D., et al. “A Low-Cost Geostationary Minisatellite Platform.” *Proceedings of the 54th International Astronautical Congress*. Bremen, Germany. Oct 2003

Lunar and Planetary Institute. “Apollo 11 Solar Wind Composition Experiment”. Available at:

<http://www.lpi.usra.edu/lunar/missions/apollo/apollo_11/experiments/swc/>, Accessed October 2009.

Mah, T, et al. “Advanced Processing of the Optical Surface on Large Lightweight Mirrors.” *NASA Tech Days 2003.* Kirtland AFB, Albuquerque, NM. 27 Sep. 2003.

Mah, T., et al. “Advanced Rapid Mirror Assembly Processing”. *46th AIAA/ASME/ASCE/AHS/ASC Structures, Structural Dynamics & Materials Conference*. Austin, Texas. 18-21 Apr. 2005.

Matson, L. “CTE Tailored Materials for Hybrid Mirror Systems.” *NASA Tech Days 2003*. Kirtland AFB, Albuquerque, NM. 27 Sep. 2003.

Matson, L.E.; Mollenhauer, D. “Advanced materials and processes for large, lightweight, space-based mirrors” *Proc. 2003 IEEE Aerospace Conference*. Vol. 4, Pp. 4_1681-4_1697. Mar. 2003.

Matson, L.E.; Chen, M.Y.; deBlonk, B.; Palusinski, I. “Silicon Carbide Technologies for Lightweighted Aerospace Mirrors.” *Proc. of AMOSTech ’08*. Maui, HI. 16-19 Sep 2008.

Matweb. “Online Materials Information Resource”. Matweb, LLC. Website. Viewed May 2012. http://www.matweb.com.

Meshishnek, M. J., Stuckey, W. K., Anderson, P. C. “Radiation Environment Predictions for Laboratory Tests”. *Aerospace Corporation Report TR 2001 (8565)-9*. Under contract to USAF Space & Missile Center, F04701-00-C-0009. Published 1 October 2001.

Monib, KM. “The Use of Silicone Adhesives in Space Applications”. *Adhesives Magazine*. 28 Oct 2003.

Mosher, Todd. “Conceptual spacecraft design using a genetic algorithm trade selection process.” *Journal of Aircraft*. Vol. 36, no. 1, pp. 200-208. Jan.-Feb. 1999.

Moulder, J.,F., et al. *Handbook of X-ray Photoelectron Spectroscopy.* Eden Prairie, MN: Perkin-Elmer Corp., 1992.

Nakamura, H., Nakamura, T., Noguchi, T., Imagawa, K. “Photodegradation of PEEK Sheets Under Tensile Stress”. *Polymer Degradation and Stability*. Vol. 91, Issue 4. Pp. 740-746. April 2006.

NASA Langley Research Center. “Long Duration Exposure Facility (LDEF) Archive System.” Available at: <http://setas-www.larc.nasa.gov/LDEF/index.html>. Accessed 1 October 2009.

“NASA MISSE”. http://misseone.larc.nasa.gov/. NASA. N.d. Accessed 1 Oct 2009.

National Reconnaissance Office. “Corona Fact Sheet”. National Reconnaissance Office website, n.d. Web. 1 Nov 2009

“Nuclear and space radiation effects on materials - Space vehicle design criteria”. NASA Document #SP-8053. Published June 1970.

O’Neill, MJ, et al. “Development of the Ultra-Light Stretched Lens Array”. *Proc. of the 29th IEEE Photovoltaic Specialists Conference.* New Orleans, LA. May 2002

Papakonstantinou, C.G.; Balaguru, P.; Lyon, R.E. “Comparative study of high temperature composites” *Composites Part B: Engineering.* Volume 32, Issue 8, Dec. 2001, Pages 637-649.

Perera, D., Uchida, O., Vance, E.R., Finnie, K.S. “Influence of curing schedule on the integrity of geopolymers.” *J Mater. Sci*. Vol 42, Pp. 3099-3106. 2007.

Picone, J.M., et al. "NRL-MSISE-00 Empirical Model of the Atmosphere: Statistical Comparisons and Scientific Issues," *J. Geophys. Res.* In press 2003

Pippin, H.G. “Analysis of Materials Flown on the Long Duration Exposure Facility: Summary of Results of the Materials Special Investigation Group”, *NASA Contractor Report*. Available from NASA Marshall Space Flight Center's Materials and Processes Technical Information System (MAPTIS). Published May 1995.

Pocius, A.V. *Adhesion and Adhesives Technology*. Cincinnati: Hanser Gardner Publications, 2002.

Provis, JL., Duxson, P., Van Deveter, J.S.J., Lukey, G.C. “The Role of Mathematical Modeling and Gel Chemistry in Advancing Geopolymer Technology.” *Chemical Engineering Research and Design*. Vol 83, Issue 7, July 2005. Pp. 853-860.

Sanderson, R.T. *Chemical Bonds and Bond Energy*. New York: Academic Press, 1976.

Sandia National Laboratory. "New Deployable Thin-Film, Ultralight Mirror May Be Future Of Space Telescopes And Surveillance Satellites." *ScienceDaily*. n.p., 24 May 2000. Web. 7 Dec. 2009.

Scialdone,J., Isaac, P., Clatterbuck, C., Hunkeler, R. “Material Total Mass Loss in Vacuum Obtained from Various Outgassing Systems”. NASA/TM–2000–209897. NASA Goddard Space Flight Center, Greenbelt MD. 2000.

Snead, L.L., Zinkle, S.J., White, D.P. “Thermal conductivity degradation of ceramic materials due to low temperature, low dose neutron irradiation”. *Journal of Nuclear Materials*, Vol. 340, No 2-3, Pp. 187-202. 2005.

Stahl, H.P.; et al. “Preliminary cost model for space telescopes.” *Proc. SPIE-UV/Optical/IR Space Telescopes: Innovative Technologies and Concepts IV*. Vol. 7436. 3 Aug 2009.

Stahl, H.P. “Design study of 8 meter monolithic mirror UV/optical space telescope.” *Proc. of Space Telescopes and Instrumentation 2008: Optical, Infrared, and Millimeter, SPIE*. Vol. 7010, 2008.

Stockman, HS. “James Webb Space Telescope.” *Proc. of the International Astronomical Union.* Vol. 2. Pp. 522-3. (2006)

Tao, L., et al. “Space Atomic Oxygen Erosion Effects on Epoxy and Silicone Adhesives Used in LEO Spacecraft”. *Proceedings of the 9th International Conference: Protection of Materials and Structures From Space Environment.*, Amer. Inst. Phys. Conf. Proc. 1087, pp. 83-89. 20–23 May 2008, Toronto (Canada).

Tribble, A.C. *The Space Environment: Implications for Spacecraft Design.* Princeton: Princeton University Press. 2003.

Tribble, A.C., et al. “8.1.5 Radiation and Associated Degradation.” In W.J. Larson & J.R. Wertz (Eds.) *Space Mission Analysis and Design, 3rd Edition*. Pp. 214 – 221. El Segundo: Microcosm Press. 2004.

"U.S. Standard Atmosphere 1976". National Oceanic and Atmospheric Administration. Document # NOAA –S/T 76-1562.

Van Jaarsveld, JGS, et al. "Potential Use of Geopolymeric Materials to Immobilize Toxic Metals: Part I. Theory and Applications." *Minerals Engineering*. Vol 10, No 7. Pp 659-669. 1997.

Visentine, J.T., "Atomic Oxygen Effects Measurements for Shuttle Missions STS-8 and 41-G," *NASA Technical Memorandum.* No. 100459, Vol. I, pp. 2-1 – 2-10, Sep. 1988.

Wallace, T.J., Rossiter, W.J. *Roofing Research and Standards Development*. Chelsea: ASTM Publishing. 1990.

Wang, Y.M., J. Li, A. V. Hamza, and T. W. Barbee, Jr., "Ductile Crystalline-Amorphous Nanolaminates," *Proc. Natl. Acad. Sci. USA* 104 11155-11160 (2007)

Xu, H.; Van Deventer, J.S.J. "The geopolymerisation of alumino-silicate minerals." *International Journal of Mineral Processing.* Volume 59, Issue 3, Pp. 247-66. June 2000.

Zeus Industrial Products. "UV Properties of Plastics: Transmission and Resistance". Technical White Paper. Published 2006. Available at <http://www.zeusinc.com/UserFiles/zeusinc/Documents/Zeus_UV_Properties.pdf>

Vita

CONTACT INFORMATION

Brandon Timothy Cesul
961 Hickory Lane, Troy, OH 45373
Phone: 937-335-4518, Email: Brandon.cesul@us.af.mil

EDUCATION

University of Michigan, Ann Arbor, MI. Master of Engineering, Space Systems, Awarded May 2002

University of Michigan, Ann Arbor, MI. Bachelor of Science in Engineering, Major: Chemical Engineering, Awarded May 2001

PROFESSIONAL EXPERIENCE

2002-2012: National Air & Space Intelligence Center, WPAFB, OH. Space Systems Engineer

PUBLICATIONS / BOOKS

Cesul, BT; Ohlweiler J; Szopko R. "The Icarus Student Satellite Project". 1999 Sigma Xi Annual Conference Proceedings.

Cesul BT; Gilchrist B, Goldberg H. "The Icarus Student Satellite Program - Michigan's First Autonomous Satellite". Proceedings of the 16th Annual (2002)AIAA/Utah St University Small Satellite Conference. Logan UT.

Cesul, BT; Mall, S; Matson, L.; Lee, H. "Inorganic Polymers for Space Applications", Proceedings of the 22nd Annual (2008) AIAA/Utah St University Small Satellite Conference. Logan UT. 11-14 Aug 2008.

Cesul, BT; Mall, S; Matson, L; Lee, H. "Suitability of Geopolymers for Spacecraft Applications", Proceedings of the 59th International Astronautical Congress. Glasgow UK. 29 Sep – 3 Oct 2008. IAC-08-C2.4.7

Classified Literature: Over 100 peer reviewed contributions to the IC literature

PROFESSIONAL AFFILIATIONS

Sigma Gamma Tau, Tau Beta Pi, American Polish Engineering Association, American Institute of Chemical Engineers, The Mars Society

AWARDS

National Air & Space Intelligence Center Civilian of the Year, Cat III, 2009; NASIC Commander's Award for Merit, Technology and Subsystems Assessments, 2005; Wright-Patterson AFB Civilian of the Year, Cat II, 2004; Patterson Memorial Scholarship, University of Michigan, 2000

REPORT DOCUMENTATION PAGE

Form Approved
OMB No. 074-0188

1. REPORT DATE *(DD-MM-YYYY)*	2. REPORT TYPE	3. DATES COVERED *(From – To)*
13-09-2012	Dissertation	Jan 2005 – Sep 2012

4. TITLE AND SUBTITLE

Investigation into Suitability of Geopolymers (Illite & Metakaolin) for the Space Environment

5a. CONTRACT NUMBER

5b. GRANT NUMBER

5c. PROGRAM ELEMENT NUMBER

6. AUTHOR(S)

Cesul, Brandon T.

5d. PROJECT NUMBER

5e. TASK NUMBER

5f. WORK UNIT NUMBER

7. PERFORMING ORGANIZATION NAMES(S) AND ADDRESS(S)

Air Force Institute of Technology
Graduate School of Engineering and Management (AFIT/EN)
2950 Hobson Way, Building 640
WPAFB OH 45433-8865

8. PERFORMING ORGANIZATION REPORT NUMBER

AFIT/DS/ENY/12-14

9. SPONSORING/MONITORING AGENCY NAME(S) AND ADDRESS(ES)

Intentionally left blank

10. SPONSOR/MONITOR'S ACRONYM(S)

11. SPONSOR/MONITOR'S REPORT NUMBER(S)

12. DISTRIBUTION/AVAILABILITY STATEMENT

APPROVED FOR PUBLIC RELEASE; DISTRIBUTION UNLIMITED. CASE NUMBER 88ABW-2012-3723, CLEARED 06 JUL 2012

13. SUPPLEMENTARY NOTES

14. ABSTRACT

Suitability of non-organic polymers for space application is studied. Materials included are illite and metakaolin. Bulk material suitability was investigated for exposure to ultraviolet radiation, atomic oxygen, and high energy charged particles. Outgassing phenomenon of the materials was studied. Curing shrinkage reduction techniques were identified as well.

15. SUBJECT TERMS

Geopolymers, space environment, illite, metakaolin, curing shrinkage, outgassing

16. SECURITY CLASSIFICATION OF:			17. LIMITATION OF ABSTRACT	18. NUMBER OF PAGES	19a. NAME OF RESPONSIBLE PERSON
a. REPORT	b. ABSTRACT	c. THIS PAGE			Shankar Mall, Prof, AFIT/ENY
					19b. TELEPHONE NUMBER *(Include area code)*
U	U	U	UU	207	(937) 255-6565, ext 4587 (Shankar.mall@afit.edu)

Standard Form 298 (Rev. 8-98)
Prescribed by ANSI Std. Z39-18